JOURNAL OF GEOPHYSICAL RESEARCH, VOL. 91, NO. B12, PAGES 12,587–12,631, NOVEMBER 10, 1986

Earthquakes, Quaternary Faults, and Seismic Hazard in California

STEVEN G. WESNOUSKY[1]

Seismological Laboratory, California Institute of Technology

Data describing the locations, slip rates, and lengths of Quaternary faults are the primary basis in this work for constructing maps that characterize seismic hazard in California. The expected seismic moment M_o^e and the strength of ground shaking resulting from the entire rupture of each mapped fault (or fault segment) are estimated using empirical relations between seismic moment M_o, rupture length, source to site distance, and strong ground motions. Assuming a fault model whereby the repeat time T of earthquakes on each fault equals M_o^e/M_o^g (where the moment rate M_o^g is proportional to fault slip rate), it is observed that the moment-frequency distribution of earthquakes predicted from the geologic data agrees well with the distribution determined from a 150-year historical record. The agreement is consistent with the argument that the geologic record of Quaternary fault offsets contains information sufficient to predict the average spatial and size distribution of earthquakes through time in California. The estimates of T for each fault are the foundation for constructing maps that depict the average return period of $\geq 0.1g$ peak horizontal ground accelerations, and the horizontal components of peak acceleration, peak velocity, and the pseudovelocity response (at 1-period and 5% damping) expected to occur at the level of 0.1 probability during a 50-year period of time. A map is also formulated to show the probability that $\geq 0.1g$ horizontal ground accelerations will occur during the next 50 years. The maps serve to illustrate the potential value of Quaternary fault studies for assessing seismic hazard. Interpretation of available slip rates indicates that the largest and most frequent occurrence of potentially destructive strong ground motions are associated principally with the San Andreas, San Jacinto, Calaveras, Hayward, and Ventura Basin fault zones. Other regions of similarly high hazard may yet remain unrecognized. This inadequacy results primarily from an incomplete data set. Numerous faults, for example, are mapped along the coastal region of northern California and within the Modoc Plateau, but relatively few studies relating to fault slip rate are reported. A similar problem exists for other stretches of coastal California where marine reflection studies provide evidence of active faulting offshore yet yield little or no information of fault slip rate. Geological and geophysical field studies can work to remove these deficiencies. A concerted effort to locate and define rates of activity on all faults in California is the most promising means to further quantify present levels of seismic hazard in California.

INTRODUCTION

The causal relation between earthquakes and faulting was well described some 100 years ago by *Gilbert* [1884] during his discussion of earthquakes in the Great Basin. *Koto* [1893] independently noted the same causality during his study of the great 1891 Nobi earthquake of Japan. Later field investigations of the great 1906 California earthquake by *Lawson* [1908] and his colleagues removed most remaining doubt of the close connection between faulting and earthquakes. Moreover, *Reid*'s [1910] geodetic study of that same earthquake provided a physical model to explain the occurrence of earthquake faulting, the now well-known concept of elastic rebound. These observations prompted *Willis* [1923] to suggest as early as 1923 that a fault map of California was a good indicator to the sites of future earthquakes. Since these studies, knowledge of the mechanics of earthquake faulting has continued to grow, moderate to large earthquakes have consistently been observed to rupture along mapped faults, and faults that break Quaternary deposits are now commonly accepted as sources of seismic hazard. The purpose of this work is to use our current understanding of fault mechanics to interpret data that describe the average rates of offset across Quaternary faults, with an aim toward developing maps that depict long-term seismic hazard in California: specifically, the average size and spatial distribution of earthquakes through time and, of more practical consequence, the expected occurrence rate of the resulting strong ground motions.

The motivation for this study resides in the uncertainties inherent to more conventional forms of seismic hazard analysis, which are based primarily on earthquake frequency statistics obtained from historical catalogues of seismicity. The uncertainty in such analyses is large when the historical record is too short to define secular rates of seismicity, which is the usual case, particularly when relatively small regions are considered. In contrast to historical data, the geologic record of Quaternary fault offsets contains information on the occurrence of earthquakes through periods of time many orders longer than the average repeat time of large earthquakes on individual faults and orders of magnitude greater than periods covered by historical records. Observations such as these have recently led a number of investigators to argue that geologic information of fault offset rates may be used to reduce uncertainties associated with estimates of long-term seismicity and, in turn, seismic hazard [e.g., *Allen*, 1975; *Anderson*, 1979; *Molnar*, 1979]. The following exercise is thus an attempt at placing this idea into a quantitative framework for analysis of seismic hazard in California. The approach I will take follows that developed in a recent study of seismic hazard in Japan [*Wesnousky et al.*, 1984]. The underlying premise of that work was that moderate to large earthquakes occur on mappable Quaternary faults and that the occurrence rate of

[1] Now at Tennessee Earthquake Information Center, Memphis State University.

Copyright 1986 by the American Geophysical Union.

Paper number 5B5769.
0148-0227/86/005B-5769$05.00

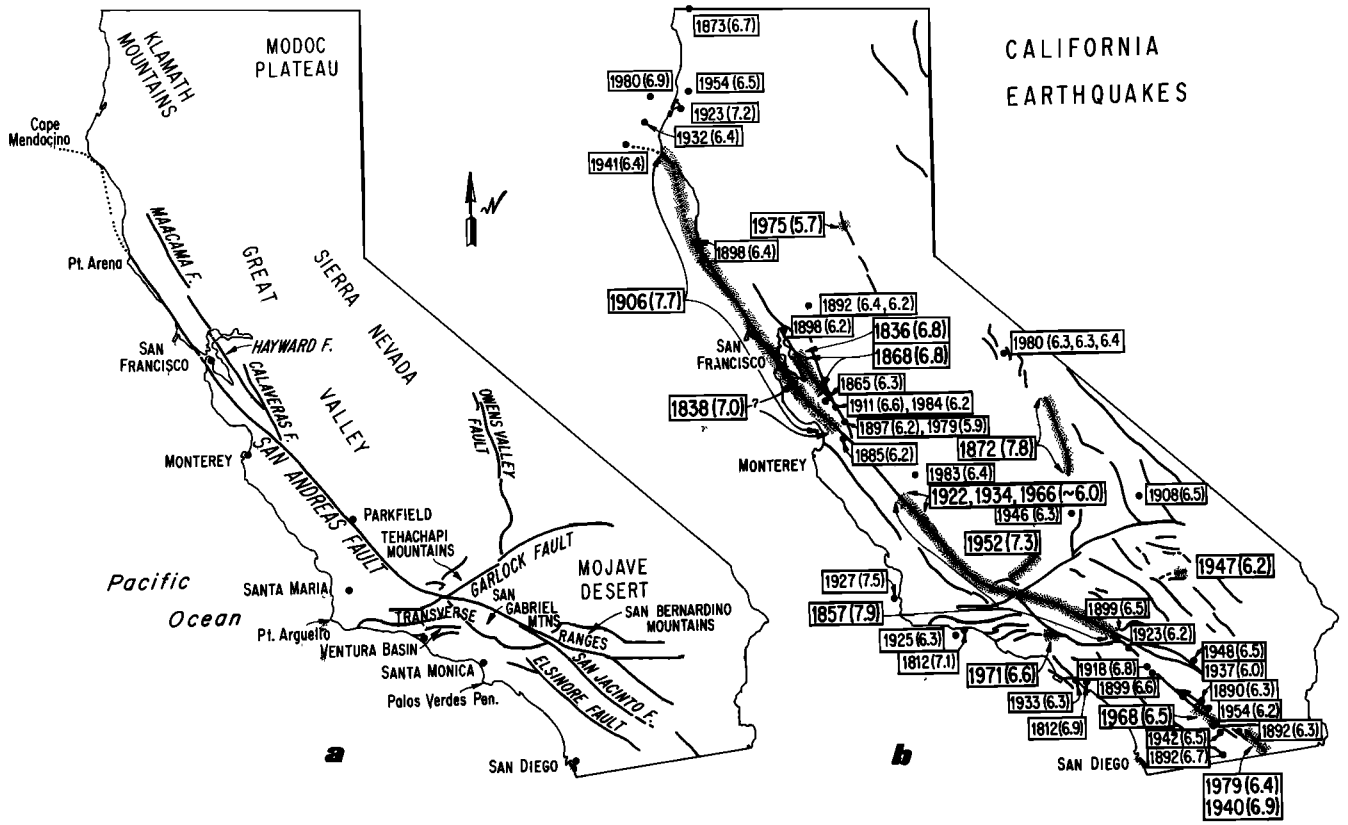

Fig. 1. (a) Major active faults, physiographic features, and (b) locations of historically recorded moderate to large earthquakes that have occurred in California. Faults that have produced coseismic surface ruptures are stippled. Onshore and offshore events of $M \geq 6.2$ are listed in Tables 1 and 3, respectively.

earthquakes on each fault is proportional to the Quaternary fault slip rate.

It is the parameter of seismic moment M_o that allows the quantitative assessment of seismicity rates from fault slip rate data [*Brune*, 1968]. The seismic moment M_o is a more fundamental measure of earthquake strength than is earthquake magnitude M and, like M, may be measured directly from a seismogram. M_o, however, may be related directly to physical parameters that describe the earthquake source, whereas M can only be indirectly related through its empirical relation with M_o [e.g. *Hanks and Kanamori*, 1979]. Specifically, seismic moment M_o is defined to equal $\mu\bar{U}A$, where μ is the shear modulus, A is the fault area, and $\bar{U}$ is the average slip occurring across the fault [e.g., *Aki and Richards*, 1980]. Thus, for a fault on which a number n of earthquakes have occurred during a period of time T_1, the rate of seismicity on the fault may be characterized by the seismic moment rate

$$\dot{M}_o = \left[\sum_{i=1}^{n} M_o^i\right] / T_1$$

Further, if a geologic marker of age T_2 is displaced across the fault by distance U, the long-term rate of seismicity on the fault may be expressed as $\dot{M}_o = \mu A(U/T_2)$ [*Brune*, 1968]. This assumes that fault displacements are not the result of aseismic creep but rather are the cumulative result of many earthquakes through geologic time. Using the concept of seismic moment, a near coincidence of historical rates of seismicity to rates of seismicity averaged over longer periods of geologic time has now been observed for the regions encompassing southern California [*Anderson*, 1979], Utah [*Doser and Smith*, 1982], and intraplate Japan [*Wesnousky et al.*, 1982], as well as a number of plate boundaries [*Brune*, 1968; *Davies and Brune*, 1971]. The observed coincidence in seismicity rates over these broad regions provides support for the suggestion [*Allen*, 1975; *Anderson*, 1979] that the geologic record of Quaternary fault offsets is well suited for estimating long-term rates of seismicity and hence seismic hazard in regions characterized by shallow seismicity, Quaternary faulting, and a short recorded history. California possesses each of these attributes. Let me then briefly review the available data concerning seismicity, faulting, and fault slip rates in California.

Data And Observations

Earthquakes and Faulting

Earthquakes in California, and in other regions of similar tectonic style, generally rupture along faults that show evidence of prior Quaternary movements [*Allen*, 1975; *Matsuda*, 1977]. It is also generally recognized in California that the occurrence of earthquakes is limited primarily to the upper 15 km of the earth's crust [e.g., *Sibson*, 1982]. The epicentral distribution of moderate to large earthquakes that have occurred in California during historical time is pictured on a simplified fault map of California in Figure 1. Onshore earthquakes of $M \geq 6.2$ are further listed in Table

TABLE 1. Earthquakes Onshore California

Date	Location	Magnitude*	Mappable Fault†	Surface Rupture†	References ‡
April 9, 1857	San Andreas	7.9§	Yes	Yes	1
March 26, 1872	Owens Valley	7.8	Yes	Yes	2,21
April 18, 1906	San Andreas	7.7§	Yes	Yes	3
July 21, 1952	Kern County	7.3§	Yes	Yes	4
Jan. 22, 1923	Humboldt#	7.2	--	--	9,25
June 1838	San Andreas	7.0	Yes	Yes	5
Dec. 8, 1812	Los Angeles#	6.9	--	--	7
May 19, 1940	Imperial Valley	6.9§	Yes	Yes	6
June 10, 1836	Hayward	6.8	?	?	5,7
Oct. 21, 1868	Hayward	6.8	Yes	Yes	3
April 21, 1918	San Jacinto	6.8	Yes	--	7,8
Nov. 23, 1873	Oregon border	6.7	--	--	18
Feb. 24, 1892	San Diego County	6.7	--	--	7
Dec. 25, 1899	San Jacinto	6.6	Yes	--	8,9
July 1, 1911	Santa Clara	6.6	Yes	--	7,11
Feb. 9, 1971	San Fernando	6.6§	Yes	Yes	12
July 22, 1899	Cajon Pass	6.5	--	--	7,8
Nov. 4, 1908	Inyo	6.5	--	--	9
March 10, 1922	Parkfield	6.5	Yes	?	13,23
Oct. 21, 1942	San Jacinto	6.5	Yes	--	7,8
Dec. 4, 1948	Desert Hot Springs	6.5	?	?	14
Dec. 21, 1954	Humboldt	6.5	--	--	18
April 9, 1968	Borrego Mountain	6.5§	Yes	Yes	15
April 19, 1892	Winters	6.4	--	--	16
Oct. 15, 1979	Imperial Valley	6.4§	Yes	Yes	19
May 2, 1983	Coalinga	6.4	No	No	20
May 25, 1980	Mammoth	6.4,6.3		?	?
Oct. 8, 1865	San Jose	6.3	--	--	7
Feb. 9, 1890	San Jacinto	6.3	--	--	7,8
May 28, 1892	San Jacinto	6.3	--	--	7,8
July 23, 1923	Riverside	6.3	--	--	8,9
March 11, 1933	Long Beach	6.3	Yes	No	17
March 15, 1946	Walker Pass	6.3	?	?	21
May 27, 1980	Mammoth	6.3	?	?	10,26
April 12, 1885	Salinas	6.2	--	--	7
April 21, 1892	Winters	6.2	--	--	7
June 20, 1897	Gilroy	6.2	Yes	?	7
March 31, 1898	Rodgers Creek	6.2	--	--	7
April 10, 1947	Manix	6.2	Yes	Yes	21
March 19, 1954	Santa Rosa Mountain	6.2	Yes	--	8,22
April 24, 1984	Morgan Hill	6.2	Yes	No	24

* Magnitudes are from *Toppozada et al.* [1981], *Toppozada and Parke* [1982], and *Toppozada et al.* [1986] for the periods prior to 1900, 1900 to 1950, and post-1950, respectively.

† Answers are provided to (1) whether or not instrumental, isoseismal, or field studies indicate that the earthquake was associated with displacement along a mappable fault, and (2) whether or not the earthquake produced tectonic surface ruptures along the fault trace. Observations, particularly for older events, are often equivocal and, in such cases, are marked by a query. Pair of dashes indicates that data are insufficient to consider possible association of event to a specific mapped fault.

‡ 1, *Sieh* [1978*b*]; 2, *Whitney* [1872]; 3, *Lawson et al.* [1908]; 4, *Buwalda and St. Amand* [1955]; 5, *Louderback* [1947]; 6, *Brune and Allen* [1967]; 7, *Toppozada et al.* [1981]; 8, *Sanders and Kanamori* [1984]; 9, *Toppozada and Parke,* [1982]; 10, *Taylor and Bryant* [1980]; 11, *Reasenberg and Ellsworth* [1982]; 12, *Barrows et al.* [1973]; 13, *Bulletin of the Seismological Society of America* [1924]; 14, *Richter et al.* [1958]; 15, *Clark* [1972]; 16, *Wong* [1984]; 17, *Barrows* [1974]; 18, *Toppozada et al.* [1986]; 19, *Sharp et al.* [1982]; 20, *Clark et al.* [1983]; 21, *Richter* [1958]; 22, *Magistrale et al.* [1984]; 23, *Bakun and McEvilly* [1984]; 24, *Cockerham and Eaton* [1984]; 25, *Lajoie and Keefer* [1981]; 26, *Clark and Yount* [1981].

§ Magnitude determined from seismic moment M_o via empirical relation $M=2/3\times\log M_o-10.7$ [*Hanks and Kanamori,* 1979], assuming value of M_o listed in Table 2.

Near coast, possibly offshore.

1. The data in Table 1 serve to illustrate the close association between earthquakes and Quaternary faults. Examination of Table 1 shows that as a general rule, earthquakes of $M \geqslant \sim 6.5$ produce observable surface ruptures along preexisting and mappable Quaternary faults, when attention is limited to those earthquakes for which data exist to bear upon this observation. Similarly, further examination of Table 1 shows that the moderate events of magnitude $M <$ 6.5 may also generally be demonstrated to be the result of displacement along faults with mappable surficial traces, though surface ruptures are not commonly in evidence.

The distribution of onshore faults with Quaternary dis-

TABLE 2. Earthquake Data

Date	Location	Moment			Length			Type[§]	
		10^{19} N-m	Reference *	Data †	km	Reference *	Data ‡		
			North America						
Jan. 6, 1857	Southern California	53-90	1,16	d	360-400	1,16	h	S	P
May 3, 1887	Sonora, Mexico	7-15#	61	d	76	61	h	N	I
April 18, 1906	Northern California	35-43	1,29	d	420-470	1,29	h	S	P
Oct. 2, 1915	Pleasant Valley, Nevada	3-8#	17	d	34	17	h	N	I
June 7, 1934	Parkfield, California	0.15	6	b	20	7	g	S	P
May 19, 1940	Imperial, California	2.6#- 8	8,9,5	d,b	60	8,9	h	S	P
July 21, 1952	Kern County, California	11	10	d	75	10	f	R	I
July 6, 1954	Fallon Rainbow, Nevada	0.3	4	a	18	19	h	N	I
Aug. 23, 1954	Fallon Stillwater,Nevada	0.7	4	a	30	19	h	N	I
Dec. 16, 1954	Dixie Valley, Nevada	1	4	a	40	18	h	N	I
Dec. 16, 1954	Fairview Peak, Nevada	5.3	4	a	45	18	h	N	I
July 10, 1958	Southeast Alaska	44	59	d	350	25	g	S	P
Aug. 17, 1959	Hebgen Lake,Montana	10	58	a	26	20	h	N	I
April 9, 1966	Borrego, California	0.7-1.1	11,12	a	30-45	13,14	h,g	S	P
June 27, 1966	Parkfield, California	0.15	2	b	37	3	h	S	P
Feb. 9, 1971	San Fernando, California	0.8-1.9	23,24	b,a	14-22	21	g,h	R	I
Oct. 15, 1979	Imperial, California	0.6	52	b	30	15	h	S	P
April 2, 1983	Coalinga	0.54	60	b	25	46	g	R	I
Oct. 28, 1983	Borah Peak	2.1-3.5	56,57	a,b	36	35,41	g,h	N	I
			Japan						
Oct. 28, 1892	Nobi, Japan	15	37	d	80	39	h	S	I
Aug. 31, 1896	Rikuu, Japan	14	39	d,e	36-50	38,39	f,h	R	I
March 27, 1927	Tango, Japan	4.6	40	d	33	40	f,g	S	I
Nov. 25, 1930	N. Izu, Japan	2.7	42	d,e	22	42,43	f,h	S	I
Sept. 21, 1931	Saitama, Japan	0.7	44	b	20	44	g	S	I
July 11, 1935	Shizuoka, Japan	0.22	45	a	11	45	g	S	I
Aug. 11, 1940	Shakotan, Japan	21	50	b	170	50	i	R	I
Sept. 10, 1943	Tottori, Japan	3.6	40	a,e	33	40	e	S	I
Jan. 31, 1945	Mikawa, Japan	0.9	47	e	12	47	f	R	I
June 28, 1948	Fukui, Japan	3.3	40	a,e	30	40	g	S	I
Aug. 19, 1961	Kita-Mino, Japan	0.9	51	a	12	51	f,g	S	I
March 26, 1963	Wakasa Bay, Japan	0.33	49	a	20	49	g	S	I
May 7, 1964	Oga Pen., Japan	4.6	50	b	50	50	g	R	I
June 16, 1964	Niigata, Japan	32	48	b	80	48	g	R	I
Jan 14, 1968	Izu-Oshima, Japan	1.1	55	a,b	17	55	g	S	I
Sept. 9, 1969	Gifu, Japan	0.35	53	c,e	18	53	f,g	S	I
Oct. 16, 1970	Akita, Japan	0.22	55	c,e	14	54	g	R	I
May 8, 1974	Izu-Hanto-oki, Japan	0.6	42	e	18	42	g	S	I
			Elsewhere						
Dec. 26, 1939	Erincan, Turkey	45	59	d	350	30	h	S	P
Dec. 20, 1942	Erba Niksar, Turkey	2.5	59	d	50	30	h	S	P
Feb. 1, 1944	Gerede-Bolu, Turkey	24	59	d	190	30	h	S	P
March 18, 1953	Gonen-Yenice, Turkey	7.3	59	d	58	30	h	S	P
Dec. 4, 1957	Gobi-Altai, Mongolia	130-180	31,32	b	270-300	31,32	g	S	I
July 22, 1967	Mudurnu, Turkey	3.6-8.8	11,59	a,d	80	30	h	S	P
Aug. 31, 1968	Dasht e Bayaz, Iran	6.7	11	a	80-110	34	h,g	S	I
Oct. 16, 1974	Gibbs Fracture Zone	4.5	62	b	75	62	g	S	P
Feb. 4, 1976	Guatemala	26	27	b	240-300	27,28	g,h	S	P
July 27, 1976	Tangshan, China	18	33	b	140	33	g	S	I

* Reference to published estimates of seismic moment and fault rupture length: 1, *Sieh* [1978*b*]; 2, *Tsai and Aki* [1969]; 3, *Brown and Vedder* [1967]; 4, *Doser* (unpublished manuscript, 1986); 5, *Doser and Kanamori* [1986]; 6, *Bakun and McEvilly* [1984]; 7, *Wilson* [1936]; 8, *Brune and Allen* [1967]; 9, *Trifunac* [1972]; 10, *Stein and Thatcher* [1981]; 11, *Hanks and Wyss* [1972]; 12, *Burdick and Mellman* [1976]; 13, *Clark* [1972]; 14, *Hamilton* [1972]; 15, *Sharp et al.* [1982]; 16, *Hanks and Kanamori* [1979]; 17, *Page* [1935]; 18, *Slemmons* [1957]; 19, *Tocher* [1956]; 20, *Witkind* [1964]; 21, *Sharp* [1975]; 22, *Allen et al.* [1975]; 23, *Wyss* [1971]; 24, *Canitez and Toksoz* [1972]; 25, *Sykes* [1971]; 26, *Plafker et al.* [1978]; 27, *Kanamori and Stewart* [1978]; 28, *Bucknam et al., 1978; 29, Kanamori and Stewart* [1976]; 30, *Ambraseys* [1970]; 31, *Okal* [1976]; 32, *Chen and Molnar* [1977]; 33, *Butler et al.* [*1979*]; *34, Ambraseys and Tchalenko* [1969]; 35, *Crone et al.* [1985]; 36, *Matsuda* [1974]; 37, *Mikumo and Ando* [1976]; 38, *Matsuda et al.* [1980]; 39, *Thatcher et al.* [1980]; 40, *Kanamori* [1973]; 41, *Richins et al.* [1985]; 42, *Abe* [1978]; 43, *Matsuda* [1972]; 44, *Abe* [1975*a*]; 45, *Takeo et al.* [1979]; 46, *Urhammer et al.* [1983]; 47, *Ando* [1974]; 48, *Abe* [1975*b*]; 49, *Abe* [1974]; 50, *Fukao and Furumoto* [1975]; 51, *Kawasaki* [1975]; 52, *Kanamori and Regan* [1982]; 53, *Mikumo* [1973]; 54, *Mikumo* [1974]; 55, *Shimazaki and Somerville* [1979]; 56, *Doser and Smith* [1985]; 57, *Tanimoto and Kanamori* [1986]; 58, *Doser* [1985]; 59, *Sykes and Quittmeyer* [1981]; 60, *Kanamori* [1983]; 61, *Herd and McMaster* [1982]; 62, *Thatcher* [1975].

placement is shown in Plate 1. The location of onshore faults is based primarily on the work of *Jennings* [1975] and *Clark et al.* [1984]. Also shown in Plate 1 is the distribution of major offshore faults which are known from marine seismic reflection or drillhole studies to reach to or near the seafloor and hence may also be characterized by Quaternary displacement. The offshore fault distribution is adapted from several separate studies. Offshore faults south of Palos Verdes are reported by *Legg and Kennedy* [1979] and *Greene et al.* [1979], offshore Santa Monica by *Junger and Wagner* [1977], north of Ventura to Point Arguello by *Yerkes et al.* [1981], and northward of Point Arguello to Cape Mendocino by *Field et al.* [1980].

Fault Slip Rates

Recent years have witnessed an increased effort toward the recognition of Quaternary faults and the collection and use of fault slip rate data. *Anderson* [1979] compiled slip rates for a study of seismic risk in southern California. *Bird and Rosenstock* [1984] made a similar compilation to construct a kinematic model of deformation in southern California. The most comprehensive collection of slip rate information currently available is the result of an effort by geologists at the U. S. Geological Survey [*Clark et al.*, 1984]. It is these three works that provide the primary data base for this study. Faults in California for which some information on slip rate has been inferred from either Quaternary displacements or offsets of older Pliocene to Miocene age units are marked in Plate 1. Plate 1 shows that estimates of slip rate exist for most of the major onshore fault zones, whereas virtually no slip rate information exists for the offshore faults. Rates of slip determined from older Pliocene and Miocene deposits may be less representative of present rates of seismic activity than are rates assessed from the offset of younger deposits. In this work, slip rates derived from offset Pliocene and Miocene units are used only when rates determined from younger deposits are not available and, initially, attention is limited to earthquakes and faulting onshore California.

Slip rate estimates are generally coupled with large uncertainties. For that reason, slip rates of individual faults are most often reported as a range of values which bracket the investigator's best estimate. Frequently, only a maximum or minimum value is reported. Uncertainties inherent to slip rate estimates are detailed by *Clark et al.* [1986], are significant, and should be considered when interpreting the maps resulting from this analysis. The range of slip rates reported for onshore faults in Plate 1, references to the data, and the value of slip rate used for each fault in calculations are provided in Table A1 of the appendix. Faults in Table A1 for which no slip rate data are available are assigned a very low slip rate of 0.01 mm/yr.

ANALYSIS

Fault Length and Earthquake Size

The seismic moment rate $\dot{M}_o$ characterizes the average rate of seismic activity on a fault. The release of seismic moment on a fault occurs, however, in the discrete form of earthquakes. Hence seismic hazard analysis requires an estimate of both the expected size and the occurrence rate of earthquakes on faults in a region of interest. Empirical relations between earthquake magnitude M and rupture length l derived from recent earthquakes are commonly the basis for estimating the expected size of earthquakes on mapped faults [e.g., *Albee and Smith*, 1966; *Slemmons*, 1977; *Bonilla et al.*, 1984], with the inference that the size of an earthquake on a fault will be proportional to the mapped fault length. A similar approach is taken here, except the measure of seismic moment is substituted for earthquake magnitude. Seismic source parameters for earthquakes from California and other regions of similar tectonic style are presented in Table 2. The seismic moment M_o versus rupture length l of each event is plotted in Figure 2. The solid symbols in Figure 2 indicate events that occurred on major plate bounding faults generally characterized by slip rates of about a centimeter per year or more. The open symbols represent earthquakes that occurred on faults with lesser slip rates. In spite of significant scatter, the two groups form distinct populations. Empirically, the separation indicates that for two faults of similar length, earthquakes rupturing the more slowly slipping fault will produce a greater amount of slip and hence a greater seismic moment. The physical consequences of this separation are discussed by *Scholz et al.* [1986] and *Kanamori and Allen* [1986]. For present purposes, lines of the form $\log M_o = A + B \times \log l$ are fit through the two groups of data and shall provide the basis for estimating the expected earthquake size from mapped fault length (Figure 2). For the sake of completeness, the earthquakes in Table 2 are also divided according to the earthquake mechanism. It is found that strike-slip, reverse, and normal faulting events do not form distinct populations when M_o is plotted versus rupture length (Figure 2).

The estimation of expected earthquake size from mapped fault length is simple in concept but difficult in practice. Earthquakes in California commonly do not rupture along the entire extent of the faults on which they occur. Thus there arises the critical problem of identifying the segments of faults that will be the source of future earthquakes. A growing body of empirical evidence indicates that the end points of earthquake ruptures are controlled by structural or physical discontinuities along fault strike. This is clearly demonstrated on the San Andreas fault by the rupture characteristics of the 1906 and 1857 earthquakes. Each of

† Moment estimated with a, long-period body waves; b, long-period surface waves; c, short-period body waves; d, rupture parameters determined from geologic observations; or e, rupture parameters determined from geodetic observations.

‡ Rupture length inferred from f, geodetic data; g, aftershock distribution; h, extent of surface offsets; or i, tsunamai data

§ Earthquake displacment predominantly S, strike-slip; N, Normal; or R, reverse. Earthquake occurred on P, plate boundary or I, intraplate or plate boundary related fault inferred to have long-term slip rate greater than or less than about 1 cm/yr, respectively.

Estimated here from rupture parameters summarized in respective references.

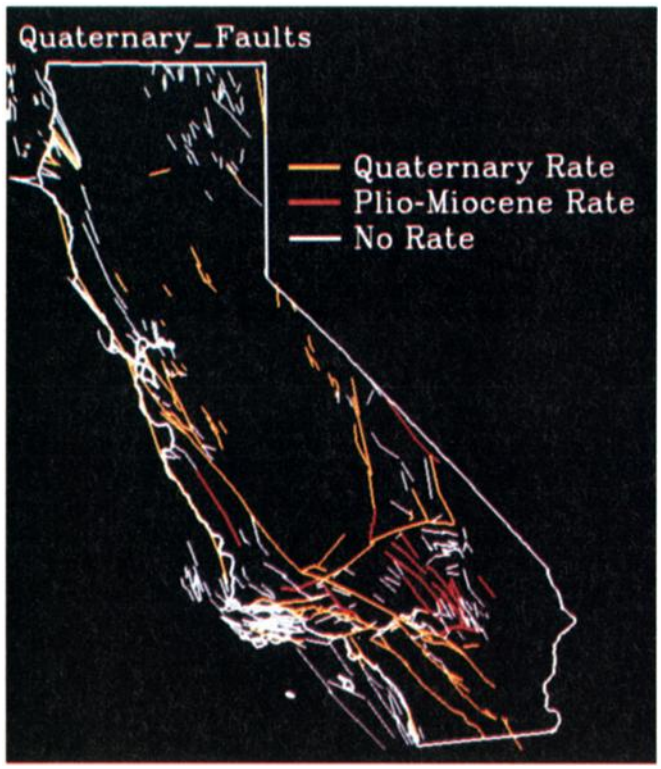

Plate 1. Distribution of faults in and offshore California that displace Quaternary rocks (Table A1) and near seafloor marine deposits, respectively. Fault slip rate estimates assessed from Quaternary offsets and displaced Pliocene to Miocene age rocks have been reported for sites along the faults marked in yellow and orange, respectively. Distribution of onshore faults adapted primarily from *Jennings* [1975] and *Clark et al.* [1984]. References to distribution of offshore faults provided in text.

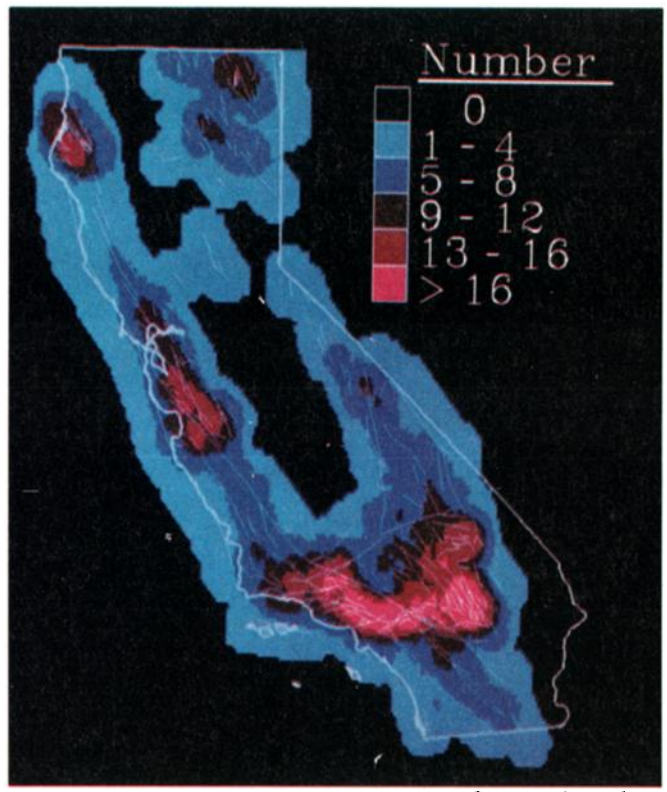

Plate 2. Contour map shows the number of mapped, onshore Quaternary faults capable of producing $\geqslant 0.1g$ peak horizontal ground accelerations at any locality in California.

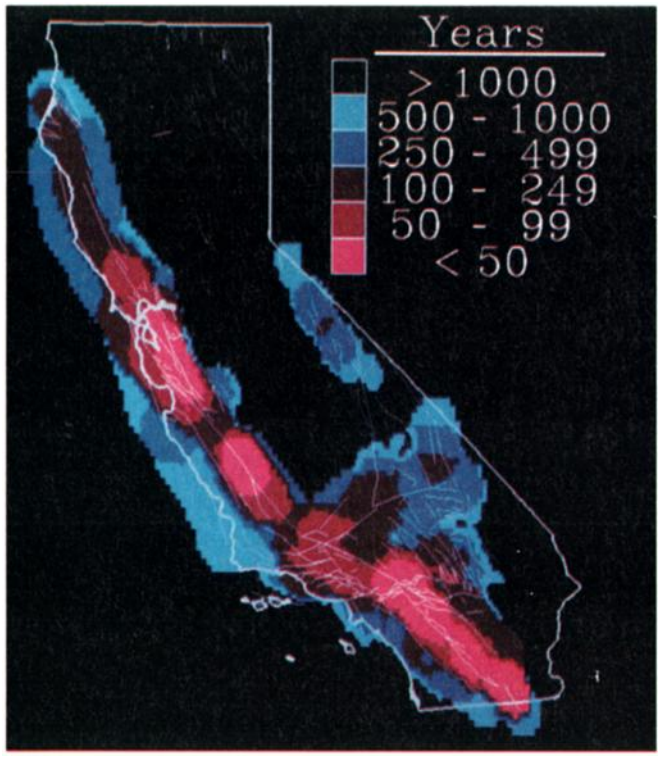

Plate 3*a*. Contour map shows the average expected return time of $\geqslant 0.1g$ peak horizontal ground acceleration expected due to the repeated occurrence of earthquakes on mapped Quaternary faults onshore California.

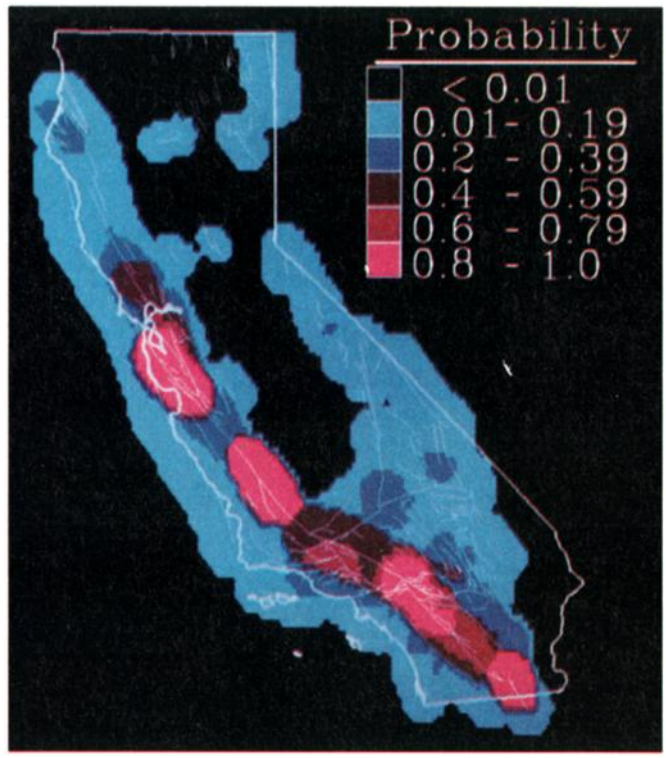

Plate 3*b*. Contour map shows estimated probability that onshore Quaternary faults mapped in California will produce peak horizontal ground accelerations of $\geqslant 0.1g$ during the next 50 years.

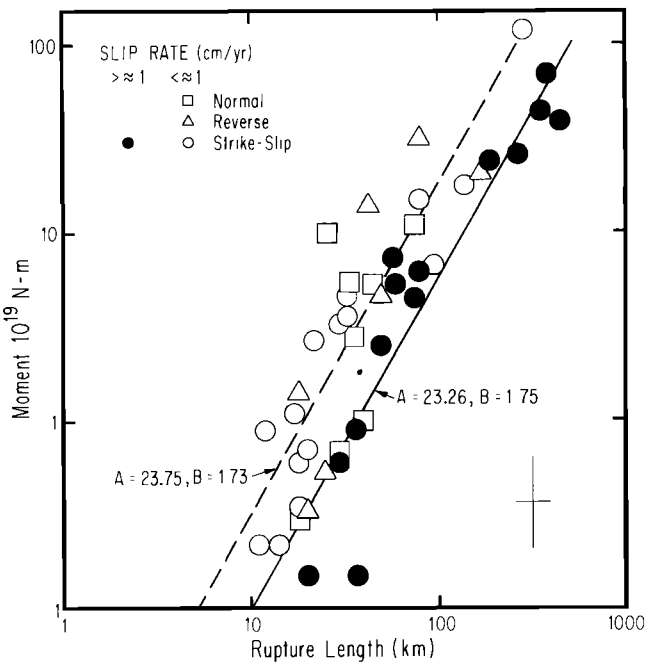

Fig. 2. Seismic moment M_o versus rupture length l for earthquakes listed in Table 2. Solid symbols indicate earthquakes on major plate boundary faults generally characterized to have slip rates of 1 cm/yr or greater. Earthquakes on faults with lesser slip rates are shown by open symbols. Lines of form $\log M_o = A + B \times \log l$ are fit through the solid and open symbols, respectively. Squares, triangles, and circles correspond to normal, reverse, and strike-slip type earthquakes, respectively. The vertical and horizontal bars of the cross in lower right corner of plot correspond to a factor of 3 in M_o and 50% in l, respectively.

the events ruptured different segments of the San Andreas. The 1906 and 1857 rupture zones are separated by the creeping section of fault extending from San Juan Bautista to Parkfield. The southern margin of the 1857 rupture is a site marking the complex juncture of several different fault zones (i.e., the Cucamonga, San Jacinto, San Andreas, Cleghorn fault zones). The northern end of the 1906 rupture is at the junction of the San Andreas with the Mendocino escarpment. It seems likely that these points of tectonic complexity will mark the end of fault ruptures along the San Andreas in the future. Another example is the Sierra Madre fault system that produced the 1971 San Fernando earthquake rupture. The 1971 event ruptured only a 20-km segment of this system. Detailed examination of the Sierra Madre fault zone has shown that the freshness of scarps or recency of faulting varies along different segments of the zone [*Crook et al.*, 1986]. In addition, investigators have noted that the Sierra Madre fault zone appears to be segmented into a series of arcuate salients convex toward the San Gabriel Valley [e.g., *Procter et al.*, 1972]. These observations have led investigators to argue that segments of the San Gabriel range, each 15-25 km in length, behave as independent seismic entities [*Crook et al.*, 1986]. Similarly, *Wallace and Whitney* [1984] studied the distribution and recency of range bounding fault scarps in central Nevada and suggested that individual mountain blocks may at times behave independently and that block boundaries may determine the extent of future surface faulting. Examination of the White Wolf fault, which produced the 1952 Kern County earthquake, shows that the fault rupture is overridden on the southwest by the Pleito thrust fault and terminates on the northeast at an abrupt northward bend in the fault zone. En echelon steps along strike-slip faults have been observed to be controlling factors in the rupture length of the 1966 Parkfield [*Lindh and Boore*, 1981], 1968 Borrego Mountain [*Clark*, 1972], 1979 Coyote Lake [*Reasenberg and Ellsworth*, 1982], and 1984 Morgan Hill [*Bakun et al.*, 1984] earthquakes. Physical explanations of the controlling nature of en echelon steps on the fault rupture process have been suggested in the work of *Segall and Pollard* [1980] and *Sibson* [1986]. The observations and arguments given above are the basis in this study for assuming that certain faults in California are segmented and that the segments will produce earthquakes independently. The observations and decisions used to characterize the segmented nature of each of the major fault zones in California are discussed further in the appendix. Some of the decisions regarding fault segmentation are largely subjective. Nonetheless, the decisions used here are an estimate of the future behavior of faults based on our current understanding of geology and the faulting process.

Occurrence Rate of Earthquakes

Estimates of the occurrence rate of earthquakes on faults, from geologic data of fault length and fault slip rate, require the assumption of a fault model. Seismological literature includes two extremes of thought concerning the mechanical behavior of faults. A number of investigators [e.g., *Nur*, 1978; *Hanks*, 1979; *Andrews*, 1980; *von Seggern*, 1980] have assumed that seismicity particular to a single fault or fault segment satisfies the relation $\log N = a - bM$, where N is the number of events with magnitude greater than or equal to M, and a and b are empirical constants [e.g., *Ishimoto and Iida*, 1939; *Gutenberg and Richter*, 1944]. A consequence of this assumption is that during the repeat time T of one maximum magnitude earthquake on a fault, some fault slip is also accommodated by the occurrence of smaller though potentially hazardous earthquakes. A separate view of fault behavior, initially implied in the work of geologists [e.g., *Allen*, 1968; *Wallace*, 1970; *Matsuda*, 1977], is that faults or fault segments produce earthquakes of a characteristic size that is a function of fault length and tectonic setting and that these events together with their foreshocks and aftershocks account for all seismic slip on a fault. For the sake of consistency with earlier papers [*Wesnousky et al.*, 1983, 1984], this latter behavior is referred to here as the maximum magnitude earthquake model.

The assumption of which model best depicts fault behavior is of both scientific and practical significance and has been discussed at length by *Wesnousky et al.* [1983]. A growing body of seismological and geological observations points to the maximum magnitude earthquake model as the more accurate picture of the mechanical behavior of individual faults. *Allen* [1968], for example, examined the seismic character of the San Andreas and noted that the segments of the fault which ruptured in historical time are essentially devoid of seismicity down as far as the microearthquake level. He suggested that this behavior is typical of the past and future behavior of these fault segments. A number of investigations along convergent plate

margins report evidence to suggest that plate boundaries generally rupture along specific segments and that rupture of the segments occurs cyclically [e.g., *Kelleher*, 1970, 1972; *Ando*, 1975; *Sykes and Quittmeyer*, 1981]. Earthquake frequency statistics, where compiled for various segments of the world plate margins, show that the earthquake frequency distribution along each segment is dominated by the repeated occurrence of main shocks and the accompanying aftershocks [*Utsu*, 1971; *Singh et al.*, 1981, 1983; *Lahr and Stephens*, 1982; *Davison and Scholz*, 1985]. *Bath* [1981] interpreted earthquake frequency statistics observed for regions of Europe in a similar manner. Site-specific geologic investigations are also consistent with the maximum magnitude model. *Sieh and Jahns* [1984] interpreted displaced geomorphic features along segments of the San Andreas fault to indicate the repeated occurrence of similar sized events. *Schwartz and Coppersmith* [1984] arrived at a similar conclusion during their study of the Wasatch range front in Utah. They interpreted that future earthquake ruptures along the Wasatch will be limited to specific segments of the range front, based on the existence of structural discontinuities and differing values of repeat time that they estimated from trench studies at sites along strike of the frontal fault zone. Trenching [*Schwartz and Crone*, 1985] and scarp morphology [*Salyards*, 1985] studies along the recent 1984 Borah Peak earthquake fault have also been used to suggest that that fault has previously ruptured in a similar fashion during late Quaternary time. In Japan, *Wesnousky et al.* [1983] observed that the earthquake frequency distribution predicted from geologic data describing the slip rates of Quaternary faults, and with the assumption that faults behave according to a maximum magnitude model, matched well with the distribution derived from a 400-year record of seismicity. In this work then it is assumed that the mechanics of faulting is described by the maximum magnitude model.

The maximum magnitude model of fault behavior may be cast in terms of seismic moment. The average expected repeat time of earthquakes on a fault that is described by the maximum magnitude model can be approximated to equal

$$T = M_o^e / \dot{M}_o^g \qquad (1)$$

years, where the seismic moment M_o^e of the expected event on the fault is proportional to the fault length and the geologically assessed moment rate $\dot{M}_o^g$ of the fault is a function of the fault slip rate. Estimation of average earthquake repeat times in this manner is conceptually consistent with the well-known and supported concept of elastic rebound [e.g., *Imamura*, 1930; *Fitch and Scholz*, 1971; *Kanamori*, 1973; *Shimazaki*, 1974; *Thatcher*, 1975; *Scholz and Kato*, 1978]. Hence in equation (1), M_o^e is a measure of the average strain drop during an earthquake and $\dot{M}_o^g$ is a function of the strain accumulation rate, and it is assumed that the two parameters remain constant for each fault through time.

Predicted Versus Observed Seismicity

The size distribution of earthquakes in a region generally obeys the relationship $\log N = a - c \times \log M_o$, where N is the number of events with seismic moment $\geq M_o$ and a and c are empirical constants. A correct analysis of regional seismic hazard must incorporate this observation. The expected moment-frequency distribution of earthquakes resulting from slip on all mapped faults in California may be computed from the information of fault length and slip rate compiled in Table A1. The seismic moment M_o^e expected for an earthquake rupturing the entire length of each fault or fault segment in Table A1 is considered a function of fault length and is computed with the empirical relations in Figure 2. The moment rate $\dot{M}_o^g = \mu l w \dot{u}$ of each fault is a function of the mapped fault length l and the respective fault slip rate $\dot{u}$ and is determined assuming that the width w of each fault is 15 km and that the shear modulus μ of the crust is equal to 3×10^{11} *dyn/cm*^{2}. Insertion of the estimates of M_o^e and $\dot{M}_o^g$ into equation (1) defines the average repeat time T of M_o^e earthquakes for each of the mapped faults. The cumulative rate of seismicity, computed in this manner, resulting from slip on all onshore faults listed in Table A1 is compared in Figure 3 to the historical rate of seismicity averaged over the last 150 years. The observed and predicted earthquake frequency distributions exhibit a similar shape and indicate earthquake occurrence rates that generally agree to within a factor of about 2. Speculation as to the cause of the differences in the predicted versus observed curves is not warranted, since the differences are small with respect to the uncertainties associated with this analysis. The cumulative seismic moment rate $\sum \dot{M}_o$ predicted from the geologic data (2.1×10^{19} N -m/yr) is also found to differ by less than a factor of 2 from the rate computed from the historical record (1.6×10^{19} N -m/yr). The similarity between the observed and

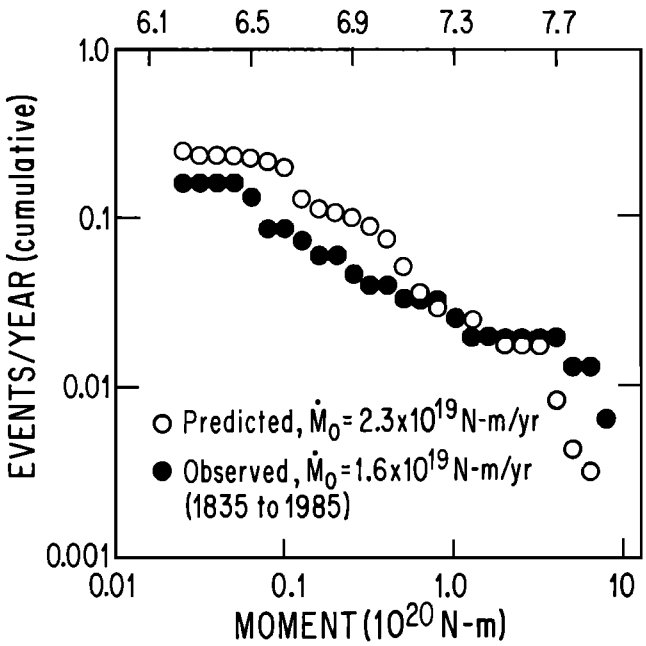

Fig. 3. Earthquake frequency distribution expected from slip on all mapped Quaternary faults onshore California (open symbols) compared to the distribution (solid circles) computed from the 150-year historical record of seismicity in Table 1. Magnitudes of events in Table 1 are converted to seismic moment with the empirical relation $\log M_o = 1.5\ M + 16.1$ [*Hanks and Kanamori*, 1979], except for those events where direct measurements of M_o are available (Table 2).

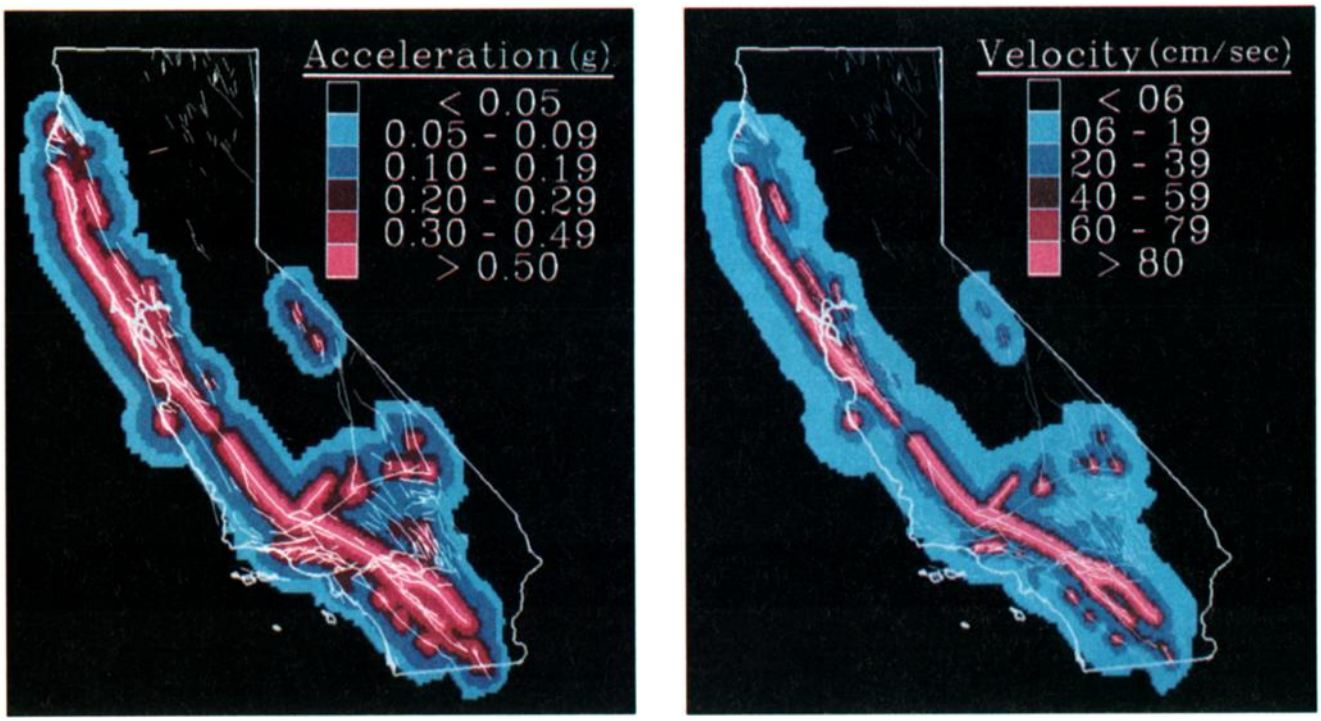

Plate 4. Contour maps show the (*a*) peak horizontal ground acceleration and the (*b*) peak horizontal ground velocity at 1-second period expected to be exceeded on rock sites at the 10% probability level during a 50-year period of time due to earthquakes on Quaternary faults mapped onshore of California.

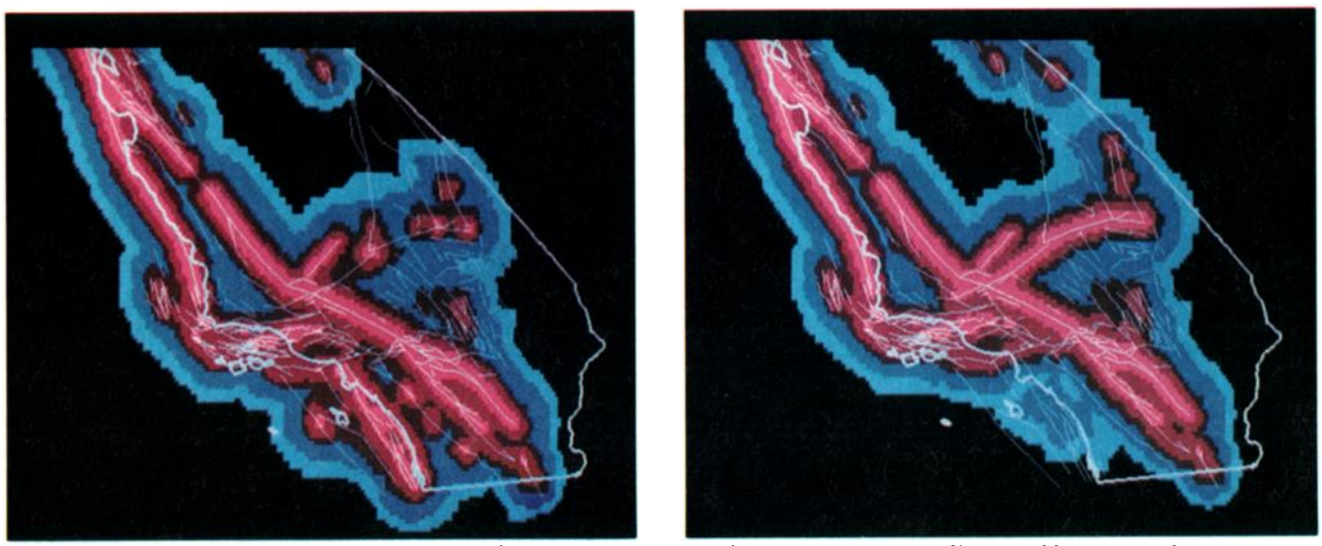

Plate 5. Contour maps show the peak horizontal ground acceleration expected at the 10% probability level during a 50-year period in southern California assuming that (*a*), in addition to slip rates reported for onshore faults, mapped offshore faults further accommodate ~2 cm/yr of slip and (*b*) total relative plate motion between the Pacific plate and North America is 5.6 cm/yr and primarily accommodated by onshore faults according to the model of *Bird and Rosenstock* [1984]. See Plate 4*a* for color key.

predicted values of $\sum \dot{M}_o$ as well as the earthquake frequency distributions computed with the two data sets is encouraging, for it is in accord with the hypothesis that current knowledge of Quaternary fault offsets and fault mechanics provides sufficient information to predict both the average spatial and size distribution of earthquakes in California through time.

Construction of Seismic Hazard Maps

The data reviewed thus far are consistent with the idea that in areas characterized by shallow seismicity and surface faulting, rates of seismicity derived from fault slip rate data are representative of present-day rates. Evidence also points to a simple model of fault behavior, whereby the average repeat time of earthquakes on a fault can be approximated to equal $T = M_o^e/\dot{M}_o^s$ years (equation (1)). Thus a foundation is set upon which we may begin to base estimates of long-term seismic hazard. Specifically, with empirical relations between seismic moment, source to site distance, and strong ground motions [*Joyner and Fumal*, 1985], the equation (1) and data describing the length and average slip rate of faults in California are used to compute the average expected frequency f of occurrence of seismic shaking over a range of different strengths. The value f, for a given level of strong ground motion at site location j, is defined by the relation

$$f_j = \sum_{i=1}^{N} \frac{1}{T_i} \tag{2}$$

where T_i are the average repeat times of the N faults that are capable of producing a specific strength of ground motion at site location j. The probability of occurrence of a given ground motion is a function of the frequency of occurrence of the specified ground motion and the time period for which one is concerned. More concisely, the probability that the occurrence time S of a certain strength of strong ground motion will occur during the period of time from t_1 to t_2 conditional to t_1 years having elapsed since the last occurrence of similar ground shaking is generally expressed as

$$P(t_1 \leqslant S < t_2 \mid S > t_1) = \frac{\int_{t_1}^{t_2} g(t)\,dt}{\int_{t}^{\infty} g(t)\,dt} \tag{3}$$

where $g(t)$ is an assumed probability density function. It is initially assumed in this work that the occurrence of specific levels of ground motion at a site is a Poisson process and hence $g(t)$ is appropriately defined by the exponential function fe^{-ft}, where f is the frequency of occurrence of the ground motion of concern and is defined by equation (2). For this case,

$$P(t_1 \leqslant S < t_2 \mid S > t_1) = 1 - e^{-f(t_2 - t_1)} \tag{4}$$

The repeated use of equations (2) and (4) for different levels of strong motion at a gridwork of sites is the basis here for constructing contour maps that depict the average return period of $\geqslant 0.1g$ peak accelerations, and the horizontal components of peak acceleration, peak velocity, and the peak pseudovelocity response (at 1-period and 5% damping) expected to occur at level of 0.1 probability during a period of 50 years.

Maps Depicting Seismic Hazard Due to Onshore Faults

The suite of maps in Plates 2-4 and Figure 4 help provide a synoptic view of our current understanding of seismic hazard in California. A detailed assessment of the maps requires a comprehensive understanding of the geological and seismological data used in compiling Table A1. Discussion is limited here to a description of the major features that characterize the maps. Specific faults and geographic regions are discussed in the appendix.

Plate 2 portrays the number of mapped faults capable of producing ground shaking at levels of peak horizontal acceleration $\geqslant 0.1$ gravity at any locality in California. A peak horizontal acceleration of $0.1g$ is the level at which older structures and some modern structures not engineered to withstand earthquake shaking are susceptible to significant damage. The contours in Plate 2 thus provide a picture of the relative density of faults that constitute a source of seismic hazard. The greatest concentrations of faulting are within the Transverse ranges of southern California, the southern Mojave, and adjacent to the juncture of the San Andreas and Calaveras fault systems in northern California. Sites in these regions are commonly susceptible to ground accelerations $\geqslant 0.1g$ originating from a dozen or more faults. Significant concentrations of Quaternary faults are also evident in northern California, along the coast north of Cape Mendocino and inland within the Modoc Plateau. The relative concentration of Quaternary faults, however, provides only an incomplete measure of seismic hazard. The picture of seismic hazard is altered significantly when the geologic rate of slip on each fault is further taken into account.

A second map, shown as Plate 3*a*, depicts the average expected return time of peak horizontal accelerations exceeding $0.1g$. The expected return period of $\geqslant 0.1g$ peak horizontal ground accelerations is less than 50 years in several regions of California (Plate 3*a*). The shortest values are generally associated with the San Andreas, Calaveras, Hayward, and San Jacinto fault systems. This is reasonable since it is these faults that accommodate much of the motion along the California plate boundary and, accordingly, show slip rates ranging from many millimeters to $\geqslant 1$ cm/yr. The Ventura Basin is similarly characterized by relatively short return periods, a direct consequence of the relatively high slip rates associated with faults in that area. The regions marked by short return periods are areas of relatively higher seismic hazard. Caution should be exercised, however, in concluding that hazard is low in all the regions characterized by long return periods. Long return periods predicted for several regions are possibly the consequence of insufficient geologic data, as discussed later in this section.

The most comprehensive characterization of seismic hazard is provided by the maps in Plate 4 and Figure 4. The peak horizontal acceleration expected to occur at the 10% probability level during a 50-year period is contoured in Plate 4*a*. Maps in Plate 4*b* and Figure 4 are identical to Plate 4*a*, except that the parameter contoured is peak velo-

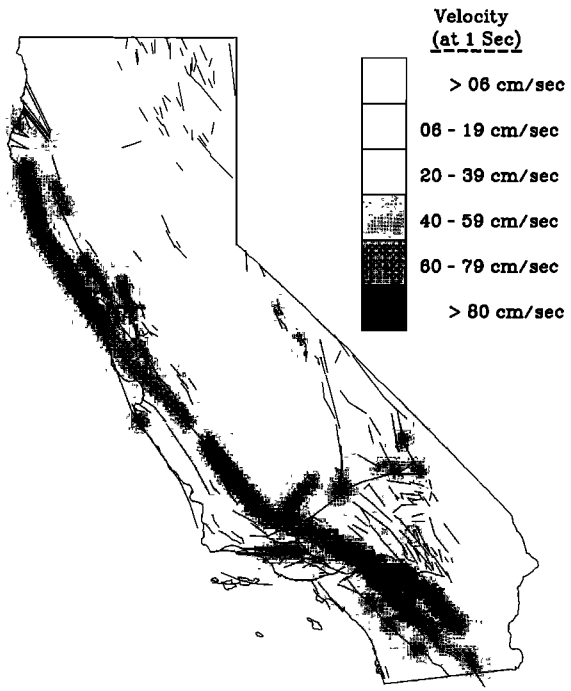

Fig. 4. Peak horizontal pseudovelocity response at 1-second period expected to be exceeded on rock sites at the 10% probability level during a 50-year period of time due to earthquakes on Quaternary faults mapped onshore of California.

city and the pseudovelocity response registered at 1-period with a 5% damping coefficient, respectively. Plate 4, unlike Plates 2 and 3*a*, simultaneously display information bearing upon both the expected size and the frequency of earthquake-induced strong ground motions. The strong ground motions contoured in Plate 4 are characterized by an average return period of $\leqslant 475$ years, as may be seen by insertion of the appropriate values of $\Delta t = t_2 - t_1$ (50 years) and probability (0.1) into equation (4). The contours of higher acceleration or velocity in these maps may, for convenience of discussion, be considered to enclose regions posing the greater seismic hazard. The maps in Plate 4 show the San Andreas fault to be a principal contributor to high levels of seismic hazard in California. Contours of strong ground motion along strike of the San Andreas are uniformly high, except along a small segment in central California where slip occurs primarily by aseismic creep. Several other regions are also characterized by levels of seismic hazard that approach levels predicted adjacent to the San Andreas. Relatively rapid rates of slip along the Calaveras, Hayward, and associated lesser faults are interpreted to indicate significant levels of hazard in the regions adjacent to San Francisco Bay. The likely transfer of slip northward from the Hayward to the Healdsberg, Rogers Creek, and Maacama fault zones implies a zone of high seismic hazard extending north of San Francisco Bay as well. To the south, reported rates of slip across the Pleito, White Wolf, and Garlock faults (Figure A6) indicate the northern boundary of the Mojave Desert as a zone of relatively high hazard. The southern Mojave is mapped as a region of comparatively high hazard due to a number of faults with moderate slip rates. Major sources of hazard within the Peninsular ranges are the San Jacinto and Elsinore fault zones. Within the western Transverse Range, slip rate information points to high hazard within the Ventura Basin region.

Attention so far has centered upon the regions characterized by high levels of seismic hazard. Examination of the parameters that lead to low levels of seismic hazard being predicted for various regions is equally important when interpreting the hazard maps. Plate 2, for example, indicates that the eastern Mojave, Great Valley, and Central Coast near Point Arguello are characterized by few or no mapped Quaternary faults. The low levels of strong ground motion predicted for these regions is contingent upon the detail of geologic mapping. The Modoc Plateau, unlike the Great Valley and eastern Mojave, is the site of numerous Quaternary faults (e.g., Plate 2). Plate 1 shows, however, that little data regarding fault slip rate is available in the area. The small values of strong motion predicted within the Modoc Plateau (Plate 4 and Figure 4) may then not be real but rather a consequence of assigning very low slip rates to those faults which have not been the subject of detailed geologic study. The same is likely true for other regions of California that are characterized by Quaternary faults but for which slip rates are unknown. Hence other regions of relatively high seismic hazard may remain unrecognized. This observation, however, should be tempered by the realization that geologists have generally aimed their efforts toward those faults recognized to be most active.

Potential Hazard Due to Offshore Faults

The hazard maps constructed thus far consider only faults onshore and within the political boundaries of California. A consequence is that the predicted levels of hazard are underestimated along the boundaries of California where active faults lie outside but near the border. The problem is most acute along coastal California where population centers are greatest, historical records describe the occurrence of several moderate to large offshore earthquakes (Table 3), and both geological and geophysical investigations have been the basis for suggesting rapid rates of slip and high seismic potential on offshore fault structures [e.g. *Anderson*, 1979; *Sieh and Jahns*, 1984; *Minster and Jordan*, 1984; *Weldon and Humphreys*, 1986, *Heaton and Kanamori*, 1984]. Observed rates of seismicity offshore and north of Cape Mendocino are, for example, comparable to rates observed onshore in southern California [e.g., *Toppozada et al.*, 1981; *Toppozada and Parke*, 1982; *Rogers*, 1980]. Seismicity offshore of the coast north of Cape Men-

TABLE 3. Earthquakes Offshore California

Date	Location	Magnitude*	References†
Dec. 12, 1812	Santa Barbara	7.1	7
April 15, 1898	Point Arena	6.4	7
June 29, 1925	Santa Barbara	6.3	9
Nov. 4, 1927	Santa Barbara	7.5	9
June 6, 1932	Humboldt	6.4	9
Oct. 3, 1941	Humboldt	6.4	9
Nov. 8, 1980	Humboldt	6.9	18

* See Table 1.
† See Table 1.

docino is generally attributed to the relative motion taking place between the Gorda plate and North America. Interpretations of seafloor magnetic lineations show that relative motion between North America and the Gorda plate is between 3 and 5 mm/yr [e.g. *Minster and Jordan*, 1978; *Riddihough*, 1980]. Observed distortion of magnetic lineations and the distributed nature of seismicity within the Gorda plate indicate that a significant portion of the relative motion may be taking place as internal deformation of the Gorda plate [*Silver*, 1971]. Interpretations of geophysical data with the assumption that the Gorda plate is rigid suggest that relative motion is being accommodated by either strike-slip motion [*Riddihough*, 1980] or thrusting of the Gorda plate beneath North America [*Minster and Jordan*, 1978]. The potential of large thrust earthquakes occurring along the north coast is discussed in detail by *Heaton and Kanamori* [1984]. It is beyond the scope of this work to examine the effect of assuming the different interpretations of plate deformation on predicted levels of hazard along the coast north of Cape Mendocino.

Faulting along the coast south of Cape Mendocino is generally interpreted to accommodate right-lateral transform motion between the Pacific plate and North America. *Minster and Jordan* [1978] estimated the plate velocity vector along the California plate margin to equal 5.6 cm/yr and to parallel the strike of the central San Andreas. Their rate is the result of a global inversion of plate velocity data and is averaged over the last few million years. It has since been recognized that the cumulative geologic slip rate across major mapped faults in most regions of the western United States is only 3-4 cm/yr, insufficient to account for the rate predicted by *Minster and Jordan* [1978] [*Sieh and Jahns*, 1984; *Minster and Jordan*, 1984; *Weldon and Humphreys*, 1986]. Either of two conclusions may be drawn from this discrepancy if it is accepted that the rates predicted by *Minster and Jordan* [1978] are representative of present-day plate rates. The first is that geologic data are now incomplete and that further onshore field investigations will reveal the missing 1-2 cm/yr of slip. The second possibility is that the missing slip is being accommodated by offshore fault structures. Data are insufficient to conclusively argue either of the interpretations. The two interpretations, however, predict markedly different distribution of seismic hazard along the southern coast of California. The maps in Plate 5 illustrate these differences.

Plate 5*a* is a contour map of the peak acceleration expected to occur in southern California at the 10% probability level during a 50-year period. The data and method used to construct Plate 5*a* are identical to those used earlier for Plate 4, except that 2 cm/yr of additional slip is assumed to be equally distributed across faults that have been identified with marine seismic reflection methods offshore of southern California (Plate 1). Specifically, south of about Santa Monica, 2 cm/yr of slip is distributed along the major fault structures west of and including the Palos Verdes, Newport-Inglewood, and Rose Canyon fault zones (Plate 1 and Figure A2). Deformation in the offshore region north of Santa Monica to about Point Arguello is characterized by folding and reverse faulting that indicate a northerly contraction of the crust [*Yeats*, 1983*a*; *Yerkes et al.*, 1981]. Slip rates are assigned to faults within this offshore province so that the cumulative slip rate along any north-south transect is 2 cm/yr. Between Point Arguello and San Francisco, the 2 cm/yr of slip is assumed to transfer to the San Gregorio-Hosgri fault system. The San Gregorio-Hosgri fault system is the only major offshore structure mapped along the stretch of coast between Point Arguello and San Francisco. No major fault systems are mapped offshore of the coast extending farther north from San Francisco to Cape Mendocino that may accommodate significant amounts of plate motion. The possibility exists that the proposed 2 cm/yr of slip is transferred onshore near San Francisco, but geodetic and geologic studies along the San Andreas near Point Reyes do not support such an idea [*Prescott and Yu*, 1986; *Hall et al.*, 1983]. Because of these enigmas, Plate 5*a* encompasses only the part of California south of San Francisco. The obvious result of assigning large values of slip to offshore faults is a significant increase in the expected level of strong ground motion for the entire coastal region reaching south of San Francisco to the Mexican border (Plate 5*a*).

A different picture of seismic hazard results when the constraint is imposed that 5.6 cm/yr of plate motion in southern California is taken up principally by mapped onshore faults (Plate 5*b*). *Bird and Rosenstock* [1984] divided southern California into a set of blocks bounded by mapped Quaternary faults. Within the limitations imposed by published fault slip rate data, they constructed a model of block movement that satisfies the restriction that the total plate motion across California is 5.6 cm/yr. The block model constructed [see *Bird and Rosenstock*, 1984, Figure 3] satisfies about 80% of the limits imposed by geological fault slip rate studies, though in many cases the assigned block movement rates are near the extreme limits rather than the preferred values of slip rate reported by geologists. The map in Plate 5*b* is constructed with the slip rates used by *Bird and Rosenstock* [1984] in their block model analysis. The Bird and Rosenstock model assigns 5.1 of the total 5.6 cm/yr of plate motion in California to occur onshore across the San Andreas and San Jacinto faults. The most obvious consequence, with respect to Plate 5*a*, is a decrease in the predicted values of strong ground motion along the south coast. Also, predicted levels of strong ground motion are higher along the San Gabriel range front and the Garlock fault zone. The large strong ground motions predicted along the San Gabriel range front result from the kinematic constraint of the block model that ~5 cm/yr of slip must be taken up by convergence within the Transverse ranges, a significant portion of which is assigned to the San Gabriel range front fault system. Such large (>1 cm/yr) slip rates imposed along the range front are, however, in conflict with the geologic study of *Crook et al.* [1986] which suggests that the repeat time of rupture along many individual segments of the range front is of the order of 5000 years.

The disparate patterns of seismic hazard depicted in Plate 5 underscore the importance of furthering our knowledge of both the distribution and rate of slip across Quaternary faults in California. The exercise of constructing the maps also points to a number of problems that should be the continued targets of geophysical and geological investigation during the immediate future. A fundamental problem is determining whether or not the 5.6 cm/yr of plate movement that *Minster and Jordan* [1978] found representative

of the last few million years is actually representative of present-day plate rates. Satellite-based methods of geodetic measurement may ultimately provide a corroboration of the 5.6 cm/yr rate of plate motion [e.g., *Christodoulidis et al.*, 1985]. Ground-based geological and geodetic studies are, however, also necessary to document the spatial distribution and total amount of fault displacement occurring across California. Little is known, for example, about the activity of the Rinconada, Elsinore, Healdsberg-Rogers Creek, and Maacama fault zones, all of which are major elements in the Quaternary structure of California (Figures A2, A9, and A10). Marine seismic reflection techniques have shown little potential for assessing slip rates of offshore faults. Certain major offshore faults mapped along the southern coastal borderland are, however, reported to trend onshore in Mexico to form the Agua Blanca fault zone [*Allen et al.*, 1960; *Legg and Kennedy*, 1979]. Investigations of that fault zone may provide clues to the slip rate of the corresponding offshore faults. *Weldon and Humphreys* [1986] suggest that the occurrence of 2 cm/yr of northward convergence within the Transverse Range kinematically limits the location of 2 cm/yr of transform motion to be located on faults within the southern coastal borderlands and near the coastline. Further study of possible variations in the convergence rate along the Ventura basin may provide clues to the distribution of slip rate between faults within southern coastal borderlands.

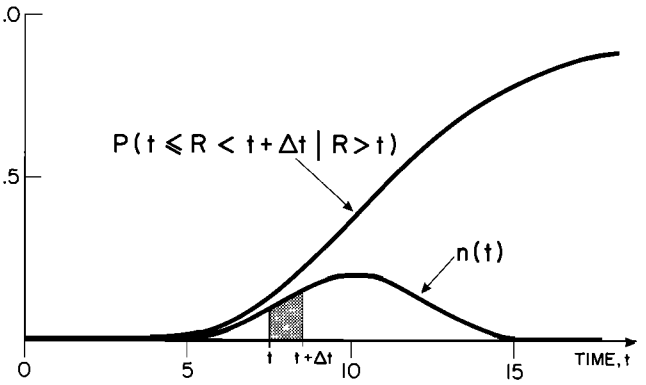

Fig. 5. The conditional probability that a fault will rupture at time R during the period t_1 to t_2 years conditional that t_1 years are past since the time of last rupture (R_l=0), for the specific case where R_p, σ, and t_2-t_1 are arbitrarily taken to equal 10, 2, and 1, respectively. The standard normal probability density function n(t) for the same set of parameters is also shown.

Seismic Hazard as a Function of Time

A major assumption underlying the hazard maps in Plates 4 and 5 and Figure 4 is that the occurrence of ground shaking at a given site is a Poisson process. As a result, the maps convey an estimate of hazard that remains constant through time and independent of the recent history of large earthquakes. This is evident when noting that the probabilities resulting from equation (4) and used to construct the maps are a function of the period considered (t_2-t_1) and not the beginning of the period (t_1) of interest. It is now generally accepted, however, that the seismic hazard, or probability of another large earthquake, on a specific fault, excluding possible aftershocks, is lowest during the period immediately following a major earthquake, the time when accumulated strain on a fault is minimal. Accordingly, seismic hazard should be an increasing function of time as strain accumulates along a fault. Added information regarding the times that faults have ruptured in the past may then, in certain regions, significantly modify the picture of seismic hazard as conveyed in Plates 4 and 5.

Only a small number of all the mapped faults in California have ruptured during the relatively short period of recorded history. A brief examination of how those earthquakes may affect present levels of seismic hazard is warranted. Toward that end, it is convenient to follow the method taken by *Wesnousky et al.* [1984] in their study of Japan and also adopted by *Lindh* [1983] and *Sykes and Nishenko* [1984] in their studies of the the San Andreas and San Jacinto fault systems. *Wesnousky et al.* [1984] defined the expected date R_p of rupture on a fault to equal R_l+RT, where R_l is the date of the last earthquake rupture and RT is the estimated time necessary to accumulate strain equal to that released in the previous earthquake. It was also assumed that the actual recurrence times distribute normally about predicted values of RT and hence estimates of R_p may be described with the normal probability density function

$$n(t) = \frac{1}{\sigma\sqrt{2\pi}} e^{-\frac{1}{2}\left(\frac{t-R_p^2}{\sigma^2}\right)} \tag{5}$$

where the standard deviation σ is assigned to represent the confidence given to a predicted value of R_p. The likelihood that the rupture time R of a fault will occur during the next $\Delta t=t_2-t_1$ years conditional to t_1 years having elapsed since R_l can then be expressed as the conditional probability

$$P(t_1 \leqslant R < t_2 \mid R > t_1) = \frac{\int_{t_1}^{t_2} n(t)\,dt}{\int_{t_1}^{\infty} n(t)\,dt} \tag{6}$$

The conditional probability (equation (6)) as function of time t_1 since R_l is schematically illustrated in Figure 5 for arbitrarily chosen values of R_p, Δt, and σ. Figure 5 reflects the concept that the probability of an earthquake on a fault in the time period following R_l is minimal and then increases as a function of time.

Large earthquakes that have ruptured mapped faults in California during historical time are listed in Table 4. Included in Table 4 are the date R_l and the estimate of RT for each fault. The estimates of RT are taken to equal the values of T for the respective faults in Table A1. The uncertainties associated with the estimates of RT are described in the appendix, though a rigorous treatment of potential errors is not a requisite for this exercise. Present purposes are served by assuming that the distribution of actual recurrence times on a given fault about the predicted value of RT is Gaussian and characterized by a standard deviation σ equal to 1/3 the predicted repeat time RT. Conditional (equation (6)) and Poisson (equation (4)) estimates of the probability that each fault will again rupture during the next 50 years are compared in Table 4. The assumption of a time-dependent or Poisson-type behavior results in differences between the predicted values of proba-

TABLE 4. Poisson Versus Conditional Estimates of Seismic Hazard: An Illustration

Fault	Earthquake R_I	Estimated Return Time,* years	Probability†	
			Poisson	Conditional
San Andreas (Carrizo Plain)	1857	345	0.1	<0.1
San Andreas (Hwy. 166 to Cajon Pass)	1857	170	0.3	0.4
San Andreas (Chalome to Hwy. 58)	1857	115	0.4	>0.9
Hayward	1868	556	<0.1	<0.1
Owens Valley	1872	3364	<0.1	<0.1
San Jacinto (Casa Loma segment)	1899	128	0.3	0.3
San Andreas (Los Altos to San Juan Bautista)	1906	95	0.4	0.8
San Andreas (Shelter Cove to Los Altos)	1906	300	0.1	<0.1
San Jacinto (Claremont segment)	1918	107	0.4	0.6
White Wolf	1952	300	0.2	<0.1
San Andreas (Slack Canyon to Cholame)	1966	22	0.9	>0.9
San Jacinto (Borrego Mountain)	1968	150	0.3	<0.1
San Fernando	1971	200	0.2	<0.1
Imperial	1979	700	0.8	>0.9
Calaveras (segment A - Coyote Lake)	1979	82	0.5	0.2
Calaveras (segment B - Morgan Hill)	1984	150	0.3	<0.1

* Return times RT are taken to equal values of T listed for respective faults in Table A1.

† Probability that earthquake will repeat during the next 50 years assuming Poisson (equation (4)) and conditional (equation (6)) modes of earthquake recurrence.

bility for many of the faults. The differences work to illustrate the potential benefit of including the time dependence of the earthquake cycle in hazard assessment.

The maps that display the value of strong ground motion expected at the 10% probability level during a 50-year period of time (e.g., Plate 4) are a convenient basis for initially examining Table 4. Information leading to an increase or decrease of the probability of given levels of ground motion to above or below 10% probability, respectively, will result in changes in the map contours. Assumption of a time-dependent, rather than Poisson, behavior results in drops in probability from above to below 10% for 6 of the fault segments in Table 4: The Carrizo Plain and Shelter Cove to Los Altos segments of the San Andreas (Figure A11) that ruptured in 1857 and 1906, respectively; the Borrego Mountain fault that broke in 1968; the segment of the Calaveras fault that ruptured in 1984; and the White Wolf and San Fernando faults that broke in 1952 and 1979, respectively. In no case does the reverse occur. Seismic hazard adjacent to these six fault segments may then be less than depicted in Plates 4 and Figure 4, if the respective estimates of RT and σ are accepted as representative of the faults. The decreases in probability realized by the use of the conditional probability function reflect an interpretation that the six fault segments are now in the early stages of their respective strain accumulation cycles. Conversely, the two segments of the San Andreas that extend from Los Altos to San Juan Bautista and Cholame to Hwy. 58 near the Carrizo Plain (Figure A11) are estimated to have average repeat times that are nearly equivalent to the time since the faults last ruptured. The conditional estimates reflect this observation by yielding probabilities that are markedly greater than the respective Poisson estimates.

A contour map of the estimated probability that mapped faults will produce $>0.1g$ ground accelerations during the next 50 years is displayed in Plate 3*b*. For construction of the map, equation (6) is used to compute the conditional probability of fault rupture for those faults in Table 4. The occurrence of shaking expected from the remaining faults (Table A1) is again taken to satisfy a Poisson distribution (equation (4)), and the probabilities are computed accordingly. Plate 3*b* demonstrates how the added knowledge of where in time faults reside with respect to the earthquake cycle may be incorporated into a map of seismic hazard. The map indicates that the likelihood of shaking is generally greatest along various segments of the San Andreas and San Jacinto fault zones. Interpretation of Plate 3*b*, as with the maps constructed previously, is contingent upon an understanding of the assumptions and data on which it is founded. Withstanding the uncertainties, Plate 3*b* conveys information in a format that may prove useful for decisions regarding the siting of hazard mitigation procedures and the deployment of seismic instrumentation.

DISCUSSION AND CONCLUSIONS

This paper demonstrates how we may begin to use geologic data and current understanding of the mechanics of earthquake faulting to characterize seismic hazard in Calfornia. The resulting maps provide useful information regarding the distribution of seismic hazard in California, but caution should be exercised in their interpretation. Slip rate data are presently incomplete. Further geologic studies will likely prove some of the slip rates in Table A1 incorrect, or inapplicable to the present. A significant number of Quaternary faults probably remain unrecognized. Lack of geologic data pertaining to the locations and slip rates of faults in a region may result in an apparently low and incorrect characterization of seismic hazard in that region. It should be further emphasized that the hazard maps presented are not the result of a rigorous statistical treatment. Errors and uncertainties, for example, associated with individual slip rate estimates for each fault are generally large and have not been used in construction of the maps. Rather, specific values within the range of reported rates have been used. The resulting estimates of seismic hazard may in certain regions be altered sharply by use of other acceptable slip rates within the range of presently

reported values. Similarly, uncertainties in the empirical relationship between seismic moment and rupture length (Figure 2) used to estimate the expected size of future earthquakes are not incorporated into the analysis. A rigorous treatment of the errors will surely be desirable in the future development of these maps. It is unwise, however, to think that such treatment will substitute for inadequate geologic data. The greatest contribution that can be made to reducing uncertainties associated with this type of analysis will be the further acquisition and understanding of geological and geophysical data relating to the locations, offset rates, and faulting histories of Quaternary faults. It is perhaps this ability to actively collect data that represents the greatest advantage over conventional forms of seismic hazard analysis, which are limited by the existing and limited historical data set [e.g., *Algermissen et al.*, 1982]. A concerted effort to increase studies of active faulting, both onshore and offshore, may well be the most efficient means of increasing our understanding of seismic hazard in California.

Fundamental research toward understanding the phenomena which control the lateral extent of earthquake ruptures is clearly of critical importance to the further development of this work. The studies of *Segall and Pollard* [1980], *Sibson* [1986], and *King and Nabelek* [1985] are steps in this direction. The historical record of earthquakes clearly indicates that the entire length of major fault zones in California does not rupture during a single earthquake. A number of observations have been drawn upon in this study to suggest that the extent of earthquake ruptures is strongly controlled by structural or physical discontinuities along fault strike. These observations, in conjunction with knowledge of the location of past earthquake ruptures, provided the basis for estimating which fault segments will rupture independently during future earthquakes. It should be recognized, however, that the specific decisions regarding fault segment length (Table A1) used in constructing the hazard maps are largely tentative and coupled with large uncertainties, since there are now relatively few data on which to rest such decisions.

It is useful to briefly examine how the maps developed here might have fared if constructed 40 years ago. Several large earthquakes have occurred during the subsequent span of time, including the 1952 Kern County and 1971 San Fernando earthquakes. Neither of the faults that these events ruptured were known to displace Quaternary rocks prior to the occurrence of the earthquakes and thus would not have been included in estimates of the seismic hazard of their respective regions. It is, however, now recognized that these faults did show mappable evidence of Quaternary displacements before the earthquakes occurred. The occurrence of events like the 1952 and 1971 earthquakes does not then negate the premise upon which this work is built but, rather, emphasizes that the extent to which the maps represent seismic hazard is a direct function of the amount and quality of field investigations that have been conducted in an area.

To summarize, seismic hazard analyses are fundamentally based on estimates of the average occurrence rate of earthquakes in a region of interest. Estimates of this parameter are conventionally made with earthquake frequency statistics obtained from data listed in historical catalogues of seismicity [e.g., *Algermissen et al.*, 1982]. Conventional forms of seismic hazard analysis are, as a consequence, associated with large uncertainties when historical data are not sufficient to define secular rates of seismicity. In contrast, the geologic record of Quaternary fault offsets contains information on the occurrence of earthquakes through periods of time many orders longer than covered by historical records. This work and that described by *Wesnousky et al.* [1983, 1984] are supportive of the hypothesis that a complete knowledge of the geologic record of Quaternary fault offsets is sufficient to predict both the spatial and size distribution of earthquakes through time in a region characterized by shallow seismicity and active faulting. California is characterized by each of these attributes. This analysis and the resulting maps illustrate how quantitative estimates of the long-term seismic hazard in California may eventually be based primarily on geologic data describing the average slip rates and repeat times of Quaternary faults, rather than the historical record of seismicity. Use of geologic data in this manner should, at minimum, provide a firm complement to estimates of seismic hazard based on earthquake statistics and may, as more and better data become available, provide a better characterization of the seismic hazard resulting from moderate to large earthquakes on Quaternary faults in California.

APPENDIX

The seismic hazard maps developed in this study are the result of a specific interpretation of the seismic behavior of each mapped fault in California. The purpose of this appendix is to summarize as concisely as possible the data and assumptions used to interpret that behavior. The faults are grouped according to geographic province (Figure A1), and listed accordingly in Table A1. Table A1 references geologic maps and reports on the location and slip rate for each fault and further summarizes the results of those studies. Also included in Table A1 are the specific estimates of the expected moment magnitude M and estimated average repeat time T of earthquakes on each fault which were used in constructing the seismic hazard maps. Major faults and fault zones in each province are discussed separately. Maps accompany the discussion to illustrate the location and mapped length of each fault and fault segment listed in Table A1.

Peninsular Range-Salton Trough

San Jacinto fault zone. The San Jacinto fault zone (SJFZ) is historically the most seismically active fault zone in California. Extensive summaries and interpretations of the earthquake history along SJFZ are given by *Thatcher et al.* [1975] and *Sanders and Kanamori* [1984]. Epicenters of earthquakes with magnitudes $\geqslant 6$ that occurred along San Jacinto since about 1890 are denoted by stars in Figure A2.

Offsets across the SJFZ are predominantly right-lateral. Geologic data presented by *Sharp* [1981] place a minimum limit of 8-12 mm/yr of slip along the SJFZ near Anza (Figure A2) during the last 0.73 m.y. South of Anza, along the fault trace that ruptured during the 1968 Borrego Mountain earthquake (Table 2), *Sharp* [1981] interprets geologic relations to show slip has averaged 2.8-5.0 mm/yr and 1.6-2.2 mm/yr during the last 400± and 6000± years, respectively,

Fig. A1. Geographic provinces of California (adapted from *Clark et al.* [1984]). Discussion and tabulation of fault data in the appendix and Table A1, respectively, are indexed according to the geographic province where the faults are located.

but some question exists whether these rates reflect the total deformation across the SJFZ at that latitude. *Thatcher et al.* [1975] determined and summed the seismic moments of earthquakes along the entire fault zone since about 1890 to determine a seismic slip rate of about 8 mm/yr. *Brune* [1968] computed a slip rate of about 15 mm/yr based on similar calculations and a lesser data base. Geodetic and trilateration measurements spanning the periods 1969-1975 and 1973-1981 are consistent with 11-18 mm/yr of slip being stored elastically in a 10-15-km-thick crust [*Savage and Prescott*, 1976; *King and Savage*, 1983]. In summary, geologic, geodetic, and seismologic observations generally point to an average slip rate of at minimum 8-12 mm/yr across the SJFZ during late Quaternary time. Though a higher rate cannot be ruled out, the hazard maps are constructed with the assumption that right-lateral the slip rate across the entire SJFZ averages 10 mm/yr.

The historical record of earthquake ruptures [e.g., *Thatcher et al.*, 1975] and mapped complexities and discontinuities along strike of the fault zone [e.g., *Sharp*, 1975*a*,*b*] give reason to consider the zone as consisting of many separate segments, each of which may rupture in separate earthquakes. For this analysis, the fault zone is divided into nine segments (Figure A2). Where individual segments strike subparallel, the constraint is imposed that the cumulative slip rate across the segments sums to near 10 mm/yr. The expected seismic moments M_0^e and repeat times T of earthquakes for each segment that are listed in Table A1 are computed using the relation in Figure 2 that corresponds to major plate boundary faults. Data describing the location, extent, slip rate, and earthquake history of each fault segment are summarized in Table A1 and discussed in more detail below. The fault nomenclature follows approximately that used by *Jennings* [1975].

The Lytle Creek-Glenn Helen-Claremont segment of the SJFZ here refers to the stretch of the SJFZ that extends northwest into the San Gabriel mountains from a point near San Jacinto (Figure A2), where the fault trace shows a major right-step [*Matti et al.*, 1985]. Isoseismal and instrumental evidence have led investigators to suggest that the July 22, 1899 (M = 6.5), the July 23, 1923 (M = 6.3), and the April 21, 1918 (M = 6.8) earthquakes ruptured along this segment of the SJFZ [*Thatcher et al.*, 1975; *Sanders and Kanamori*, 1984]. No firm evidence of surface rupture is known for any of these events, however, and the large uncertainties associated with locating such historical events do not eliminate the possibility that one or more of the earthquakes were the result of slip on other nearby faults. This segment of the SJFZ is mapped as a narrow zone as it trends northwest from San Jacinto until it reaches the San Gabriel Mountains where it splays into several or more strands, forming a wider zone of about 3.5 km that includes the Glenn Helen and Lytle Creek faults. *Mezger and Weldon* [1983] interpret offset terrace deposits to indicate a maximum horizontal slip rate of 2.5 mm/yr across the Lytle Creek fault, but this rate probably does not reflect the entire deformation rate across this segment of the SJFZ [e.g., *Morton*, 1975]. For this analysis, the Lytle Creek-Glenn Helen-Claremont segment is treated as a single seismogenic source that is accumulating the equivalent of 10 mm/yr of slip.

The Casa Loma fault is the right step and southward continuation of the Claremont fault (Figure A2). The Casa Loma fault appears continuous with the Clark fault to the southeast, the trace of each being separated only by some very young alluvial deposits [*Sharp*, 1967]. For this work, the Casa Loma and Clark faults are treated as a single earthquake source and referred to as the Casa Loma-Clark segment. This segment was a possible locus for the magnitude 6.6 earthquake of December 25, 1899 [*Sanders and Kanamori*, 1984; *Thatcher et al.*, 1975]. Moderate-sized earthquakes of about magnitude 6 also occurred along this section of the SJFZ on March 25, 1937, and March 19, 1954 [Figure A2; *Thatcher et al.*, 1975; *Magistrale et al.*, 1984], but neither can definitely be attributed to displacement along the major mapped faults in this area. Geologic relations near Anza indicate that slip along this segment has averaged 8-12 mm/yr or greater during the last 0.73 m.y. [*Sharp*, 1981], at least along the reach northwest of Anza. The entire segment is assigned a 10 mm/yr slip rate for the hazard analysis.

The Hot Springs and Thomas Mountain faults strike subparallel to the Casa Loma fault [*Hill*, 1981]. *Sharp* [1967] briefly discusses the character of displacement along these two faults but reports no evidence of slip rates. He notes that the rounded topographic character of scarps along the Hot Springs fault suggests that little movement has occurred in recent geologic time and that no evidence of Quaternary movement was found along the Thomas Mountain fault except at a point near Burnt Valley where Pleistocene deposits are cut by a thin gouge zone. The faults are included in this analysis but each is assigned a very low slip rate of 0.01 mm/yr.

South of Anza, displacement along the SJFZ is also accommodated by the Buck Ridge and Coyote Creek faults. Each fault strikes subparallel to the Clark fault. *Sharp* [1967] reports that total horizontal separation across the

TABLE A1. Quaternary Faults

Fault	Location* lat	Location* lon	S†	L‡	M§	C#	Slip Rate δ mm/yr Mn	Slip Rate δ mm/yr Mx	Slip Rate δ mm/yr Pr	T**	D††	A‡‡	Reference§§
Peninsular Ranges and Salton Trough													
Chino	34.0	117.7	rr?	28	6.8	B	0.0	0.2	0.1		v	q	*Yerkes et al.* [1965]b *Heath et al.* [1982]c
Elsinore A (Whittier)	33.8	117.7	rl	74	7.3	A	0.6	9.0	4.0	730	h	h	see segment D
Elsinore B	33.5	117.2	rl	51	7.1	A	0.6	9.0	4.0	553	h	h	see segment D
Elsinore C	33.2	116.7	rl	64	7.2	A	0.6	9.0	4.0	651	h	h	see segment D
Elsinore D	32.8	116.2	rl	69	7.2	A	0.6	9.0	4.0	694	h	h	see appendix and *Crowell and Sylvester* [1979]b *Lamar et al.* [1973]a *Lowman* [1980]b *Sage* [1973]a *Weber* [1977]a *Pinault and Rockwell* [1984]
Imperial-Brawley (1979 rupture)	32.8	115.5	rv?	40	6.7	AA	20.0			32†‡	t	h	see the appendix and *Sharp* [1980]c *Sharp* [1982]c *Sharp et al.* [1982]c *Sharp and Lienkaemper* [1982]c *Clark et al.* [1984]
Imperial-Brawley (1940 rupture)	32.7	115.4	rv	69	6.9	A		8.6		700†‡	h	h	see 1979 segment
La Nacion	32.7	117.1		19	6.6	C							*Jennings* [1975]
Newport - Inglewood A	33.7	118.1	rv?	34	6.9	A	0.1	6.0	1.0	1650	v	h	see segment B
Newport - Inglewood B	33.9	118.3	rv?	28	6.8	A	0.1	6.0	1.0	1454	v	h	see the appendix and *Castle* [1960]c *Castle and Yerkes* [1976]c *California Department Water Resources* [1968]c *Poland and Piper* [1956]c *Wright et al.* [1973]a *Yeats* [1973]b
Palos Verdes	33.8	118.3	rr?	45	7.0	A	0.02	0.7	0.7	2905	v	h	*Yerkes et al.* [1965]a,b *Darrow and Fisher* [1983]c
Rose Canyon	32.8	117.2	rr?	50	7.1	A	0.0	2.2	1.5	1458	t	q	*Artim and Streiff* [1981]
San Jacinto Fault Zone (reference summary)													*Ferrand et al.* [1981] *Kennedy* [1975a]b *Kern* [1977]c *Moore and Kennedy* [1975]c *Sharp* [1981] *Bartholomew* [1970]b *Clark et al.* [1972] *Savage and Prescott* [1976] *King and Savage* [1983] *Sharp* [1967] *Thatcher et al.* [1975] *Brune* [1968]
San Jacinto (Lytle Creek-Glenn Helen - Claremont)	34.5	117.2	rl	78	7.0	AA			10.0	107	h	q	see the appendix
San Jacinto (Hot Springs)	33.7	116.8		29	6.8	C							see the appendix
San Jacinto (Thomas Mountain)	33.6	116.6		15	6.5	C							see the appendix
San Jacinto (Casa Loma - Clark)	33.5	116.6	rl	100	7.1	AA	8.0		10.0	128	h	q	see the appendix
San Jacinto (Buck Ridge)	33.5	116.5	rl	35	6.6	A			2.0	294	h	q	see the appendix
San Jacinto (Coyote Creek)	33.3	116.4	rl	38	6.6	A			2.0	314	h	q	see the appendix
San Jacinto (Borrego Mountain)	33.1	116.1	rl	30	6.5	A	1.6	5.0	2.0	150†‡	h	h	see the appendix
San Jacinto (Superstition Mountain)	32.9	115.8	rl	26	6.4	A			1.0	468	h	q	see the appendix
San Jacinto (Superstition Hills)	33.0	115.8	rl	22	6.4	A			1.0	422	h	q	see the appendix

TABLE A1. (continued)

Fault	Location* lat	lon	S†	L‡	M§	C#	Slip Rate δ mm/yr Mn	Mx	Pr	T**	D††	A‡‡	s	Reference§§
Transverse Ranges														
Arrastre Canyon Narrows	34.4	117.1		11	6.3	C								*Meisling* [1984]
Arrowhead Springs •	34.2	117.2		11	6.3	C								*Jennings* [1975]
Arroyo Parida	34.4	119.5	r?	44	7.0	B	0.35	0.4		5350	v		q	*Rockwell* (1983]c *Rockwell et al.* [1984]
Beaumont Fault Zone	33.9	117.0	n	8	6.1	C								*Matti et al.* [1985]
Benedict Canyon	34.1	118.3	r?	11	6.3	C								*Weber* [1980]
Big Pine	34.7	119.3	ll	67	7.2	A	0.8	2.0	1.0	2699	h		p	*Kahle et al.* [1966]b *Lamar et al.* [1973]a
Chatsworth Reservoir •	34.2	118.6		12	6.3	C								*Jennings* [1975]
Clearwater	34.6	118.6		33	6.9	C								*Jennings* [1975]
Cleghorn	34.3	117.4	ll	20	6.6	A	1.5	18.0	3.0	380	h		q	*Meisling* [1984]
Crofton Hills	34.0	117.1	n	21	6.6	C								*Matti et al.* [1985]
Cucamonga	34.2	117.6	r	20	6.6	A	2.9	6.4		700†‡	t		h	*Morton et al.* [1982]c *Weldon and Sieh* [1980]c *Weldon* [1983]c *Matti et al.* [1982]
Eagle Rock - San Rafael	34.1	118.2	r?	11	6.3	C								*Weber* [1980]
Frazier Mountain North	34.8	119.0	r	13	6.4	C								*Jennings* [1975]
Frazier Mountain South	34.7	119.0	r	11	6.3	C								*Jennings* [1975]
Glen Annie	34.4	119.8		21	6.6	C								*Sylvester and Darrow* [1979]
Hollywood	34.1	118.3	r?	14	6.4	B	0.3	0.8		1627	v		h	*Weber* [1980]c
Holser	34.4	118.7		19	6.6	C								*Jennings* [1975] *Yeats* [1983a]
Javon Canyon	34.3	119.4	r	8	6.2	C	0.7	2.5	0.01		t		h	see the appendix and *Sarna-Wojcicki et al.* [1979]c, *Yeats* [1982]c
Lavigia	34.4	119.7		9	6.2	C								*Yeats and Olson* [1984]
Malibu Coast	34.0	118.7	r	34	6.9	C	0.04	0.09			t		q	*Clark et al.* [1984]
Mesa	34.4	119.7		7	6.1	C								*Yeats and Olson* [1984]
Mission Hills	34.3	118.5	r?	8	6.1	C								*Weber* [1980]
More	34.4	119.8		19	6.6	C								*Yeats and Olson* [1984]
Morongo Valley	34.1	116.6	ll	18	6.5	C								*Jennings* [1975]
Northridge Hills	34.3	118.6	r?	21	6.6	C								*Weber* [1980]
Oak Ridge (onshore)	34.3	119.0	r	39	6.9	A			3.5	521	t		q	*Yeats* [1983a]
Ocotillo Ridge (fold)	34.4	117.1	r	14	6.4	C								*Meisling* [1984]
Ord Mountain	34.4	117.2	r	11	6.3	B		1.2	0.1		v		q	*Meisling* [1984]
Pine Mountain	34.6	119.1		59	7.1	C								*Jennings* [1975]
Pinto Mountain	34.1	116.3	ll	73	7.3	A	0.3	5.3	1.0	2885	h		m	*Dibblee* [1968a]b *Dibblee* [1975]a *Garfunkle* [1974]a
Raymond	34.1	118.1	lr?	22	6.7	B	0.1	0.2		3000†‡	v		h	*Yerkes et al.* [1965]a,b *Allen et al.* [1978]b *Crook et al.* [1986]
Red Hill	34.1	117.6		14	6.4	C								*Jennings* [1975]
Red Mountain	34.4	119.4	r?	25	6.7	A	0.9	2.3		831	d		q	*Lajoie et al.* [1982]c *Lee et al.* [1979]c *Sarna-Wojcicki et al.* [1979]c *Yeats et al.* [1982]c *Sarna-Wojcicki and Yerkes [1982]*
San Antonio North •	34.2	117.6		18	6.6	C								*Jennings* [1975]
San Antonio South •	34.2	117.6		18	6.5	C								*Jennings* [1975]
San Cayetano	34.4	119.0	r	49	7.1	A	0.9	9.0	5.0	429	d		q	*Yeats* [1983a] *Rockwell* [1983]
San Fernando (1971)	34.3	118.4	r	17	6.5	A				200†‡			h	*Bonilla* [1973]
San Gabriel A	34.6	118.7	rl	47	7.0	B		5.0			h		m	see segment B
San Gabriel B	34.4	118.4	rl	24	6.7	B		5.0			h		m	*Ehlig* [1973]ab *Crowell* [1973]a
San Gorgonio Mtn. •	34.1	116.8		20	6.6	C								*Jennings* [1975]
San Jose	34.1	117.8		23	6.7	C								*Jennings* [1975]
Santa Ana Fault •	34.2	117.1		16	6.5	C								*Jennings* [1975]

TABLE A1. (continued)

Fault	Location*		S†	L‡	M§	C#	Slip Rate$^{\delta}$ mm/yr			T**	D††	A‡‡	Reference§§
	lat	lon					Mn	Mx	Pr				
Santa Cruz Island	34.1	119.9	r	94	7.4	B	0.2	0.9	0.9	4035	h	q	*Junger and Wagner* [1977] *Patterson* [1979]c *Yerkes et al.* [1981]
Santa Monica	34.1	118.4	r?	24	6.7	B	0.1	1.0	0.3	3955	v	q	*Yerkes et al.* [1965]b *Lamar* [1961]b *McGill* [1981,1982]b,c *Yerkes and Wentworth* [1965]a
Santa Rosa Island	34.0	120.2		47	7.0								*Yerkes et al.* [1981]
Santa Susana	34.4	118.6	r	38	6.9	A	1.2	4.5		630	d	q	*Barnhart and Slosson* [1973]a *Yeats* [1979]
Santa Ynez (west)	34.5	120.1	lv	46	7.0	B	0.2	0.6	0.4	5152	v	h	*Clark et al.* [1984]
Santa Ynez (east)	34.5	119.4	ll	84	7.3	B	0.1	6.7	1.0	3195	t	h	*Sylvester and Darrow* [1979]b *Dibblee* [1966]b *Gordon* [1979]b *Keaton* [1978]c *Clark et al.* [1984]
Saw Pit Canyon	34.2	118.0		13	6.4	C							*Jennings* [1975]
Sierra Madre A	34.3	118.2	r?	14	6.4	A				5000†‡	v	h	*Crook et al.* [1986]
Sierra Madre B	34.3	118.2	r?	17	6.5	A		0.4	4.0	5000†‡		q	*Crook et al.* [1986]
Sierra Madre C	34.2	118.1	r?	15	6.5	A				5000†‡		q	*Crook et al.* [1986]
Sierra Madre D	34.2	117.9	r?	14	6.4	A				5000†‡		q	*Crook et al.* [1986]
Sierra Madre E	34.1	117.8	r?	14	6.4	A				5000†‡			see the appendix
Simi	34.3	118.9		36	6.9	C							*Yeats* [1983b]
Sky High Ranch (Fifteen Mile Valley)	34.4	117.0	rl	11	6.3	A	0.3	15.0	1.3	578	h	q	*Meisling* [1984]
Slide Peak •	34.2	117.0		20	6.6	C							*Jennings* [1975]
Soledad	34.5	118.3		11	6.3	C							*Jennings* [1975]
Summit Valley	34.3	117.3	r	16	6.5	C							*Meisling* [1984]
Tunnel Ridge Lineament	34.3	117.2		10	6.3	C							*Meisling* [1984]
Ventura	34.3	119.3	lr	7	6.1	C	0.8	2.4	0.01		d	p	*Sarna-Wojcicki et al.* [1976]c *Gardner and Stahl* [1977]c *Lee et al.* [1979]c *Yerkes and Lee* [1979]c *Sarna-Wojcicki and Yerkes* [1982]c
Verdugo	34.2	118.3	r?	21	6.6	C							*Weber* [1980]
Walnut Creek	34.1	117.9		16	6.5	C							*Jennings* [1975]
Waterman Canyon	34.2	117.2		18	6.6	C							Jennings (1975)
						Mojave Desert							
Avawatz Mountain •	35.5	116.2		16	6.5	C							*Jennings* [1975]
Baker •	35.3	116.1		15	6.5	C							*Jennings* [1975]
Bitter Spring A •	35.2	116.5		17	6.5	C							*Jennings* [1975]
Bitter Spring B •	35.2	116.6		12	6.4	C							*Jennings* [1975]
Blake Ranch	34.8	117.6		27	6.8	C							*Jennings* [1975]
Blackhawk Springs •	34.3	116.8		12	6.4	C							*Jennings* [1975]
Blackwater	35.3	117.3	rl	42	7.0	B	0.4			4746	h	p	*Dibblee* [1968a]b
Blue Cut	33.9	116.1		27	6.8	C							*Hope* [1969]b
Bristol Mountain	34.7	115.8	rl	40	7.0	B	0.3	3.0		1133	h	p	*Dokka* [1983] *Miller and Morton* [1980]
Bullion A	34.5	116.3	rl	27	6.8	C							*Jennings* [1975]
Bullion B	34.3	116.0	rl	39	6.9	C							*Jennings* [1975]
Bullion C	34.1	115.9	rl	19	6.6	C							*Jennings* [1975]
Bullion D	34.5	116.3	rl	13	6.4	C							*Jennings* [1975]
Bullion Mountain A •	34.5	116.2		17	6.5	C							*Jennings* [1975]
Bullion Mountain B •	34.4	116.0		21	6.6	C							*Jennings* [1975]
Bullion Mountain C •	34.4	115.9		9	6.2	C							*Jennings* [1975]
Bullion Mountain D •	34.3	115.8		8	6.1	C							*Jennings* [1975]
Cady	34.9	116.5		21	6.6	C							*Jennings* [1975]
Calico A	35.0	116.9	rl	12	6.4	A	0.4	5.0	1.0	786	h	p	inferred from segment B

TABLE A1. (continued)

Fault	Location*		S†	L‡	M§	C#	Slip Rate δ mm/yr			T**	D††	A‡‡	Reference§§
	lat	lon					Mn	Mx	Pr				
Calico B	34.8	116.7	rl	34	6.9	A	0.4	5.0	1.0	1657	h	p	*Dokka* [1983]c *Miller and Morton* [1980] *Garfunkle* [1974]a
Calico C	34.6	116.4	rl	44	7.0	A	0.4	5.0	1.0	1983	h	p	inferred from segment B
Camp Rock	34.7	116.7	rl	32	6.8	A	0.8	2.0	1.0	1580	h	p	*Dokka* [1983]c *Morton et al.* [1980]c *Garfunkle* [1974]a
Covington Flat •	34.1	116.3		16	6.5	C							*Jennings* [1975]
Coyote Lake A	35.1	116.9		19	6.6	C							*Jennings* [1975]
Coyote Lake B	35.1	116.6		25	6.7	C							*Jennings* [1975]
Deep Spring	34.9	117.6		26	6.8	C							*Jennings* [1975]
Dome Mountain •	35.4	117.5		12	6.4	C							*Jennings* [1975]
Emerson A	34.5	116.6	rl	27	6.8	B	0.6	1.2		1544	h	m	*Garfunkle* [1974]a
Emerson B	34.4	116.4	rl	22	6.7	B	0.6	1.2		1351	h	m	*Garfunkle* [1974]a
Emerson C	34.3	116.3	rl	12	6.4	C							*Jennings* [1975]
Emerson D	34.2	116.3	rl	13	6.4	C							*Jennings* [1975]
Emerson E	34.5	116.5	rl	10	6.3	C							*Jennings* [1975]
Garlic Spring	35.2	116.6		12	6.4	C							*Jennings* [1975]
Garlock (west)	35.1	118.4	rl	103	7.4	A	0.7	30.0	7.0	527†‡	h	h	see Garlock (east)
Garlock (east)	35.5	117.2	rl	148	7.6	A	0.7	30.0	7.0	685†‡	h	h	*Astiz and Allen* [1983] *Burke and Clark* [1978]c *Carter* [1980,1982]c *Clark and Lajoie* [1974]c *La Violette et al.* [1980]c *Michael* [1966]a *Smith* [1962]a *Smith* [1975]c
Garlock Splay A •	34.9	118.6		18	6.6	C							*Jennings* [1975]
Garlock Splay B •	34.9	118.4		20	6.6	C							*Jennings* [1975]
Goldstone •	35.3	117.0		32	6.8	C							*Jennings* [1975]
Granite Mountain A •	35.5	116.8		39	6.9	C							*Jennings* [1975]
Granite Mountain B •	35.5	116.5		26	6.7	C							*Jennings* [1975]
Harper A	35.2	117.5	rl	30	6.8	B	0.2			6302	h	p	inferred from segment B
Harper B	35.1	117.2	rl	25	6.7	B	0.2			5582	h	p	*Dibblee* [1968b]b
Harper C	35.0	117.0	rl	17	6.5	B	0.2			4223	h	p	inferred from segment B
Helendale A	34.8	117.3	rl	26	6.7	A	0.2	1.5	1.0	1379	h	p	*Dokka* [1983] *Miller and Morton* [1980]c *Morton et al.* [1980]c
Helendale B	34.5	117.1	rl	39	6.9	A	0.2	1.5	1.0	1835	h	p	inferred from segment A
Helendale C	34.3	116.8	rl	29	6.8	A	0.2	1.5	1.0	1479	h	p	inferred from segment A
Hidalgo	34.3	116.3	rl	30	6.8	C							*Jennings* [1975]
Hidalgo East	34.3	116.2		14	6.4	C							*Jennings* [1975]
Homestead	34.4	116.5		24	6.7	C							*Jennings* [1975]
Johnson Valley	34.4	116.6		37	6.9	C							*Jennings* [1975]
Lenwood	34.6	116.8	ss	51	7.1	A	0.1	2.5	1.0	2234	h	p	*Dokka* [1983] *Miller and Morton* [1980]c *Garfunkle* [1974]a
Lockhart	35.0	117.4	ss	76	7.3	A	0.9	2.5		1742	h	m	*Garfunkle* [1974]a
Ludlow	34.7	116.1		67	7.2	C							*Jennings* [1975]
Manix	35.0	116.5		20	6.6	C							*Jennings* [1975]
Mesquite Lake	34.2	116.1		22	6.7	C							*Jennings* [1975)
Mirage Valley	34.7	117.7		32	6.8	C							*Jennings* [1975]
Old Woman Springs	34.4	116.7		35	6.9	C							*Jennings* [1975]
Pipes Canyon	34.2	116.6	rl	23	6.7	C							*Jennings* [1975]
Pisgah	34.7	116.4	rl	34	6.9	A	0.3	7.0	1.0	1668	h	p	*Dokka* [1983] *Miller and Morton* [1980]c *Garfunkle* [1974]a
Rock Creek •	34.6	117.8		21	6.6	C							*Jennings* [1975]
Red Pass Lake •	35.2	116.3		18	6.6	C							*Jennings* [1975]
Rodman	34.7	116.5	rl	16	6.5	B	0.3	0.7	0.5	1891	h	p	*Dokka* [1983] *Miller and Morton* [1980]c *Garfunkle* [1974]a
Soda Mountains •	35.3	116.2		14	6.4	C							*Jennings* [1975]

TABLE A1. (continued)

Fault	Location* lat	Location* lon	S†	L‡	M§	C#	Slip Rate δ mm/yr Mn	Slip Rate δ mm/yr Mx	Slip Rate δ mm/yr Pr	T**	D††	A‡‡	Reference§§
South Lockhart	35.0	117.5		25	6.7	C							*Jennings* [1975]
Tiefort Mountain A •	35.3	116.6		30	6.8	C							*Jennings* [1975]
Tiefort Mountain B •	35.3	116.8		11	6.3	C							*Jennings* [1975]
Tiefort Mountain C •	35.3	116.4		14	6.4	C							*Jennings* [1975]
Tiefort Mountain D •	35.3	116.5		15	6.5	C							*Jennings* [1975]
						Sierra Nevada - Great Basin							
Auburn Shear (Dewitt fault)	39.0	121.1	n	13	6.4	C		0.07			v	q	see Swains Ravine
Auburn Shear (Rescue fault)	38.9	121.1	n	29	6.8	C		0.07			v	q	*Woodward-Clyde Consultants* [1977]c *Harwood and Helley* [1982]c *Borchardt et al.* [1978]c *Harden and Marchand* [1980]c
Auburn Shear zone (Swains Ravine fault)	39.3	121.4	n?	32	6.8	C		.01			v	q	*Woodward-Clyde Consultants* [1977]c *Borchardt et al.* [1978]c *Harden and Marchand* [1980]c
Auburn Shear zone (Spenceville fault)	39.0	121.3	n	31	6.8	C		0.07			v	q	see Swains Ravine
Battle Creek	40.4	122.0	n	33	6.9	B	0.1	1.0	0.4	5412	t	q	*Harwood et al.* [1980, 1981]c *Helley et al.* [1981]c
Carson Valley	38.7	119.8	n	35	6.9	A	0.7	1.6	1.0	1684	t	q	*Clark et al.* [1984]
Fish Springs	37.2	118.3	n	28	6.8	B	0.1	1.4	0.4	3623	t	q	*Bachman* [1974]b *Clark* [1979]c *Clark et al.* [1984]
Furnace Creek	36.9	117.2	rl	139	7.6	B		0.7		6574	h	m	*Wright and Troxel* [1967]b
Hartley Springs	37.8	119.1	n	23	6.7	B	0.1	0.2	0.2	8424	t	h	*Clark et al.* [1984]
Hilton Creek Fault	37.6	118.8	n	19	6.6	A	1.3	2.6	2.0	554	t	h	*Clark and Gillespie* [1981]c
Independence	36.7	118.2	n	65	7.2	B	0.1	0.2	0.1		t	q	*Gillespie* [1982]c
Inyo Mountains •	37.3	118.0		22	6.7	C							*Jennings* [1975]
Keough Springs •	37.3	118.4		17	6.5	C							*Jennings* [1975]
Mt. Humphreys •	37.3	118.6		16	6.5	C							*Jennings* [1975]
Mono Lake	38.1	119.1	n	27	6.8	C	1.8	3.3	2.5	557	t	h	*Clark et al.* [1984]
North Death Valley	37.5	118.0		43	7.0	C							*Jennings* [1975]
Owens Valley	36.7	118.1	rn	91	7.4	A	0.3	2.0	1.0	3364	t	h	*Lubetkin* (1980)c *Lubetkin and Clark* [1980]c
Owl Lake	35.7	116.8		20	6.6	C							*Jennings* [1975]
Panamint Valley (East)	36.3	117.3	n?	35	6.9	C							*Jennings* [1975]
Panamint Valley (West)	36.2	117.4	n?	30	6.8	C							*Jennings* [1975]
Panamint Valley (South)	35.8	117.1	rn	56	7.1	A	1.0	2.6	2.0	1192	t	h	*Smith* [1979]c
Parker Lake	37.9	119.2	n	31	6.8	B	0.2	0.8	0.5	3083	t	q	*Clark* [1979]c
Pleito Thrust	34.9	119.1	r	44	7.0	A	0.2	14.0	1.4	1470	t	h	*Clark et al.* [1984] *Hall* [1984]a
Round Valley	37.5	118.7	n	30	6.8	A	0.7	1.4	1.0	1503	t	h	*Clark et al.* [1984]
Saline Valley (North)	36.7	117.9		25	6.7	C							*Jennings* [1975]
Saline Valley (South)	36.6	117.6		36	6.9	C							*Jennings* [1975]
South Death Valley (East)	36.3	116.8	rv	52	7.1	A	0.2	5.7		761	h	q	see south segment
South Death Valley (South)	35.8	116.6	rv	55	7.1	A	0.2	5.7		800	q	m	*Troxel and Butler* [1980]b *Hooke* [1972]b
South Death Valley (West)	36.2	116.9		62	7.2	C							*Jennings* [1975]
Sierra Nevada A	36.1	118.0	n?	58	7.1	A	0.3	2.7		1633	v	q	*Saint Amand and Roquemore* [1979]b *Roquemore* [1981]c *Duffield and Smith* [1978]c *Christensen* [1966]a
Sierra Nevada B	35.7	117.9	n?	24	6.7				1.5	850	v	p	inferred from segment A
Sierra Nevada C	35.4	118.0	n?	25	6.7				1.5	897	v	p	inferred from segment A
Tank Canyon	35.7	117.3	n	18	6.5	A	0.5	1.6	1.0	1031	t	h	*Smith et al.* [1968]c
West Walker	38.6	119.5	n	22	6.7	C	0.3	0.9	0.6	1996	t	q	*Clark* [1967]
White Mountain	37.3	118.3	n?	56	7.1	B			0.8	2956	v	h	*Wallace* [1978]b

TABLE A1. (continued)

Fault	Location* lat	lon	S†	L‡	M§	C#	Slip Rate δ mm/yr Mn	Mx	Pr	T**	D††	A‡‡	Reference§§
White Wolf	35.2	118.8	r	62	7.2	A	3.0	8.5		300	d	q	*Stein and Thatcher* [1981] *Lamar et al.* [1973]a
Wilson Canyon	35.8	117.5		37	6.9	C							*Jennings* [1975]
						Modoc Plateau							
Honey Lake	40.1	120.3		52	7.1	C							*Jennings* [1975]
Likely	41.3	120.6		94	7.4	C							*Jennings* [1975]
Suprise	41.5	120.1	n	102	7.4	A	0.8	2.7	1.0	3669	v	q	*Hedel* [1980]c
Susanville	40.4	120.6	rn	33	6.9	B	0.1	0.4	0.2	8096	t	q	*Roberts and Gross* [1982]c
						Central Coast							
Carmel •	36.6	121.9		28	6.8	C							*Jennings* [1975]
Cuyama Valley •	35.0	119.8		44	7.0	C							*Jennings* [1975]
Hosgri	35.6	121.3	rv	199	7.8	A	4.6	9.0	7.0	852	h	q	*Weber* [1981]c
King City	36.0	121.6		57	7.1	C							*Jennings* [1975]
La Panza	35.4	120.4		33	6.9	C							*Jennings* [1975]
Lions Head	34.8	120.5		26	6.7	C							*Sylvester and Darrow* [1979]
Little Pine	34.7	120.0	r	31	6.8	C							*Jennings* [1975]
Los Alamos-Baseline	34.7	120.1		44	7.0	C							*Sylvester and Darrow* [1979]
Ozena	34.8	119.5		36	6.9	C							*Jennings* [1975]
Rinconada	35.8	120.9	rl	136	7.6	A	2.4	12.0	2.4	1883	h	p	*Durham* [1965]b *Hart* [1976]b
San Gregorio	37.1	122.3	rl	190	7.7	A	7.0	19.0	7.0	824	h	q	*Weber and Cotton* [1981]c *Weber and Lajoie* [1981]c *Clark et al.* [1984]c *Weber and Cotton* [1981]c
San Juan	35.4	120.1		69	7.2								*Jennings* [1975]
Santa Maria	34.9	120.4		23	6.7	C							*Sylvester and Darrow* [1979]
Seaside •	36.5	121.7		23	6.7	C							*Jennings* [1975]
						North Coast and Great Valley							
Antioch A	38.1	121.8		10	6.3	C							*Jennings* [1975]
Antioch B	38.0	121.8		19	6.6	C							*Jennings* [1975]
Bay Entrance	40.7	124.2	r	20	6.6	A	1.4	2.2	1.8	632	d	q	*Woodward-Clyde Consultants* [1980]
Bear River	40.4	124.2		30	6.8	C							*Carver et al.* [1982]
Big Valley	39.0	122.9	rl	16	6.5	B	0.3			2675	h	q	*Hearn et al.* [1976]c *Clark et al.* [1984]
Blue Lake	40.8	123.9	r	65	7.2	A	1.1	1.6		1965	t	q	*Carver* [1985]
Browns Valley •	36.9	121.3		29	6.8	C							*Jennings* [1975]
Burdell Mountain	38.1	122.6		21	6.6	C							*Jennings* [1975]
Calaveras A (Coyote Lake)	37.0	121.5	rl	28	5.7	A			17.0	82†‡	h	h	*Prescott et al.* [1981] *Savage et al.* [1979]
Calaveras B (Morgan Hill)	37.3	121.7	rl	28	6.3	A	7.0	17.0		150†‡	h	h	*Prescott et al.* [1981] *Savage et al.* [1979]
Calaveras C	37.5	121.8	rl	31	6.3	A			7.0	150†‡		h	see the appendix
Calaveras D	37.7	122.0	rl	23	6.3	A			7.0	150†‡	h	h	see the appendix
Collayami	38.9	122.8	rl	18	6.6	B		1.0	0.1		h	q	*Hearn et al.* [1976]c
Concord	38.0	122.0	rl	24	6.7	A			4.0	319			see the appendix and *Harsh and Burford* [1982]
Cordelia	38.3	122.1		22	6.7	C							*Herd and Helley* [1977]
Corral Hollow •	37.7	121.6		17	6.5	C							*Jennings* [1975]
Fickle Hill	40.7	123.9	rr	63	7.2		0.4	0.8		4335	t	q	*Carver* ([1985]
Freshwater	40.8	124.1		32	6.8	C							*Jennings* [1975]
Goose Lake	40.6	124.2	rr	22	6.7	B	0.3	1.0	1.0	6108	t	q	*Carver et al.* [1982] *Clark et al.* [1984] *Woodward-Clyde Consultants* [1980]c
Green Valley	38.2	122.1		35	6.9	A			4.0	424			see the appendix and *Herd and Helly* [1977] *Frizzell and Brown* [1976]
Greenville	37.7	121.7	rv	28	6.8	B	0.1	0.7		3585	h	h	*Wright et al.* [1982]

TABLE A1. (continued)

Fault	Location* lat	lon	S†	L‡	M§	C#	Slip Rate δ mm/yr Mn	Mx	Pr	T**	D††	A‡‡	Reference§§
Grogan's	41.0	123.8		94	7.4								*Carver et al.* [1982]
Hayward A (Coyote and Silver Creek faults)	37.2	121.7	ll	18	6.6	A			4.0	264	h	h	see the appendix
Hayward B (Evergreen fault)	37.4	121.8	rl	25	6.7	A			4.0	335	h	h	see the appendix
Hayward C	37.6	122.1	rl	51	7.1	A	6.0	8.0	4.0	556	h	h	*Prescott et al.* [1981] *Prescott and Lisowski* [1982]
Hayward D	37.9	122.3	rl	25	6.7	A			4.0	336	h	h	see the appendix
Healdsberg	38.6	122.8	rl	32	6.8	A			7.0	228			see the appendix and *Jennings* [1975]
Lagoons	40.9	123.8		89	7.3								*Carver et al.* [1982]
Lake Mountain–Island Mountain	39.9	123.4		94	7.4	A			7.0	494			see the appendix and *Herd* [1978] *Carver et al.* [1982]
Las Positas	37.6	121.7	ln	10	6.3	B	0.04	1.6		872	t	q	*Carpenter and Clark* [1982]c *Herd and Brabb* [1979]
Little Salmon	40.6	124.1	r?	29	6.8	A	1.8	3.0	2.4	609	d	q	*Woodward-Clyde Consultants* [1980]c *Carver et al.* (1982)
Livermore	37.7	121.8		8	6.2	C							*Jennings* [1975]
Los Altos •	37.3	122.1		14	6.4	C							*Jennings* [1975]
Los Gatos •	37.2	121.9		15	6.5	C							*Jennings* [1975]
Maacama	39.1	123.1		151	7.6	A			7.0	696			see the appendix and *Pampeyan et al.* [1981] *Herd* [1978] *Herd and Helley* [1977]
Mad River	40.7	123.9		64	7.2	B	0.6	1.1		3075			*Carver* [1985]
Mckinleyville	40.8	123.9	rr	67	7.2	B	0.2	0.7		6017	t	q	*Woodward-Clyde Consultants* [1980]c *Carver* [1985]
Midway	37.7	121.6	r	11	6.3	B	0.1	0.5		2651	t	q	*Shedlock et al.* [1980]c
Oneill	36.9	121.0	r	18	6.5	A	0.3	1.8		984	t	q	*Lettis* [1982]c
Ortigalita A	37.1	121.2	?	25	6.7	C	0.01	0.04		10000†‡	v	q	*Anderson et al.* [1982] *Clark et al.* [1984]
Ortigalita B	37.0	121.1	?	18	6.6	C	0.01	0.04		10000†‡	v	q	see segment A
Ortigalita C	36.9	121.0	?	18	6.6	C	0.01	0.04		10000†‡	v	q	see segment A
Ortigalita D	36.7	120.9	?	21	6.6	C	0.01	0.04		10000†‡	v	q	see segment A
Paicines	36.8	121.3	rl	36	6.9	A	5.0	13.0	1.0	1726		h	see the appendix and *Harsh and Pavoni* [1978] *Ellsworth* [1975] *Savage et al.* [1973] *Lisowski and Prescott* [1981]
Panoche Pass •	36.6	121.1		22	6.6	C							*Jennings* [1975]
Pleasonton	37.7	121.9		9	6.2	C							*Jennings* [1975]
Rogers Creek	38.3	122.6		38	6.9	A			7.0	255			see the appendix and *Jennings* [1975]
Russ	40.5	124.2		30	6.8								*Carver et al.* [1982]
San Benito	36.6	121.1	rl	24	6.7	A	5.0	13.0	1.0	1291			see Paicines fault
San Joaquin	36.9	120.8	?	21	6.6	A	0.2	2.0		1083	v	q	*Lettis* [1982]c
Sargent-Berrocal	37.0	121.7	rr	51	7.1	A		4.0	1.0			h	*Savage et al.* [1979] *Hay et al.* [1980]
Tolay	38.2	122.5		14	6.5	C							*Jennings* [1975]
Trinidad	40.8	123.9	r	74	7.3		0.1	0.9		5900	t	q	*Clark et al.*, [1984]c *Carver* [1985]
Vaca	38.3	122.0	rl	7	6.1	A	0.3	4.0		260	h	q	*Knuepfer* [1977]c
Verona	37.6	121.8	r	8	6.2	B	0.02	0.1	0.1	9735	t	q	*Herd and Brabb* [1980]c
West Napa	38.3	122.3		17	6.5	C							*Herd and Helley* [1977]
Zamora	38.8	121.9	n	21	6.6	A	0.2	0.5	0.3	4631	v	q	*Harwood et al.* [1981]c *Harwood and Helley* [1982]c
Zayante-Vergales	37.0	121.8	rr	50	7.1	B	0.1	1.3		3130	t	q	*Coppersmith* [1979]c *Dupre* [1975]c

TABLE A1. (continued)

Fault	Location* lat	Location* lon	S†	L‡	M§	C#	Slip Rate δ mm/yr Mn	Mx	Pr	T**	D††	A‡‡	Reference§§
						San Andreas							
San Andreas (Shelter Cove to San Juan Bautista)	38.5	122.8	rl	420	7.8	AA	6.9	30.0	12.0	300†‡	h	h	*Hall* [1984]b *Cummings* [1968] *Prescott and Yu* [1986] *Addicott* [1969] *Clark et al.* [1984]
San Andreas- (Los Altos to San Juan Bautista)	37.1	121.9	rl	85	7.0	AA			12.0	140†‡	h	h	*Prescott et al. (1981)* *Hall* [1984]b
San Andreas (San Juan Bautista to Bitterwater)	36.6	121.2	rl	86	7.0	AA	10.0	39.0	5.0	228	h	h	see the appendix and *Burford and Harsh* [1980] *Clark et al.* [1984]
San Andreas (Bitterwater to Slack Canyon)	36.2	120.7	rl	51				33.9	0.01				*Burford and Harsh* [1980]
San Andreas (Slack Canyon to Cholame)	35.9	120.4	rl	37	6.6	AA			33.9	28†‡	h	h	*Bakun and McEvilly* [1984]
San Andreas (Slack Canyon to Hwy 58)	35.7	120.2	rl	85	7.0	AA			33.9	140†‡	h	h	*Sieh* [1984] *Sieh and Jahns* [1984]
San Andreas (Slack Canyon to Cajon Pass)	35.2	119.0	rl	337	7.7	AA	5.8	67.0	33.9	345†‡	h	h	*Rust* [1982a,b]c *Sieh* [1984]
San Andreas (Hwy. 166 to Cajon Pass)	34.6	118.4	rl	177	7.4	AA				360†‡		h	*Sieh* [1978a,1984]
San Andreas (Cajon Pass to Salton Sea)	33.9	116.7	rl	210	7.5	AA	10.0	35.0	25.0	170†‡	h	h	*Weldon and Sieh* [1985] *Rasmussen* [1982] *Keller et al.* [1982] *K. E. Sieh* (personal communication, *1986)*

* Location of fault. Coordinates mark approximate latitude (°N) and longitude (°W) of fault midpoint.

• Fault name assumed without reference to earlier studies.

† Fault type (e.g., reverse (r), normal (n), right-lateral (rl), left-lateral (ll), right-reverse (rr), left-reverse (lr), right-vertical (rv), left-vertical (rv), right-normal (rn), left-normal (ln)).

‡ Fault length (kilometers).

§ Moment-magnitude M_w of earthquake expected for rupture of entire fault length, estimated with slip rate dependent empirical relations between seismic moment M_o and fault length in Figure 2, and assuming the empirical relation $\log M_o = 1.5M_w + 16.1$ [*Hanks and Kanamori,* 1979].

Slip rate class: AA ⩾ 10 mm/yr; A ⩾ 1 mm/yr; B ⩾ 0.1 mm/yr; C ⩾ 0.01 mm/yr. Faults are assumed to be class C when no slip rate data are available and assigned a slip rate equal to 0.01 mm/yr for hazard map development.

δ The minimum (Mn) and maximum (Mx) values of slip rate reported by referenced investigators. The preferred (Pr) value of rate, when listed, is used for estimating T. Otherwise, T is estimated with either the minimum, maximum, or average of the minimum and maximum reported rates, depending on which limits are placed on the respective faults.

** Repeat time of rupture for each fault estimated with equation (1) unless marked by †‡ . Repeat times estimated to be greater than 10,000 years are not listed.

†† The reported slip rate is determined primarily from the horizontal (h), vertical (v), dip-slip (d), or the total (t) component of displacement.

‡‡ Youngest feature used to determine slip rate and/or repeat time along entire fault zone; Holocene (h), Pleistocene (q), Pliocene (p), or Miocene (m). Range of slip rates may reflect rates determined from older offsets as well.

§§ References regarding location, slip rate, and repeat time of each fault. A letter a, b, or c following the reference indicates that values of slip rate listed are those reported by a, *Anderson* [1979]; b, *Bird and Rosenstock* [1984]; and c, *Clark et al.* [1984], respectively.

†‡ Based on historical information, trenching studies, or other geological inferences, rather than equation (1). Cases are discussed in the appendix.

Clark fault is about 19 km, whereas total horizontal separation across the Coyote Creek and Buck Ridge faults is about 5-6 km. For the hazard analysis, slip rates of the individual faults are assumed to be approximately proportional to the total separation documented across each fault, though it is recognized that no evidence is reported to document the relative youth of the three faults. The Buck Ridge and Coyote Creek faults are accordingly assigned slip rates of 2.0 mm/yr for the hazard analysis.

The 30-km section of fault that broke during the magnitude 6.8 earthquake in April of 1968 (Table 2) is here referred to as the Borrego Mountain fault (Figure A2). The Borrego Mountain fault is the only major mapped fault strand to continue immediately south of the Clark, Coyote

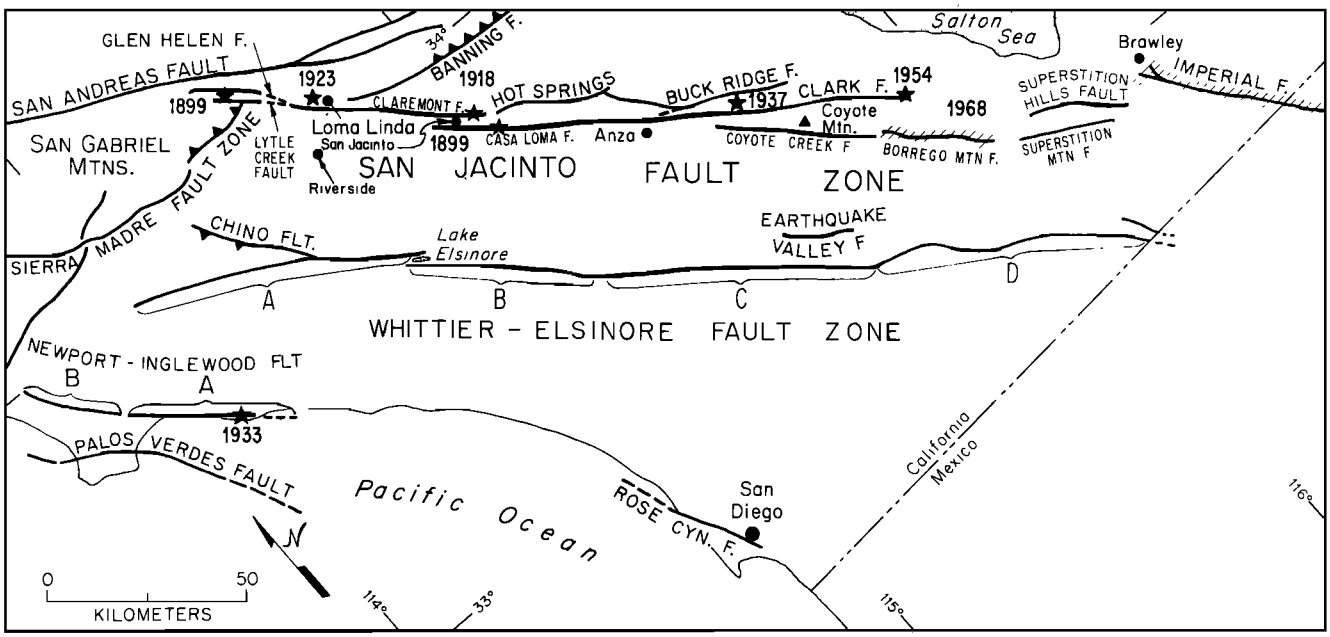

Fig. A2. Map showing location of Quaternary faults and fault segments within the Peninsular Ranges which are listed in Table A1 and used in the development of seismic hazard maps. Limits of assumed segment lengths for the Whittier-Elsinore fault and Newport-Inglewood fault zones are denoted by brackets. Epicenters of historical earthquakes with $M \geq 6$ are shown by stars. The faults that produced surface rupture during the 1968 Borrego Mountain and the 1940 and 1979 Imperial earthquakes are hatchered. Teeth are placed on hanging wall side of thrust and reverse fault traces.

Creek, and Buck Ridge faults. *Clark et al.* [1972] estimated an average recurrence interval of about 200 years for tectonic events like that of the 1968 by comparing vertical components of displacement in 1968 with earlier movements recorded in offset sediments of ancient Lake Cahuilla that ranged in age from 860 to 3080 years. With the assumption that earthquakes along this fault prior to 1968 were associated with the ratio of horizontal to vertical slip observed in the 1968 event, *Clark et al.* [1972] further interpreted vertical rates of deformation to suggest a right-lateral offset rate of about 3 mm/yr. *Sharp* [1981] cites new stratigraphic features found in a series of trenches and further reinterprets the observations of *Clark et al.* [1972] to estimate that the rate of slip has averaged 2.7-5.0 mm/yr during the last 435 years. In light of *Sharp's* [1981] data, *Clark et al.*'s [1972] observations are consistent with a lesser repeat time than they originally reported, with best estimates ranging roughly between about 100 and 200 years. *Sharp* [1981] also reports a right-lateral offset of 10.9 m measured on a buried stream channel that is between 5060 and 6820 years of age, yielding the most direct measure of horizontal slip rate along this segment equal to 1.6-2.2 mm/yr. *Louie et al.* [1985] report that aseismic creep at a site along the fault has averaged about 5 mm/yr since 1971 but acknowledge that the rate may partly reflect triggered slip due to the 1968 Borrego Mountain and 1979 Imperial earthquakes. All of the reported rates of slip are less than the rate found farther to the north by *Sharp* [1981]. The discrepancy implies that a significant amount of deformation at this latitude is being taken up along faults or structures that are not presently recognized or understood. For construction of the hazard maps, this segment is assumed to rupture each 150 years.

Strike-slip deformation south of the Borrego Mountain segment is apparently accomodated by the motion along the subparallel Superstition Hills and Superstition Mountain faults. Aseismic creep of 0.5 mm/yr is documented by *Louie et al.* [1985] at a site along the Superstition Hills fault between May 1968 and 1979. Surface displacements ranging up to about 20 mm were also triggered on the Superstition Hills fault by the 1968 Borrego Mountain and 1979 Imperial Valley earthquakes (Table 2), respectively [*Fuis*, 1982]. However, no geologic evidence that limits the slip rate of either fault over longer periods of time is recorded in the literature. Lacking firm evidence, it is speculated that the cumulative seismic slip rate for these two faults is approximately equal to the 1.6-2.2 mm/yr assessed by *Sharp* [1981] just to the north along the Borrego Mountain fault. Thus the seismic slip rate of each fault is assumed for the hazard analysis to equal 1.0 mm/yr.

Imperial Fault. The Imperial fault strikes southward from near Brawley to across the Mexican Border. The fault was the site of large earthquakes in 1940 and 1979 (Table 2), each of which produced primary surface ruptures north of the U.S.-Mexico border. A minimum slip rate of 20 mm/yr is inferred for the section of fault that broke in 1979, when it is assumed that strain released during the 1979 earthquake was accumulated during the period subsequent to the 1940 earthquake [*Clark et al.*, 1984]. Isoseismal studies also yield some evidence that an earthquake in 1915 ruptured the northern extent of the Imperial fault [*Toppozada and Parke*, 1982]. The average return time between the three earthquakes is 32 years. It is, however, important to note that surface ruptures during 1979 were limited to the fault north of the border [*Sharp*, 1982], whereas the 1940 earthquake also ruptured some 30 km into Mexico [*Brune and Allen*, 1967; *Trifunac*, 1972]. Preliminary results of a trenching study along the fault trace south of the 1979 rupture imply that no slip occurred during at least the 700 years preceding the 1940 event [*Clark et*

al., 1984]. *Clark et al.* [1984] note that this result and observations of maximum observed surface offsets in 1940 imply a maximum slip rate of 8.6 mm/yr just south of the 1979 surface rupture. The hazard maps are constructed assuming that the Imperial fault ruptures in events equivalent in location and length to the 1979 and 1940 earthquakes each 32 and 700 years, respectively.

Elsinore fault zone. The Elsinore fault zone (including the Whittier fault) strikes northwest from the Mexican border a distance of about 250 km (Figure A2). Displacement across the fault zone is predominantly right-lateral. It may be inferred from the relations in Figure 2 that complete rupture of this fault zone would produce average coseismic offsets of 2.5-7.0 m. *Pinault and Rockwell* [1984] recently interpreted offset geomorphic features along the southern Elsinore to indicate the repeated occurrence of several earthquakes during prehistorical time. The average coseismic offsets inferred for the earthquakes were interpreted to equal 1.4 m, less than would be expected from a complete rupture of the Elsinore fault. With this scant evidence, it is assumed that the Elsinore fault is characterized by moderate-sized earthquakes that do not rupture the entire extent of the fault zone and that the location and extent of future earthquake ruptures will correspond to the segments labeled A-D in Figure A2. The segments are chosen so that each is separated by a major step or bend in the fault trace. The range of slip rates reported for the Elsinore fault range from about 1 to 9 mm/yr (Table A1). Limitations placed upon the rate of slip across the Elsinore have generally been imposed by the displacement of features older than Quaternary age (Table A1). The only rate inferred from displacement of rocks of Quaternary age or younger was recently reported by *Pinault and Rockwell* [1984]. They inferred a slip rate of 4 mm/yr along segment D. The rate of 4 mm/yr is assumed here as representative of the entire fault trace, though it is emphasized that data bearing on the extrapolation of this rate along the entire fault length are few and conflicting. For example, *Clark* [1982] discusses geomorphic evidence to suggest fault activity is relatively less to the north of segment D. Preliminary reports of work along segment A, however, appear consistent with slip rates of similar order to those reported along segment D. Specifically, *Millman and Rockwell* [1985] recognize a 1.6-km offset of alluvial deposits they interpret to be mid-Quaternary in age and *Rockwell et al.* [1985] interpret sediments exposed in trenches to suggest a 200- to 300-year recurrence interval for ground rupturing earthquakes.

Displacement across the Chino fault is right-reverse [e.g., *Heath et al.*, 1982]. *Heath et al.* [1982] conclude that the Chino fault is not the principal extension of the Elsinore fault zone. Reported values of slip rate are low, ranging from 0.02 to 0.2 mm/yr. The hazard maps are constructed assuming 0.1 mm/yr of slip across the Chino fault.

Newport-Inglewood, Palos Verdes, and Rose Canyon faults. The Newport-Inglewood fault strikes southeast and offshore of Palos Verdes peninsula (Figure A2). Attention is limited here primarily to where the fault is exposed on land. The fault produced the magnitude 6.3 Long Beach earthquake of March 10, 1933 [*Richter*, 1958]. The epicenter of that event is shown in Figure A2. Aftershocks of the 1933 earthquake apparently concentrated along the approximately 30-km segment of the fault extending northwest of the epicenter [*Benioff*, 1938; *Richter*, 1958]. It is assumed here that the 1933 aftershocks delimit a characteristic rupture length for earthquakes along the Newport-Inglewood fault zone. Thus, in Figure A2, segment A of the Newport-Inglewood fault marks the inferred extent of rupture during 1933, and segment B is assumed to be capable of producing an event of size similar to the 1933 earthquake. Right-lateral slip has averaged 0.3-0.8 mm/yr since the Pliocene [*Anderson*, 1979; *Bird and Rosenstock*, 1984]. Estimates of slip rate from offset features of Holocene to Pleistocene age range between 0.1 and 6.0 mm/yr, with average and better limited values equal to about 0.6 mm/yr [*Clark et al.*, 1984]. These latter values, however, reflect only the vertical component of slip, and hence the total rate may be greater [*Clark et al.*, 1984]. The hazard analysis is made assuming that the slip rate equals 1.0 mm/yr.

The Palos Verdes fault also strikes southeast and offshore of Palos Verdes Peninsula (Figure A2). The onshore reach of the fault is assumed to be the central portion of a fault segment capable of producing earthquakes also similar in size to the 1933 Long Beach event. The segment extends from north of the Palos Verdes peninsula southward across the peninsula to about 15 km offshore (Figure A2), where beds considered of Holocene age are recognized by marine reflection methods to be offset by the fault [*Darrow and Fisher*, 1983]. Reported slip rates range between 0.02 and 0.7 mm/yr but reflect only the vertical component of movement (Table A1). The total may be greater [*Clark et al.*, 1984]. The upper bound of 0.7 mm/yr is used for the hazard analysis.

The Rose Canyon fault zone traverses San Diego and extends offshore to the northwest (Figure A2). *Greene et al.* [1979] mapped the northward extension of the fault zone with marine seismic reflection techniques. The northernmost point of the fault zone shown in Figure A2 corresponds to a pronounced right step in the fault system. It is assumed for the analysis that the 50-km stretch of the fault displayed in Figure A2 is capable of rupture during a single earthquake. *Anderson* [1979] and *Bird and Rosenstock* [1984] site offset Pliocene rocks reported by *Kennedy* [1975] to imply a 1-2 mm/yr right-lateral slip rate. Marine terraces of Pleistocene age offset in a right-reverse sense suggest a 1.2-1.5 mm/yr slip rate [*Clark et al.*, 1984]. Preliminary reports of trenching across strands within the fault zone indicate no movement during about the last 1-8 thousand years [*Artim and Streiff*, 1981; *Ferrand et al.*, 1981], but it is not clear whether the trenches span the entire zone of faulting. The maps are constructed assuming a 1.5 mm/yr slip rate.

Transverse Range

Central area. The Raymond, Hollywood, and Santa Monica faults strike southwesterly through the Los Angeles region (Figure A3). Each fault is assumed capable of complete rupture during a single earthquake for construction of the hazard maps. The Raymond fault was most recently studied by *Crook et al.* [1986]. Data obtained from excavations across the fault trace led them to estimate an average repeat time of rupture equal to 3000 years. The slip rates listed in Table A1, interpreted within the framework of

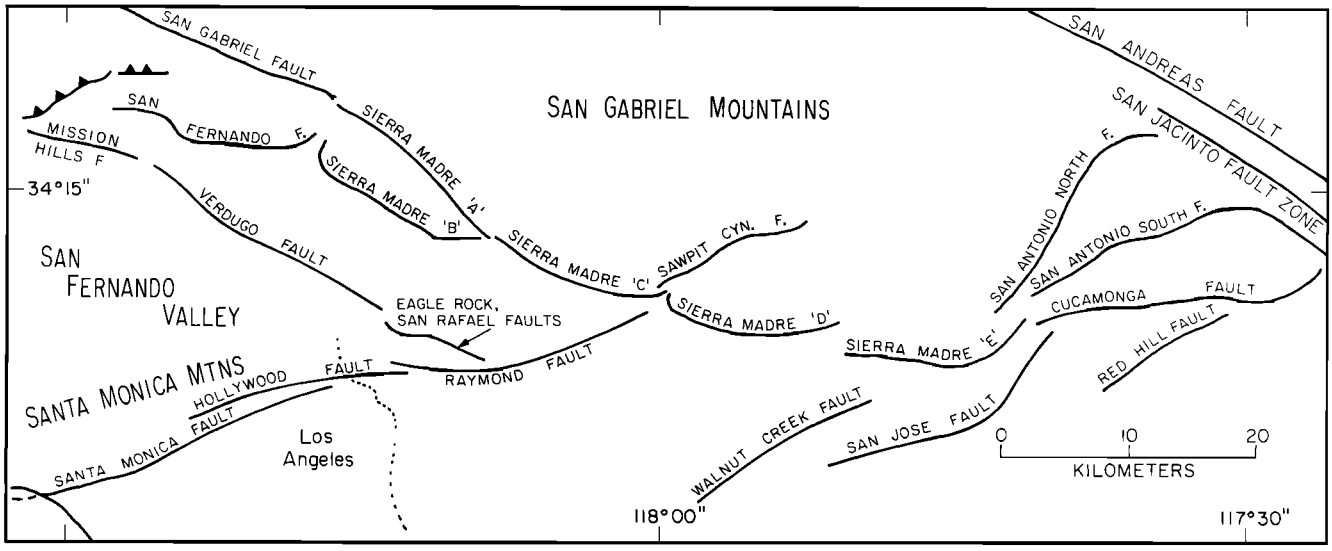

Fig. A3. Map showing location of Quaternary faults and fault segments in central Transverse Ranges which are listed in Table A1 and used in the development of seismic hazard maps. Discontinuities between segments of Sierra Madre and associated fault zones are largely schematic.

equation (1), are used to estimate the occurrence rate of rupture along the Hollywood and Santa Monica faults.

The Sierra Madre fault zone. The southern base of the San Gabriel mountains is composed of a series of north dipping thrust and reverse faults (Figure A3), one of which ruptured in the magnitude 6.6 San Fernando earthquake of February 9, 1971 (Table 1). The 1971 earthquake ruptured along a 20-km segment of the range front, labeled the San Fernando fault in Figure A3. *Procter et al.* [1972] observed that the Sierra Madre fault zone is composed of a number of discrete arcuate segments, each separated by a transverse structural discontinuity. *Ehlig* [1975] argued that due to the difference in structural character of the segments, it is unlikely that a single earthquake will be associated with rupture along more than one of the segments. The observation of *Crook et al.* [1986] that the freshness of fault related morphology varies significantly between different segments lends support to *Ehlig*'s [1975] hypothesis. These observations and arguments are accepted in this analysis. Accordingly, the segmentation of the Sierra Madre fault zone in Figure A3 and Table A1 is based on the work of *Procter et al.* [1972] and *Ehlig* [1975].

Sites along the San Fernando fault (Figure A3) were excavated immediately following the 1971 earthquake by *Bonilla* [1973]. He reported evidence of a prior rupture along the same trace between 100 and 300 years ago. A 200-year repeat time is assigned to the San Fernando fault. *Crook et al.* [1986] searched for evidence of Holocene displacements along segments of the Sierra Madre labeled 'A,' 'B,' 'C,' and 'D' in Figure A3. They recognized abundant evidence of late Pleistocene fault activity but observed no Holocene displacements. *Crook et al.* [1986] inferred from their studies that a 5000-year repeat time was probably representative of the return time of rupture along each segment. Such is the basis for assigning a 5000-year repeat time for segments A, B, C, and D of the Sierra Madre fault zone. The same return time is assumed for segment E, though site-specific studies of the Quaternary activity of this segment are not known to the author.

The Cucamonga fault is the easternmost segment of the Sierra Madre fault system. Geomorphic expression of fault related features along this fault imply a much greater degree of activity than found for segments immediately to the west [e.g., *Matti et al.*, 1982]. Estimates of the vertical component of slip across the fault range from 2.9 to 6.4 mm/yr (Table A1). *Matti et al.* [1982] concluded that the the height and age distribution of fault scarps along the Cucamonga fault zone is consistent with an average repeat time of 2-m displacements each 700 years.

Western area. Slip rates are reported for but a few faults in the western Transverse Ranges (Figure A4). A 3-4.5 mm/yr slip rate across the Santa Susana is implied by 3-4.5 km of reverse separation of a 1-m.y. horizon [*Yeats*, 1979]. Similar observations indicate reverse slip on the San Cayetano and Oak Ridge faults has averaged about 9.0 mm/yr and 3.5 mm/yr during the last 1 m.y., respectively [*Yeats*, 1983*a*]. Analysis of faulted alluvial fans by *Rockwell* [1983], however, suggests that slip along the San Cayetano has averaged a minimum of 2-3 mm/yr during the Holocene, and about 9 mm/yr during the last 160-200 thousand years. The San Cayetano is assigned a 5 mm/yr slip rate for the hazard analysis. Marine platforms offset by the Red Mountain fault are interpreted to show reverse slip has averaged 0.9-2.3 mm/yr during the last 45-60 thousand years (Table A1). Estimates of late Pleistocene slip rates along the Javon Canyon and Ventura faults range between about 1 and 3 mm/yr. *Yeats* [1982], however, argues that these latter two faults are not seismogenic. For that reason the two faults are here assigned a very low seismic slip rate of 0.01 mm/yr, though the argument of *Yeats* [1982] is not without question [*Sarna-Wojcicki and Yerkes*, 1982]. The Santa Ynez fault is treated here as two separate segments and divided at the Baseline fault intersection, approximately where total offset across the fault differs markedly to the east and west, respectively [*Sylvester and Darrow*, 1979]. Slip rates of 1.0 mm/yr and 0.4 mm/yr are assigned to the east and west segments of the Santa Ynez fault, respectively, based on studies summarized by *Clark et al.* [1984]. The

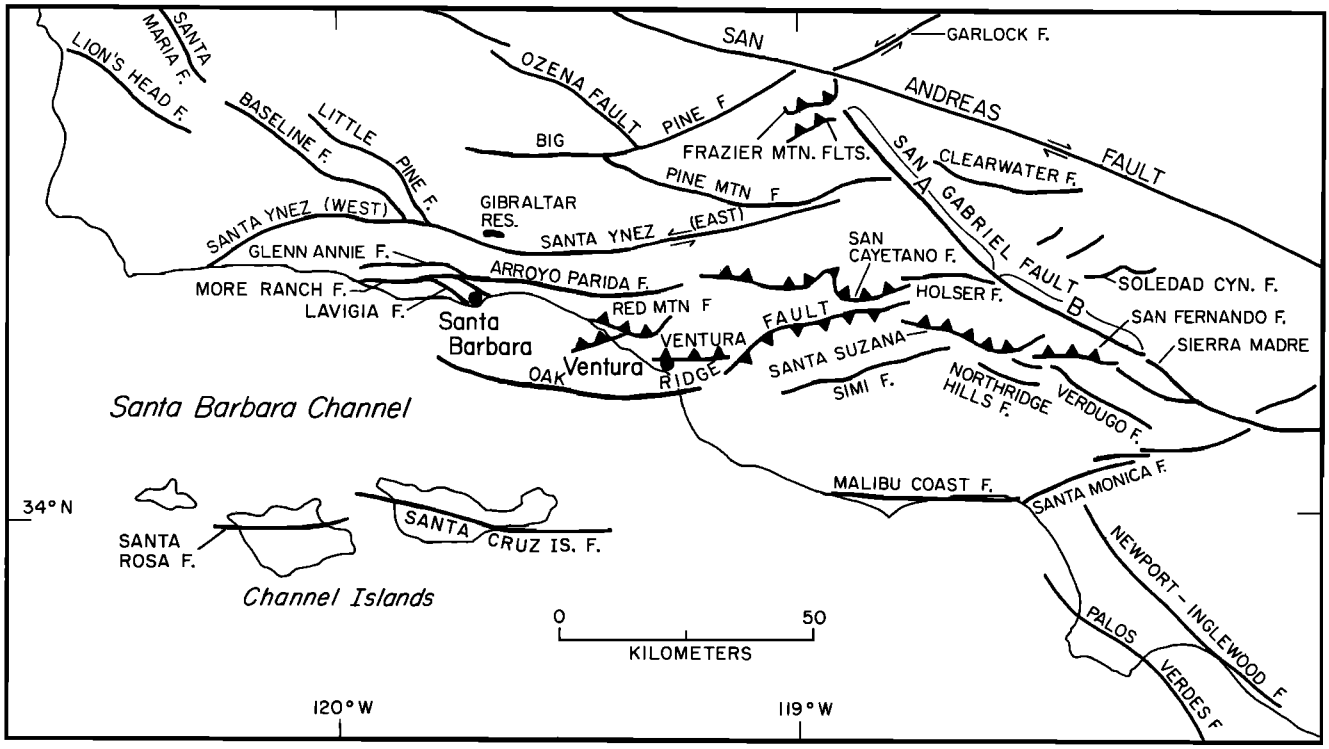

Fig. A4. Map showing location of Quaternary faults and fault segments within the western Transverse Ranges which are listed in Table A1 and used in the development of seismic hazard maps. Teeth are placed on hanging wall side of thrust and reverse faults. Sense of lateral displacement is indicated by half-sided arrows.

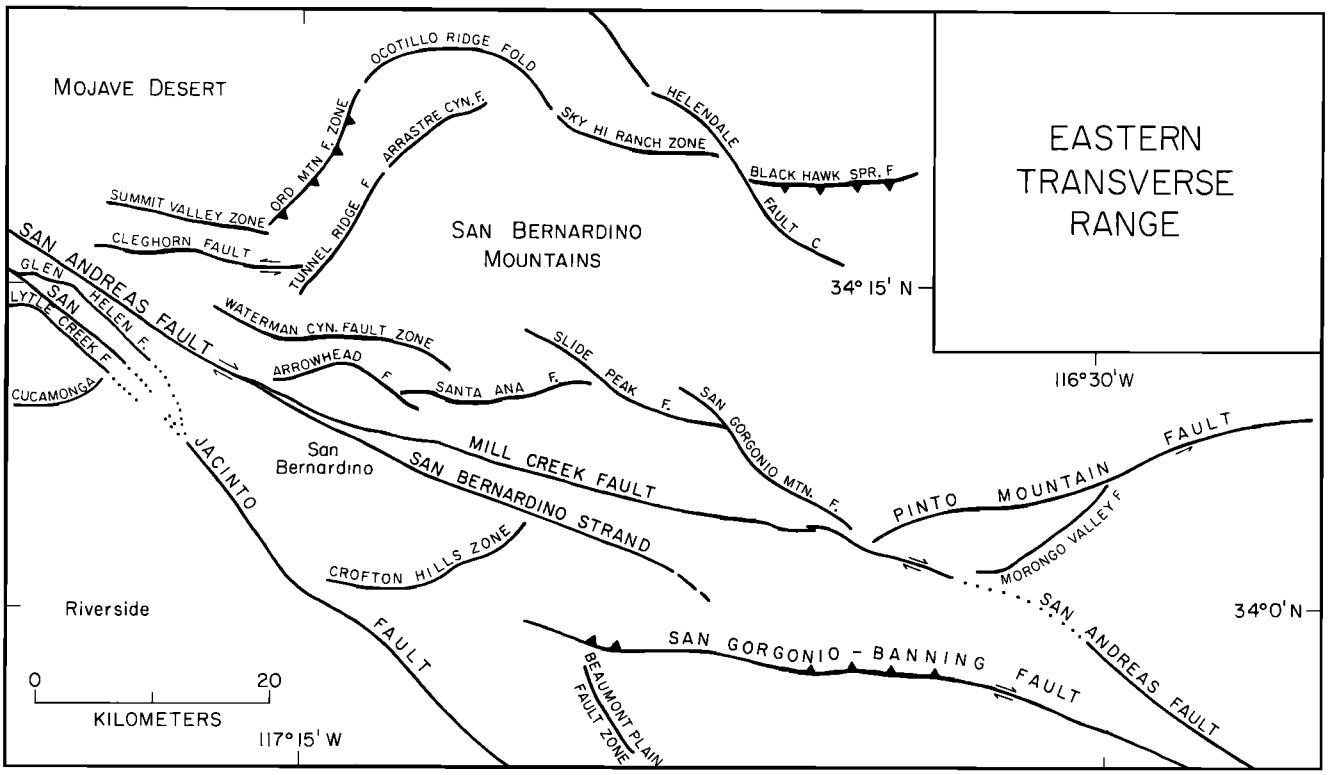

Fig. A5. Map showing location of Quaternary faults and fault segments within the eastern Transverse Ranges which are listed in Table A1 and used in the development of seismic hazard maps. Fault notation is explained in Figure A4.

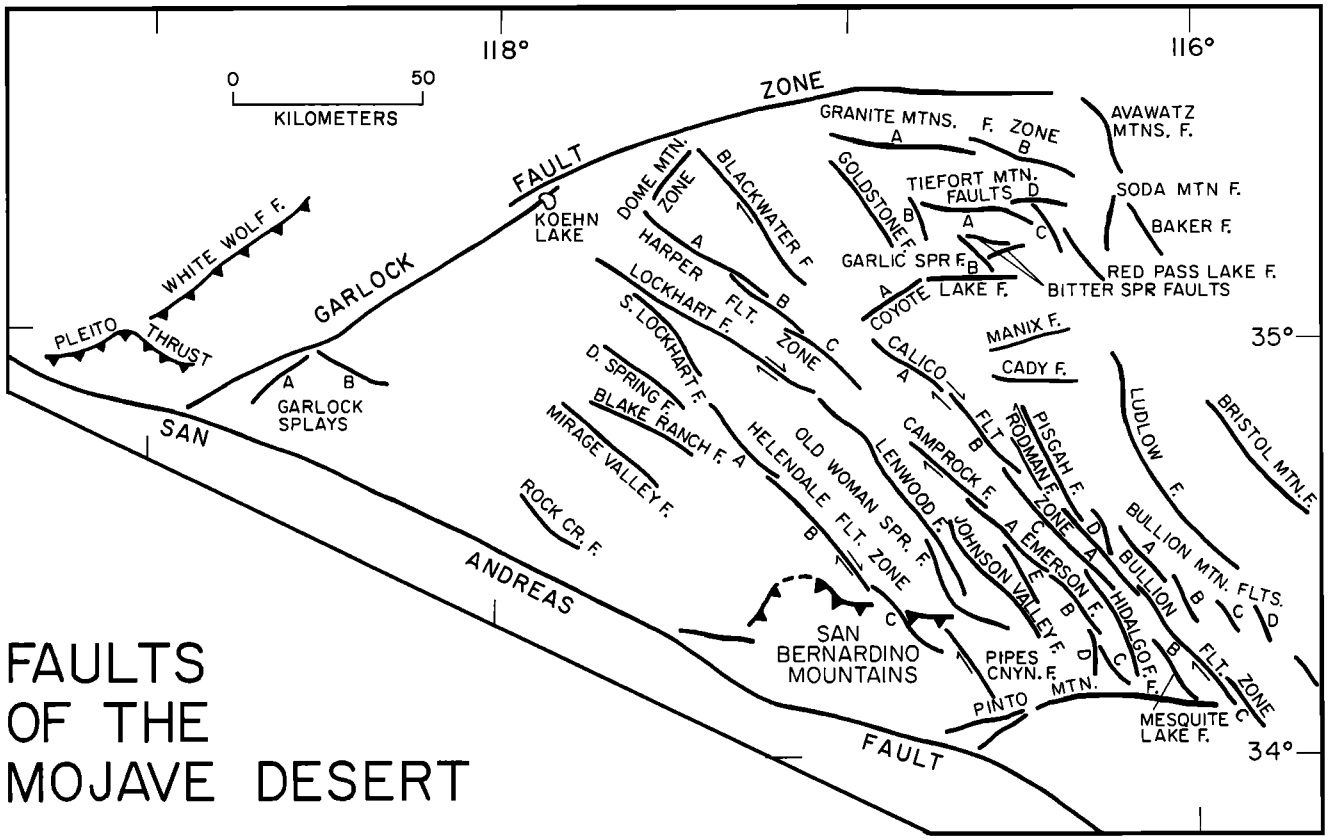

Fig. A6. Map showing location of Quaternary faults and fault segments within the Mojave Desert which are listed in Table A1 and used in the development of seismic hazard maps. Fault notation as in Figure A4.

0.35-0.40 mm/yr rate assigned to the Arroyo Parida fault (Table A1) is the vertical slip rate assessed by *Rockwell* [1983] from a study of Ventura River terraces that are offset by the fault. A speculative offset rate of 1 mm/yr is assigned to the Big Pine fault based on the documented offsets of Pliocene rocks (Table A1).

Eastern area. The eastern Transverse Range consists principally of the San Bernardino Mountains (Figure A5). Quaternary faulting along the northern San Bernardino range front was studied by *Meisling* [1984]. *Meisling* [1984] documented Quaternary displacements across the major faults that bound the the San Bernardino Mountains to the north (Figure A5) but succeeded in establishing limits of slip rate only for the Cleghorn, Ord Mountain, and Sky High Ranch faults (Table A1). The author is not aware of any published studies relating to the slip rate of faults within the southern San Bernardino mountains, and hence they are assigned a low slip rate of 0.01 mm/yr. Farther to the east, slip along the Pinto Mountain fault has reportedly averaged 0.3-5.3 mm/yr since about the Miocene (Table A1), and a slip rate of 1.0 mm/yr is assumed for the hazard analysis. The San Gorgonio, Banning, and Mill Creek faults are discussed later in the section concerning the San Andreas fault system.

Mojave Desert

Quaternary faults in the Mojave region generally show right-lateral displacements and are characterized by anastomosing and en echelon segments. The locations of structural discontinuities along strike are the basis for dividing some of the more major fault zones into smaller segments, each of which is considered to behave independently. The faults and fault segments used in computation of the hazard maps are pictured in Figure A6.

Dokka [1983] documents right-lateral displacements along the Lenwood (1.0-5.0 km), Calico (7.0-9.0 km), Rodman and Pisgah (6.4-14.4 km), and Camp Rock (1.6-4.0 km) faults. He further cites *Miller and Morton* [1980] and *Miller* [1980] for documenting simultaneous offsets along the Helendale (3.0 km) and Bristol Mountains (6.0 km) faults. The time when these displacements initiated is not well determined [*Dokka*, 1983] and may have been anywhere between about 2 m.y. and 20 m.y. ago [*Clark et al.*, 1984]. It is these values which provide the limits on the slip rates listed for these faults in Table A1. Slip rates have also been estimated for the Blackwater, Emerson, and Lockhart faults on the basis of offset Pliocene or older rocks (Table A1).

The Garlock fault defines the northern boundary of the Mojave desert, extends about 250 km in an easterly direction, and shows left-lateral displacement. Estimates of fault slip rate range from 1 to 30 mm/yr (Table A1). *Astiz and Allen* [1983] provide an extensive summary and discussion of studies relating to the earthquake history and slip rate of the Garlock fault during Holocene time. Their summary suggests that the best current estimate of the fault slip rate is 7 mm/yr, which is assumed for this analysis, and that the average recurrence interval of large earthquakes is probably

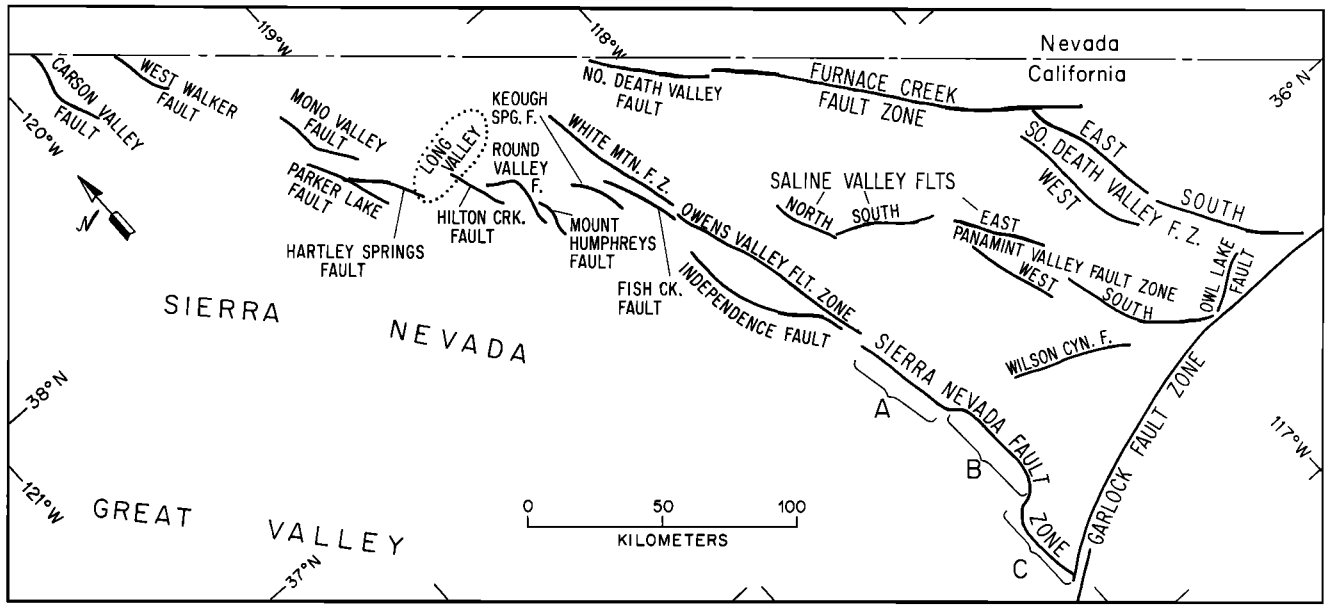

Fig. A7. Map showing location of Quaternary faults and fault segments within the Sierra Nevada and Great Basin provinces which are listed in Table A1 and used in development of the seismic hazard maps. Limits of assumed assumed segment lengths for the Sierra Nevada fault zone are denoted by brackets.

1000±500 years. The segments of the fault that strike to the east and west of a major step in the fault tract near Koehn lake (Figure A6) show distinctly different geological characteristics and seismic behavior during historical time [*Astiz and Allen*, 1983] and are treated separately in development of the hazard maps (Table A1).

Sierra Nevada-Great Basin

Few Quaternary faults are mapped within the Sierra Nevada (Figure A1). In contrast, many Quaternary faults are recognized along the eastern edge of the Sierra Nevada and within the Great Basin (Figure A7). The faults generally trend northerly, show normal and right-lateral displacements, and commonly mark the edge of long linear mountain ranges. The largest historical earthquake in this region occurred in 1872, producing surface displacements for a distance of about 100 km along the Owens Valley fault zone [*Whitney*, 1872]. Other large events, such as those recorded in Nevada during this century (Table 2), produced rupture lengths ranging from about 20 to 50 km. *Wallace and Whitney* [1984] examined the distribution of range-bounding fault scarps in central Nevada and suggested that discontinuities between individual mountain blocks may control the extent of future surface faulting events. It is that observation that provides reason here to consider several of the major fault zones in the area to be segmented. The location, segment lengths, and slip rates of faults used in this work are summarized in Figure A7 and Table A1. Only faults or fault segments of length greater than about 10 km are included for the hazard analysis, though a myriad of faults of lesser length are present and may be the source of smaller earthquakes. It also should be noted that the eastern boundary of the Sierra Nevada has been marked by volcanism during Pleistocene to recent time [e.g., *Kilbourne et al.*, 1980]. Hence some question exists whether the recurrence of earthquakes in this region is primarily controlled by regional tectonic processes or localized volcanic activity.

The White Wolf and Pleito thrust faults are located near the junction of the Sierra Nevada, Transverse Range, and Central Coast geographic provinces (Figure A6). The White Wolf fault ruptured during the magnitude 7.3 Kern County earthquake of 1952 (Table 2). *Stein and Thatcher* [1981] estimate a 3-9 mm/yr vertical slip rate for the fault based on their inference of the age (0.6-1.2 m.y) and total displacement of an ash layer that intersects the fault at depth. A 300-year repeat time is here assigned to the White Wolf fault. Based on *Stein and Thatcher*'s[1981] observation, a fault displacement rate of 3-9 mm/yr over a period of 170-450 years is sufficient to accumulate displacement equal to that produced in 1952. *Clark et al.* [1984] interpret the work of N. T. Hall to indicate that slip along the Pleito thrust has averaged between 0.2 and 14 mm/yr during the late Quaternary, though *Hall* [1984*a*] reports that a 1.3-1.4 mm/yr is most representative for the last 1500 years.

Modoc Plateau

Quaternary faults mapped within the Modoc Plateau are shown in Figure A8. Faults in this province generally strike northwestward. Only faults for which fault slip rate studies are reported are listed in Table A1 and labeled, according to fault name, in Figure A8. Those few faults generally show normal displacement. Slip rates that are reported are generally less than 1 mm/yr (Table A1). A slip rate of 0.01 mm/yr is assigned to the other mapped faults in the area. A consequence of the data and assumptions, when analyzed within the framework of equation (1), is that the expected repeat times for the separate faults in the region are largely on the order of several or more thousands of years (Table A1).

Central Coast

Quaternary faults mapped along the central coast are pictured in Figure A9. Geologic studies regarding fault slip rate are reported only for the Rinconada, San Gregorio, and Hosgri fault zones. *Bird and Rosenstock* [1984] cite the work of *Durham* [1965] and *Hart* [1976] to indicate that

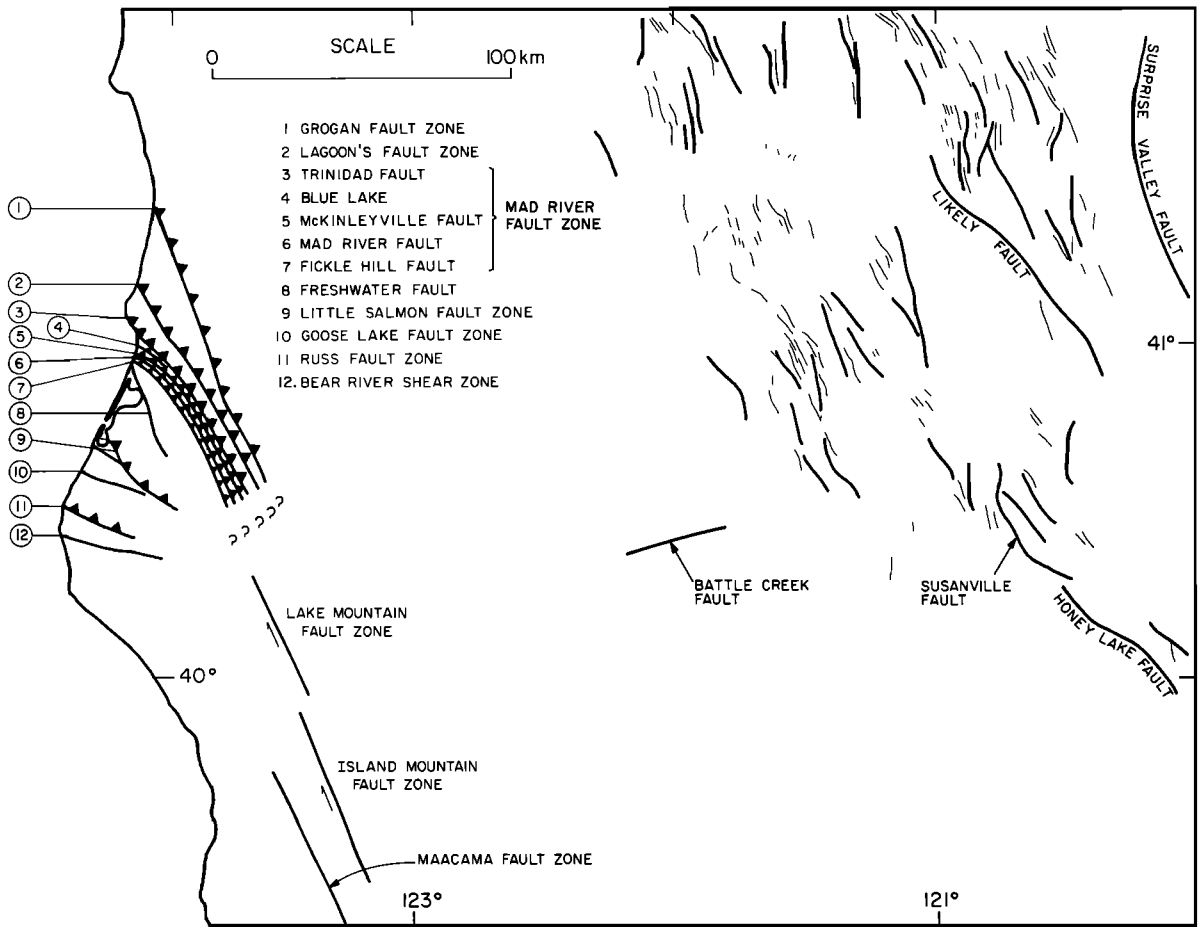

Fig. A8. Map showing location of Quaternary faults and fault segments within the Modoc Plateau and parts of the North Coast and Sierra Nevada geographic provinces (see Figure A1) that are listed in Table A1 and used in the development of seismic hazard maps. Queries indicate which southward extent of coastal thrust and reverse fault systems is not yet mapped [*Carver*, 1985; *Carver et al.*, 1982]. Unnamed faults are from *Jennings* [1975] and not listed in Table A1. Faults marked by thinner trace are not included in hazard analysis. Fault notation as in Figure A4.

right-lateral slip along the Rinconada fault zone has averaged between 2.4 and 12 mm/yr since the Pliocene. The minimum value is assumed for input to the hazard maps. It is, however, important to emphasize that estimates of slip rate based on Quaternary or younger deposits are needed to confirm whether such a rate is presently characteristic of the fault zone.

The San Gregorio and Hosgri fault zones strike a combined distance of nearly 400 km along the California coast south of San Francisco (Figure A9). Much of the fault zone is located offshore, and for that reason there remain uncertainties regarding details of the fault location, the continuity of the fault zone, the offset history, and the rate of displacement across the zone during Quaternary time. A synopsis of these problems is recounted by *Silver* [1978]. Estimates of the total right-lateral offset across the San Gregorio fault range from 80-115 km since Miocene time [*Graham and Dickinson*, 1978; *Silver*, 1974]. *Hall* [1975] argues for 80 to 100 km of post-Miocene offset along the Hosgri fault, though his estimate has been questioned [e.g., *Hamilton and Willingham*, 1977]. The San Gregorio fault was originally mapped on that section of land between Point Año Nuevo and the town of San Gregorio [*Branner et al.*, 1909; *Graham and Dickinson*, 1978]. Marine seismic reflection data are interpreted to show that the fault extends offshore to the north, through Pillar Point, to a point near the Golden Gate where it joins the San Andreas [e.g. *Graham and Dickinson*, 1978]. South of Point *Año* Nuevo, seismic profiling shows the fault to cross outer Monterey Bay and into Carmel submarine canyon near Point Sur [*Greene et al.*, 1973]. *Greene et al.* [1973] inferred that the San Gregorio trace turns landward near Point Sur to join the Palo Colorado fault. More recently, *Graham and Dickinson* [1978] interpreted geologic relations to indicate that displacements along the San Gregorio fault are not transferred to the Palo Colorado fault but, rather, are conveyed southward across Point Sur. *Silver* [1978] reviewed aeromagnetic data to conclude that "the bulk of evidence at present favors, or at least allows, the continuation of the fault zone through and to the south of the San Simeon region." The southern terminus of the San Gregorio-Hosgri fault zone is not known. It has been proposed that the fault bends into the Transverse Ranges and motion is there taken up by compression [e.g., *Hamilton and Willingham*, 1977]. *Silver* [1978] reports the suggestion that the fault is offset by east trending faults in the Santa Barbara Basin. *Crouch et al.* [1984] recently interpreted seismic reflection profiles offshore of Point Arguello to indicate major post-Miocene deformation that may mark the continuation of the San Gregorio-Hosgri system, though their observations indicate thrust movement, in contrast to indications that the predominant mode of displacement to the north is right-

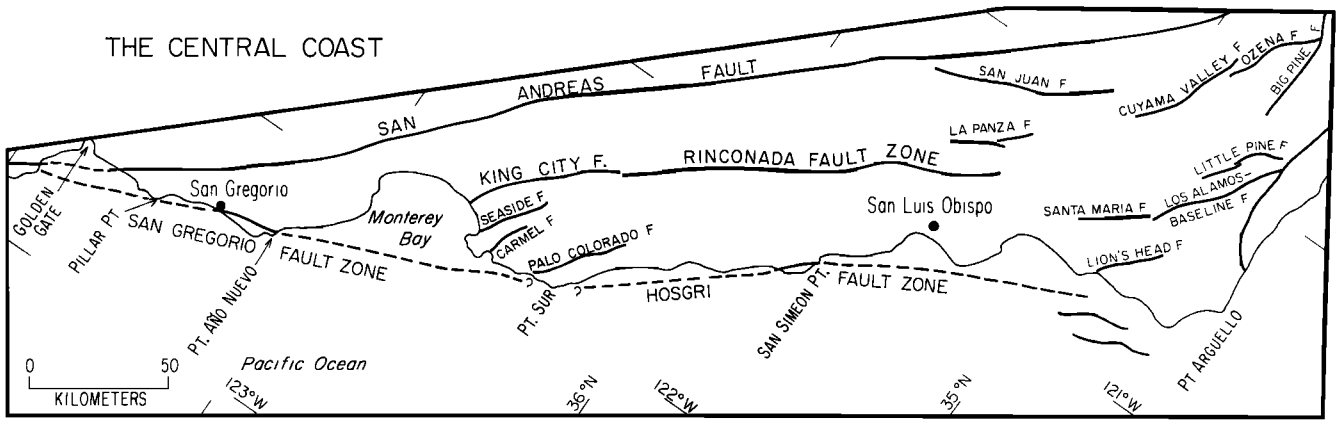

Fig. A9. Map showing location of Quaternary faults and fault segments within the Central Coast province of California which are listed in Table A1 and used in the development of seismic hazard maps. Reasons to infer offshore (dashed) extent of the San Gregorio and Hosgri fault zones are summarized in text.

lateral [e.g., *Graham and Dickinson*, 1978]. For the hazard analysis the junction of the two fault zones is placed at Point Sur, and each is treated as a continuous and independent seismic source.

Fault slip rate estimates along the San Gregorio fault zone are the result of studies near Point Año Nuevo, where the fault strikes onshore and is composed of several subparallel strands [*Clark et al.*, 1984]. Summation of the late Quaternary offset rates across the active strands range from about 7 to 19 mm/yr of right-lateral movement (Table A1). The estimates considered most reliable generally lie at the lower bound of that range [*Clark et al.*, 1984]. Along the Hosgri fault zone, slip rate studies are limited to the onshore stretch of the zone near San Simeon Point. Ancient marine shorelines that are offset by the Hosgri fault zone are interpreted to indicate 5-9 mm/yr of right-vertical movement during the late Quaternary (Table A1). For the hazard maps the San Gregorio and Hosgri fault zones are each assigned a 7 mm/yr slip rate.

North Coast

Calaveras-Hayward fault system. Estimates of the Holocene and historic slip rate of the San Andreas decrease northward from 32 mm/yr near Bitterwater [*Burford and Harsh*, 1980; *Sieh and Jahns*, 1984] to about 12 mm/yr along the San Francisco peninsula [*Hall*, 1984*a*]. The decrease in rate reflects a partitioning of slip to the Calaveras-Hayward fault system (Figure A10). A minimum slip rate of 1.4-7.1 mm/yr is estimated for the Calaveras fault from the offset of 3.5-m.y.-old volcanic rocks north of Hollister [*Herd*, 1979; *Page*, 1982; *Nakata*, 1977]. I am aware of no geologic estimates of slip rate for the Hayward fault. The transfer of slip from the San Andreas to the Calaveras-Hayward system is best evidenced by geodetic measurements that span the last 10-20 years [*Savage et al.*, 1973, 1979; *Prescott et al.*, 1981]. Geodetic observations show that at the latitude of the southern San Francisco Bay, the cumulative rate of relative motion across the San Andreas, Hayward, and Calaveras faults is equivalent to about 32 mm/yr of right-lateral displacement [e.g., *Prescott et al.*, 1981; *Savage et al.*, 1973, 1979]. Geodolite measurements of *Savage et al* [1979] are consistent with 17 ± 2 mm/yr of right-lateral slip across the section of Calaveras fault located south of the Hayward fault. Interpretation of geodetic measurements indicates that to the north, the 17 mm/yr of slip is divided between the the Hayward (7 ± 1 mm/yr) and Calaveras (7 ± 1 mm/yr) faults, with the remainder of motion being taken up by rotation of a large block to the east of the Calaveras fault [*Prescott et al.*, 1981].

Calaveras fault. Sites along the Calaveras fault are known to creep aseismically at rates of several millimeters per year or more [e.g., *Savage and Burford*, 1973; *Burford and Sharp*, 1982; *Prescott and Lisowski*, 1982]. Analyses of geodetic figures also show that little or no strain is accumulating within the crust adjacent to the Calaveras fault zone [e.g., *Prescott et al.*, 1981; *Prescott and Lisowski*, 1982]. A consequence of these observations is that the likelihood of a major rupture extending the length of the Calaveras fault zone appears very small [e.g., *Prescott and Lisowski*, 1982]. The Calaveras, however, has been the site of three moderate ($M \sim 6$) earthquakes during historical time [*Bakun et al.*, 1984; *Toppozada et al.*, 1981]. The apparent contradiction implies that the present configuration of geodetic networks is insufficient to resolve strains accumulated over a 10-year interval that are associated with the preparation of events on the Calaveras of about magnitude 6. Moreover, it appears, and is assumed in this analysis, that the characteristic size event along the Calaveras is about magnitude 6. The extent of historical earthquake ruptures and the location of mapped discontinuities in fault strike are thus used to divide the Calaveras fault zone into four separate segments, each assumed capable of producing moderate sized earthquakes. The segments, labeled A-D in Figure A10, are about 25-30 km in length and are discussed separately below.

Segment A corresponds to the zone of aftershocks registered by the magnitude 5.9 Coyote Lake earthquake of August 6, 1979 [*Reasenberg and Ellsworth*, 1982]. The northern end of this segment is approximately coincident with the bifurcation of the Calaveras and Hayward fault zones. The southern terminus is located at the fault intersection with the small left-lateral Busch fault, site of the magnitude 5.1 Thanksgiving Day earthquake of 1974 [*Reasenberg and Ellsworth*, 1982]. The seismic moment of

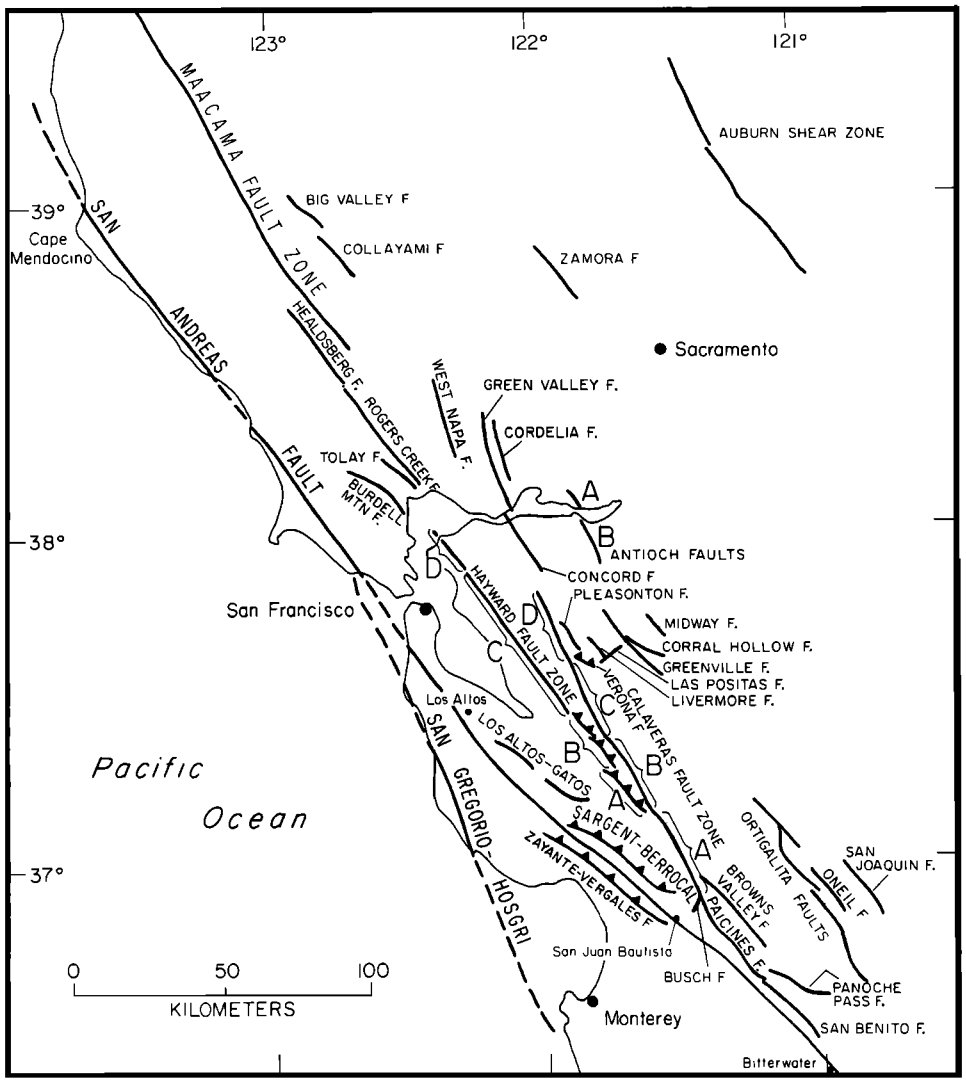

Fig. A10. Map showing location of Quaternary faults and fault segments within part of the North Coast geographic province which are listed in Table A1 and used in the development of seismic hazard maps. Limits of assumed segment lengths for the Calaveras and Hayward fault zones are denoted by brackets. Fault notation as in Figure A4.

the 1979 earthquake was $4–6\times10^{19}$ N -m [*Urhammer*, 1980; *Liu and Helmberger*, 1983; *Ekstrom and Dziewonski*, 1985]. Analysis of short-period instrumental data shows that coseismic slip during the 1979 event was primarily limited to a patch of the fault 6-14 km in length [*Bouchon*, 1982; *Liu and Helmberger*, 1983]. Little or no slip occurred outside the patch, apparently because strain release outside the patch is primarily accommodated by aseismic creep. Maximum coseismic slip on the patch during 1979 was 1.2 m [*Liu and Helmberger*, 1983]. The geodetically determined rate of slip across the fault is about 17 mm/yr [*Savage et al.*, 1979], sufficient to produce 1.2 m of slip each 70 years. Historical data also show that a similar sized earthquake ruptured this segment of the Calaveras 82 years ago on June 20, 1897 [*Toppozada et al.*, 1981; *Reasenberg and Ellsworth*, 1982]. The hazard maps are constructed assuming that this segment will produce earthquakes of $M_o=5\times10^{17}$ N -m each 82 years.

Segment B extends the length of the aftershock zone [*Cockerham and Eaton*, 1984] of the magnitude 6.1 Morgan Hill earthquake that occurred April 24, 1984. The lateral extent of rupture in 1984 is interpreted to be controlled by mapped complexities in the fault trace [*King and Nabelek*, 1985; *Bakun et al.*, 1984]. Geodetic data recorded for the Morgan Hill earthquake are consistent with a seismic moment equal to about 3×10^{18} N -m [*Bakun et al.*, 1984]. Analysis of strong ground motion data and long-period surface waves yield a similar result (*H. Kanamori*, personal communication, 1986; *Hartzell and Heaton*, 1986). *Hartzell and Heaton's* (1986) study of strong ground motion records shows that coseismic slip during the Morgan Hill earthquake was, much like observed for the 1979 Coyote Lake earthquake, confined primarily to two patches along the fault plane, each no more than about 5 km in dimension. Maximum coseismic slip on the fault plane was about 1 m. It is at this latitude that slip along the Calaveras appears to be partially transferring to the Hayward fault zone, but the exact kinematics of the slip transfer are not fully understood. Slip of about 1 m will accumulate over a period of about 60 to 150 years assuming slip rates that range from 7 to 17 mm/yr. The last event comparable in size to the 1984 earthquake to occur

on this segment of the Calaveras took place in 1911 [*Toppozada*, 1984; *Bakun et al.*, 1984], 73 years prior to the Morgan Hill earthquake. The hazard maps are constructed assuming that an earthquake with $M_o=3\times10^{18}$ N-m will rupture this segment of fault each 150 years.

The Calaveras fault extends another 55 km northward of segment B (Figure A10). Though geodetic data suggest that little, if any, elastic strain is accumulating along the fault in this region [e.g., *Prescott and Lisowski*, 1982], the possible occurrence of earthquakes similar in size to the Morgan Hill earthquake of 1984 cannot be ruled out. A moderate-sized event is, in fact, reported to have produced 8 km of surface rupture along the northern end of the Calaveras in 1861 [*Toppozada et al.*, 1981]. For computation of the hazard maps, the northern 55 km of the Calaveras fault zone is further divided into two segments (C and D in Figure A10), each similar in length to segments A and B. Segment C strikes north from segment B to a relatively sharp left bend in the fault that, in turn, coincides approximately with the point where the Verona fault strikes into the Calaveras. For the hazard analysis, segments C and D are treated identically to segment B.

Hayward fault zone. The Hayward fault zone splays off the Calaveras fault at a point south of San Francisco Bay, striking northwestward a distance of about 120 km (Figure A10). Motion across the fault is predominantly right-lateral, except along the southern reach where the fault trace is more complex and is characterized by reverse displacements [*Page*, 1982; *Bryant*, 1982]. *Prescott and Lisowski* [1982] determined strain rates from both small (1-2 km) and large (10-30 km) aperture geodetic networks that straddle the Hayward fault north of about Los Altos. They conclude that no more than 4 mm/yr of slip is presently accumulating as elastic strain in rocks adjacent to the fault, whereas the total rate of displacement measured geodetically is about 8 mm/yr [*Prescott et al.*, 1981]. The hazard maps reflect the assumption that such behavior is characteristic of the entire fault zone over the long term and that the seismic slip rate averages 4 mm/yr. The consequences of assuming other than a constant slip rate are detailed by *Prescott and Lisowski* [1982]. It is further assumed that the Hayward fault zone is composed of four segments, labeled A-D in Figure A10. The segmentation is based on the location of historical earthquake ruptures, mapped discontinuities along fault strike, and the sense of displacement registered across the fault. Segments A and B include the Silver Creek-Coyote Creek and Evergreen fault systems, respectively [*Aydin*, 1982], show predominantly reverse-type motion [e.g., *Bryant*, 1982; *Page*, 1982], and are 18-25 km long. The 50-km segment of the Hayward fault that probably ruptured in a magnitude 6.8 earthquake on October 21, 1868 [*Toppozada and Parke*, 1982] shows offset right-lateral [*Prescott et al.*, 1981] and is labeled C in Figure A10. There are also reports that a similar sized event also ruptured along segment C in 1836 [*Toppozada et al.*, 1981], though evidence for the actual location of the 1836 event is scant. Segment D is the northernmost extension of the Hayward fault zone.

Extensions of Calaveras-Hayward fault system. The Paicines and San Benito faults are the southernmost extension of the Calaveras fault zone (Figure A10). Relatively long geodolite line measurements indicate right-lateral slip rates of 8-11 mm/yr during historical time [*Ellsworth*, 1975; *Savage et al.*, 1973; *Lisowski and Prescott*, 1981]. Near-fault measurements from alignment arrays [*Harsh and Pavoni*, 1978] and short-range distance measurements [*Lisowski and Prescott*, 1981] show 5-13 mm/yr of slip at various sites along the faults. The general agreement between the long and short baseline measurements might be interpreted to indicate that most slip is taking place aseismically, rather than being accumulated as elastic strain. The data are too few, however, to yield any firm conclusion concerning the seismic behavior of these faults. For present purposes, the faults are speculatively assigned a 1 mm/yr seismic slip rate.

The Concord and Green Valley faults are the right-step northward continuation of the Calaveras fault zone [*Page*, 1982]. Alignment array measurements show an average of 4 mm/yr of fault creep at a site along the Concord fault [*Harsh and Burford*, 1982]. *Sharp* [1973] also documents a number of offset cultural features within the city of Concord that may be interpreted to indicate a similar or greater value of creep. For the hazard analysis, the assumption is made that the faults are accumulating slip at a rate of 4 mm/yr, but it is emphasized that there are presently no geologic data available that directly bear upon the correctness of this assumption.

North of San Francisco bay, the Rogers Creek, Healdsberg, Maacama, Lake Mountain, and Island Mountain fault zones (Figures A8 and A10) exhibit landforms indicative of geologically recent strike-slip movement [*Herd*, 1978; *Herd and Helley*, 1977; *Pampeyan et al.*, 1981], but geologic slip rates for the faults are not reported. The faults appear to mark the northward continuation of the Hayward fault zone [*Herd*, 1978]. *Prescott and Yu* [1986] report geodetic observations spanning a 10-year period that are consistent with such an interpretation. They observe that total right-lateral displacement distributed across a 60-km-wide zone north of San Francisco that extends between and includes the San Andreas and Green Valley faults is, within uncertainties, equivalent to the rate determined by *Prescott et al.* [1981] for the San Andreas-Hayward-Calaveras fault system south of San Francisco. An isolated measure of fault creep equal to 2 mm/yr along a strand of the Maacamma fault zone near 39.5°*N* is reported by *Harsh et al.* [1978]. The geodetic data reported by *Prescott and Yu* [1986] prohibit large amounts of fault creep, at least south of about 39°*N*. Geodetic data indicate that right-lateral slip along the Hayward fault occurs at about 7 mm/yr [*Prescott et al.*, 1981]. For the hazard analysis, the same rate is assumed to be characteristic of the northward extensions of the Hayward fault zone.

Quaternary faults north of Cape Mendocino and within the coastal region are predominantly west to northwest trending, northeast dipping, reverse and thrust faults (Figure A8) *Carver et al.*, 1982; *Carver*, 1985]. The distance the faults extend offshore is unknown, though a number of faults showing similar strike are identified offshore by *Field et al.* [1980]. It appears that this set of coastal reverse and thrust faults marks a northward continuation of the Lake Mountain-Island Mountain fault zone [*Herd*, 1978], though more mapping is necessary to determine the exact relation between the two fault regimes [*Carver*, 1985]. To construct the hazard maps, only the onshore extent of the faults as

pictured in Figure A8 is considered. *Carver* [1985] reports that the cumulative displacement rate across the Mad River fault zone has averaged about 4 mm/yr during late Quaternary time. Geologic work relating to fault slip rate is also reported for the Little Salmon, Goose Lake, and Mad River fault zones (Figure A8) and summarized in Table A1.

San Andreas Fault

The San Andreas fault is perhaps the most studied fault in California. The fault produces right-lateral offsets and extends from Cape Mendocino to the Salton Sea, a distance of about 1000 km. Seismological, geodetic, and geological information has led a number of investigators to conclude that the seismic behavior of the San Andreas varies markedly along strike [e.g., *Allen*, 1968; *Sieh and Jahns*, 1984]. The San Andreas, for example, displaces stream channels in the Carrizo Plain. Geomorphologic and geologic analyses of the displaced channels indicate that slip across the fault in the Carrizo Plain takes place during earthquakes that occur every 240-450 years and produce displacements of the order of 8 m. Earthquake displacements are, however, much smaller and more frequent along a stretch of the San Andreas near Parkfield. Rupture of the San Andreas near Parkfield since 1857 is reported to occur on average every 22 years [*Bakun and McEvilly*, 1984]. Seismological and geodetic analysis of the more recent earthquakes in this sequence shows that coseismic slip during the Parkfield events is characteristically an order of magnitude less than observed in the Carrizo Plain, averaging not more than about 30 cm [*Scholz et al.*, 1969]. The San Andreas may be characterized as a number of segments based on observations such as these, each segment being characterized by a different mode of seismic behavior and, in turn, posing a different long-term seismic hazard. The location, length, and expected repeat time of rupture of the segments used as input to the hazard maps are illustrated in Figure A11 and, from north to south, are discussed below.

Shelter Cove to San Juan Bautista. This segment of the fault broke during the San Francisco earthquake of 1906 [*Lawson*, 1908; *Sieh*, 1978*b*; *Thatcher*, 1975]. Coseismic displacements in 1906 averaged 2.5-5.0 m between Los Altos and Point Arena and a significantly less 0.5-1.5 meters south of Los Altos. Northward of Point Arena the fault is predominantly offshore, except for a small segment at Shelter Cove, where no information of the average coseismic slip exists. *Hall* [1984*b*] interprets a displaced channel on the San Francisco Peninsula, about 20 km north of Los Altos to suggest a late Holocene fault slip rate of about 12 mm/yr. Offsets of a facies of the Santa Clara formation between San Juan Bautista and San Francisco has led *Cummings* [1983] to estimate that the average rate of offset across the San Andreas has averaged about 8 ± 3 mm/yr during the last ~450,000 years.Recent geodetic surveys spanning the fault near Los Altos, during the period of 1970-1980, show strain rates that imply that 12 mm/yr of slip deficit is presently accumulating along the fault [*Prescott et al.*, 1981]. Recent geodetic surveys near Point Reyes, show similar results [*Prescott and Yu*, 1986].

Hall [1984*b*] noted that approximately five 1906-type offsets are necessary to explain the total offset of a 1130 ± 160 year old stream channel located between San Francisco and Los Altos and from that inferred a 224 ± 25 year average repeat time for 1906-type earthquakes. *Hall et al.* [1983] conducted trench studies of the San Andreas near Point Reyes and estimated the maximum return time of slip events to equal 360 ± 25 years. The average repeat time of rupture along this fault segment estimated with equation (1) is 313 years, assuming that 12 mm/yr is representative of the slip rate along the entire length of the fault segment. The average of these three estimates, 300 years, is used in formulating the seismic hazard maps.

Los Altos to San Juan Bautista. The smaller coseismic offsets (0.5-1.5 m) observed along this segment in 1906, as compared to north of Los Altos (2.5-5.0 m), give reason to further examine this stretch of the fault. Geologic and geodetic data indicate that slip to both the north and south of Los Altos occurs at about 12 mm/yr. If, as observed in 1906, it is assumed that coseismic offsets along this segment of the fault are characteristically smaller than occur to the north of Los Altos, it also requires that coseismic offsets be relatively more frequent along this segment. For input to the hazard maps, it is assumed that this segment also ruptures during the interseismic period between 1906-type events. It may be interpreted with equation (1), assuming a 12 mm/yr slip rate, that this 85-km segment will accumulate sufficient strain to produce an earthquake on average each 95 years. For the hazard maps then, rupture limited to this segment is assumed to occur each 140 years. Thus, in combination with the occurrence of 1906-type events, the hazard maps reflect an interpretation that this segment will experience large earthquakes each 95 years.

Historical documents provide evidence that a major earthquake also ruptured along the Los Altos to San Juan Bautista segment of the fault in 1838 [*Louderback*, 1947]. The 1838 earthquake is important for two reasons. The relatively short period of 68 years between 1838 and 1906 provides support for the mode of fault behavior assumed for this region. Further, accommodation of slip in this segment during 1838 may in part explain the relatively small coseismic slip observed here in 1906 as compared to farther north. This latter interpretation is, however, complicated and uncertain. *Louderback*'s [1947] account of the 1838 event indicates the event extended to the north of Los Altos as well, perhaps even to the north of San Francisco. *Louderback* [1947] further noted that the intensity of shaking in Monterey was greater in 1838 than in 1906 and on that basis, suggested that rupture during 1838 may have even extended south of San Juan Bautista. Nonetheless, the extent and variations in slip observed for the 1906 earthquake are reason to suggest the mode of fault behavior differs in this segment as compared to north of Los Altos.

San Juan Bautista to Bitterwater Valley. A late Holocene slip rate of about 34 mm/yr is estimated by Sieh and Jahns [1984] for the San Andreas fault within the Carrizo Plain. Aseismic creep is occurring at rates up to 32 mm/yr between Bitterwater Valley and Slack Canyon [*Burford and Harsh*, 1980]. North of about San Juan Bautista, however, both geologic and geodetic studies provide evidence of only about 12 mm/yr of slip. [Hall, 1984*b*; *Prescott et al.*, 1981]. This fault segment appears to mark a transition zone where a portion of the slip occurring along the San Andreas is transferred northward to the Paicines-Calaveras-

Hayward fault system. Such an interpretation is supported by the geodetic measurements of *Prescott et al.* [1981] that show the cumulative slip rate to the north of San Juan Bautista across the San Andreas, Hayward, and Calaveras faults (Figure A10) is also 33 mm/yr, as well as by observations of fault creep along the Paicines fault [*Harsh and Pavoni*, 1978; *Lisowski and Prescott*, 1981]. The slip rate along this fault segment thus increases southward from about 12 to 34 mm/yr. It is not, however, understood what portion of the slip is accumulating as elastic strain versus being released by aseismic slip. *Louderback*'s [1947] account of the large 1838 earthquake provides some suggestion that this segment may sustain significant levels of elastic strain, though the largest earthquake recorded along the segment in recent time does not exceed magnitude 5.2 [*Burford and Harsh*, 1980]. To compute the hazard maps, it is speculatively assumed that 5 mm/yr of slip is being stored as elastic strain energy and that the extent of the segment behaves as a single seismogenic source.

Bitterwater Valley to Slack Canyon. Alignment array surveys dating back to the mid-1960s show this segment to creep aseismically at about 32 mm/yr [*Burford and Harsh*, 1980]. The geologic rate of slip as averaged over the late Holocene determined at a site within the Carrizo Plain is virtually identical to this value [*Sieh and Jahns*, 1984]. It thus appears that elastic strain is not accumulating along this segment [*Burford and Harsh*, 1980; *Sieh and Jahns*, 1984]. The hazard maps are constructed assuming that negligible potential exists for a large earthquake to rupture this segment.

Slack Canyon to Cajon Pass--The 1857 rupture zone. The northern and southern ends of this segment are placed near Slack Canyon and Cajon Pass, respectively, and correspond to the probable rupture length of the great 1857 earthquake estimated by *Sieh* [1978*b*]. *Sieh and Jahns* [1984] estimated that the late Holocene slip rate within the Carrizo Plain has averaged 33.9 ± 2.9 mm/yr. A review of geomorphic evidence by *Sieh and Jahns* [1984] shows that the past three earthquakes that produced ruptures along the San Andreas in the Carrizo Plain resulted in surface offsets of between 9.5 and 12.3 m. Using these values and the late Holocene slip rate, *Sieh and Jahns* [1984] estimated the average time interval between the occurrence of such offsets is between 240 and 450 years. Hence it is assumed that the average return time of rupture for this segment is 345 years.

The largest offsets during the 1857 earthquake occurred in the Carrizo Plain [*Sieh*, 1978*b*]. Displacements during 1857 to both the north and the south of the Carrizo Plain were considerably less [*Sieh*, 1978*b*]. An assumption that the long-term rate of slip is maintained along strike of this segment requires that earthquakes be more frequent in those regions that experienced smaller offsets in 1857. This requisite is, of course, also dependent on the assumption that earthquake displacements on sections of the fault are always of a characteristic size. The long-term seismic behavior interpreted for the San Andreas and used here to construct the hazard maps is based on these assumptions. For that reason, it is useful to further examine segments of the 1857 rupture zone that extend to the north and south of the Carrizo Plain.

Slack Canyon to Cholame. Subsequent to the 1857 earthquake, moderate-sized earthquakes are also reported to have occurred relatively frequently along this segment. A moderate-sized event in 1966 produced tectonic surface ruptures extending from between Slack Canyon and Parkfield to Cholame [*Brown and Vedder*, 1967]. Isoseismal distributions determined from study of historical documents have been interpreted to suggest that similar sized events also occurred here in 1881, 1901, 1922, and 1934 [*Sieh*, 1978*c*; *Bakun and McEvilly*, 1984]. Analyses of seismograms for the 1922, 1934, and 1966 events sup-

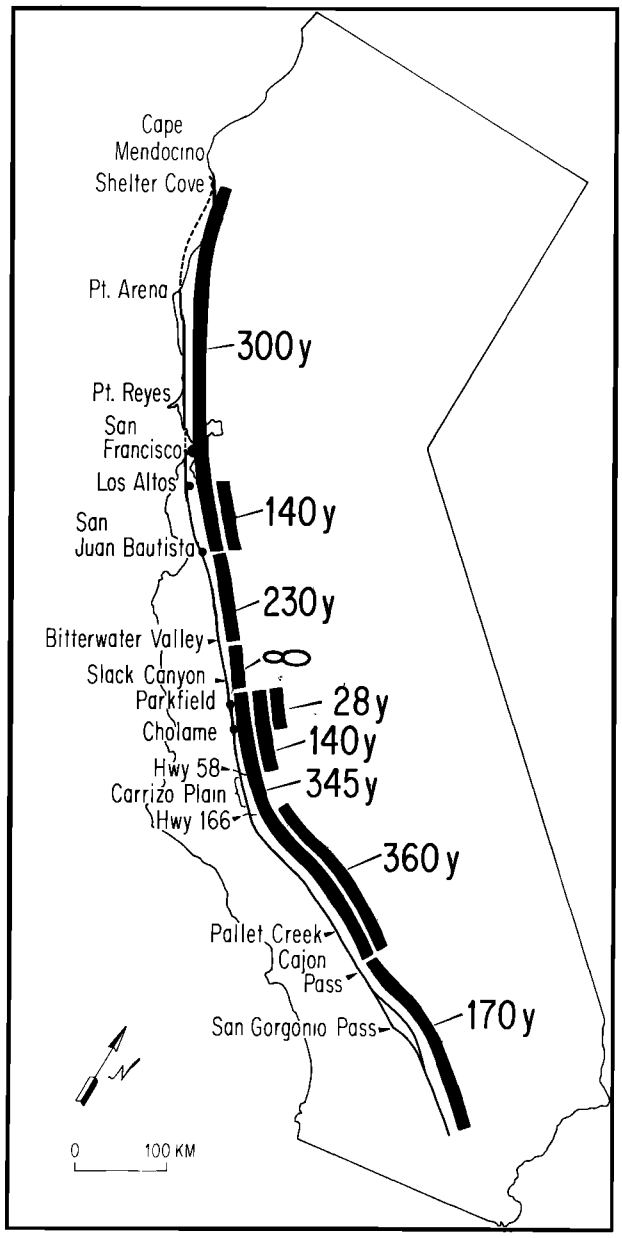

Fig. A11. Map illustrating assumed mode of rupture along the San Andreas that satisfies existing data and is assumed for development of seismic hazard maps. Solid bars adjacent to fault trace extend length assumed to rupture during single earthquakes. Overlapping of bars indicates segments of the fault that, at different times, are associated with earthquakes of different magnitude and hence rupture length. Expected average repeat times of rupture listed next to each segment are in years. Observations indicate that elastic strain accumulation is now largely being released by aseismic creep along segment marked by infinity.

port this argument, showing that the seismic moments for the three events differ at most by 20% [*Bakun and McEvilly*, 1984]. The average time interval between the six earthquakes is 22 years. To reflect that observation in the hazard maps, it is assumed that ruptures limited to this segment occur on average each 28 years. Thus, in combination with the occurrence of larger earthquakes that extend along this reach of the fault (Figure A11), the effective repeat time between earthquakes along this segment is placed at 22 years.

Slack Canyon to Hwy. 58. Offsets along this segment averaged 3-4 m directly to the south of Cholame during the great 1857 event, whereas offsets further to the south along the Carrizo Plain were on average 8-10 m [*Sieh and Jahns*, 1984]. Immediately to the south of this segment, *Sieh and Jahns* [1984] assessed the fault slip rate to have averaged 33.9 ± 2.9 mm/yr for the past 3700 years. The San Andreas is creeping at a virtually identical rate just to the north of this segment [e.g., *Burford and Harsh*, 1980]. At that rate, sufficient slip is accumulating to produce a 3.5-m offset about every 100 years. To reflect that observation in the hazard maps, ruptures limited to this segment are assumed to occur each 140 years. In conjunction with the assigned repeat time (345 years) of 1857-type ruptures then, the resultant repeat time of earthquakes along this segment is set to 100 years.

Hwy. 166 to Salton Sea. Surface rupture during the 1857 earthquake extended as far south as about Cajon Pass [*Sieh*, 1978*b*. Studies by *Sieh* [1978*a*, 1984] provide evidence that rupture of the San Andreas occurs at Pallett Creek on average every 145-200 years. *Davis* [1983] has argued, on the basis of data gathered from trench studies about 20 km south of Hwy. 166, that rupture did not extend north into the Carrizo Plain for every earthquake documented at Pallett Creek, as it did for the 1857 earthquake. No historical evidence of large earthquakes exists on the San Andreas south of Cajon Pass. There are, however, reports of 1-4 m offsets of young geomorphic features at sites along the reach of the San Andreas south of Cajon Pass that may reflect prehistoric earthquake displacements [e.g., *Weldon and Sieh*, 1985; *Keller et al.*, 1982; *Sieh*, 1978*b*] The lack of historical rupture south of Cajon Pass implies a repeat time on the order of at least 150 years, the approximate length of the historical record.

Toward reconciling available observations, it is assumed that the San Andreas between Hwy. 166 and the Salton Sea is composed of two separate segments. The first segment is taken to extend from Hwy. 166 to just north of Cajon Pass. The average repeat time of rupture of this segment is assumed to equal 360 years. Such a mode of behavior satisfies *Sieh's* [1984] conclusion that the average return time of large earthquakes at Pallett Creek is between 145 and 200 years. That is, the previously calculated occurrence of 1857-type earthquakes each 345 years, in conjunction with a rupture confined between Hwy. 166 and Cajon Pass each 360 years, is consistent with the occurrence of earthquakes at Pallett Creek on average every 170 years. A repeat time of 170 years is also assigned to the remaining southernmost segment of the fault. The 170-year repeat time is chosen to satisfy the geomorphologic and geologic analysis of sediments along the San Andreas in Cajon Pass by *Weldon and Sieh* [1985] that indicates large earthquakes occur every 150-200 years. Preliminary work by K.E. Sieh (personal communication, 1986) along the San Andreas near the Salton Sea presently appears consistent with a 170-year repeat time for large earthquakes. Other scenarios, as well as this one, have previously been put forth to explain the existing data [*Weldon and Sieh*, 1985], and all similarly infer the occurrence of large earthquakes on average each 150-200 years. Finally, it is not clear how slip along the San Andreas is transferred through the San Gorgonio pass region (Figure A11) [*Matti et al.*, 1985]. For the hazard maps, it is assumed that slip occurs simultaneously along the Mill Creek, San Gorgonio-Banning, and San Bernardino fault strands (Figure A5) during a rupture of the Cajon Pass to Salton Sea segments.

Acknowledgements. I give special thanks to Kerry Sieh and Clarence Allen, whose support and interest were instrumental to the completion of this study. I also thank Luciana Astiz, Malcolm Clark, Hiroo Kanamori, and Kerry Sieh for reviews of the manuscript, Rob Clayton for access to computer graphics hardware, Gene Humphreys for contouring programs, and David Brillinger, Gary Carver, Jim Lienkaemper, Mike Lisowski, Dave McCulloch Tom Rockwell, Mike Rymer, Robert V. Sharp, Ray Weldon, and Bob Yeats for comments and discussion regarding treatment of the geological data. Edith Huang and Barbara Pallant kindly helped prepare the manuscript. This research was supported by U.S.G.S. contracts 14-08-0001-21980 and 14-08-0001-G1184. Contribution 4253, Division of Geological and Planetary Sciences, California Institute of Technology.

REFERENCES

Abe, K., Fault parameters determined by near- and far-field data: The Wakasa Bay earthquake of March 26, 1963, *Bull. Seismol. Soc. Am., 64,* 1369-1382, 1974.

Abe, K., Static and dynamic fault parameters of the Saitama earthquake of July 1, 1968, *Tectonophysics, 27,* 223-238, 1975*a*.

Abe, K., Reexamination of the fault model for the Niigata earthquake of 1964, *J. Phys. Earth, 23,* 349-366, 1975*b*.

Abe, K., Dislocations, source dimensions and stresses associated with earthquakes in the Izu Peninsula, Japan, *J. Phys. Earth, 26,* 253-274, 1978.

Addicot, W. O., Late Pleistocene Mollusks from San Francisco Peninsula, California, and their paleogeographic significance, *Proc. Calif. Acad. Sci., 37,* 57-93, 1969.

Aki, K., and P. G. Richards, *Quantitative Seismology: Theory and Methods,* 932 pp., W. H. Freeman, New York, 1980.

Albee, A. L., and J. L. Smith, Earthquake characteristics and fault activity in southern California, in *Engineering Geology in Southern California,* edited by R. Lung and R. Procter, pp. 9-33, Association of Engineering Geologists, Glendale, Calif., 1966.

Algermissen, S. T., D. M. Perkins, P. C. Thenhaus, S. H. Hanson, and B. L. Bender, Probablistic estimates of maximum acceleration and velocity in rock in the contiguous United States, *U.S. Geol. Surv. Open File Rep., 82-1033,* 99 pp., 1982.

Allen, C. R., The tectonic environments of seismically active and inactive areas along the San Andreas fault system, in *Proceedings Conference on Geologic Problems of San Andreas Fault System,* edited by W. R. Dickenson and A. Grantz, pp. 70-82, Stanford University Press, Stanford, Calif., 1968.

Allen, C. R., Geological criteria for evaluating seismicity, *Bull. Seismol. Soc. Am., 86,* 1041-1057, 1975.

Allen, C. R., L. T. Silver, and F. G. Stehli, Agua Blanca Fault-A major transverse structure of northern Baja California, Mexico, *Geol. Soc. Am. Bull., 71,* 457-482, 1960.

Allen, C. R., T. C. Hanks, and J. H. Whitcomb, Seismological studies of the San Fernando earthquake and their tectonic implications, *Bull. Calif. Div. Mines Geol., 196,* 257-262, 1975

Allen, C. R., R. Crook, Jr., B. Kamb., C. M. Payne, and R. J. Proctor, Evidence for faulting recurrence in the Raymond and Sierra Madre fault zones, southern California, *Eos Trans. AGU, 59,* 1210, 1978.

Ambraseys, N., Some characteristic features of the Anatolian fault zone, *Tectonophysics, 9,* 143-165, 1970

Ambraseys, N. N., and J. S. Tchalenko, The Dasht-e Bayaz (Iran) earthquake of August 31, 1968: A field report, *Bull. Seismol. Soc. Am., 59,* 1751-1792, 1969.

Anderson, J. G., Estimating the seismicity from geological structure for seismic-risk studies, *Bull. Seismol. Soc. Am., 69* p. 135-158, 1979.

Anderson, L. W., M. H. Anders, and D. A. Ostena, Late Quaternary faulting and seismic hazard potential, eastern Diablo Range, California, Proceedings Conference on Earthquake Hazards in the Eastern San Francisco Bay Area, edited by E. W. Hart et al., *Calif. Div. Mines Geol. Spec. Publ., 62,* 197-206, 1982.

Ando, M., Faulting in the Mikawa earthquake of 1945, *Tectonophysics, 22,* 173-186, 1974.

Ando, M., Source mechanisms and tectonic significance of historical earthquakes along the Nankai trough, Japan, *Tectonophysics, 27,* 119-140, 1975.

Andrews, D. J., A stochastic fault model, 1, Static case, *J. Geophys. Res., 85,* 3867-3877, 1980.

Artim, E. R., and D. Streiff, Trenching in the Rose Canyon fault zone, San Diego, California, *Summ. Tech. Rep., 13,* p. 113, Nat. Earthquake Hazards Reduct. Program, U.S. Geol. Surv., Menlo Park, Calif., 1981.

Astiz, L., and C. R. Allen, Seismicity of the Garlock Fault, California, *Bull. Seismol. Soc. Am., 73,* 1721-1735, 1983.

Aydin, A., The East Bay hills, a compressional domain resulting from interaction between the Calaveras and Hayward-Rodgers Creek faults, Proceedings Conference on Earthquake Hazards in the Eastern San Francisco Bay Area, edited by E. W. Hart et al., *Calif. Div. Mines Geol. Spec. Publ. 62,* 11-21, 1982.

Bachman, S. B., Depositional and structural history of the Waucobi Lake bed deposits, Owens Valley, California, M.S. thesis, 129 pp., Univ. of Calif., Los Angeles, 1974.

Bakun, W. H., and T. V. McEvilly, Recurrence models and Parkfield earthquakes, *J. Geophys. Res., 89,* 3051-3058, 1984.

Bakun, W. H., M. M. Clark, R. S. Cockerham, W. L. Ellsworth, A. G. Lindh, W. H. Prescott, A. F. Shakal, and P. Spudich, The 1984 Morgan Hill, California, earthquake, *Science, 225,* 288-291, 1984.

Barnhart, J. T., and J. E. Slosson, The Northridge Hills and associated faults-a zone of high seismic probability?, in *Geology, Seismicity and Environmental Impact,* edited by D. E. Moran, J. E. Slosson, R. O. Stone, and C. A. Yelverton, pp. 253-256, Association of Engineering Geologists, University Publishers, Los Angeles, Calif., 1973.

Barrows, A. G., A review of the geology and earthquake history of the Newport-Inglewood structural zone, southern California, *Spec. Rep. Calif. Div. Mines Geol., 114,* 115 pp., 1974.

Barrows, A. G., J. E. Kahle, F. H. Weber, Jr., and R. B. Saul, Map of surface breaks resulting from the San Fernando, California, earthquake of Feb. 9, 1971, in *San Fernando, California Earthquake of Feb. 9, 1971,* pp. 127-136, U. S. Department of Commerce, National Oceanic and Atmospheric Administration, Washington, D. C., 1973.

Bartholomew, M. J., The San Jacinto fault zone in the northern Imperial Valley, California, *Geol. Soc. Amer. Bull., 81,* 3161-3166, 1970.

Bäth, M., Earthquake recurrence of a particular type, *Pure Appl. Geophys., 119,* 1063-1076, 1981.

Benioff, H., The determination of the extent of faulting with application to the Long Beach earthquake, *Bull. Seismol. Soc. Am., 28,* 77-84, 1938.

Bird, P., and R. W. Rosenstock, Kinematics of present crust and mantle flow in southern California, *Geol. Soc. Am. Bull., 95,* 946-957, 1984.

Bonilla, M. G., Trench exposures across surface fault ruptures associated with San Fernando earthquake in San Fernando, California, earthquake of February 9, 1971, vol. 3, pp. 173-182, U.S. Department of Commerce, Washington, D. C., 1973.

Bonilla, M. G., R. K. Mark, and J. J. Leinkaemper, Statistical relations among earthquake magnitude, surface rupture, and surface fault displacement, *Bull. Seismol. Soc. Am., 74,* 2379-2411, 1984.

Borchardt, G. A., S. Rice, and G. Taylor, Fault features in paleosols overlying the Foothills fault system near Auburn, California, *Calif. Div. Mines Geol. Open File Rep., 78-16,* 125 pp., 1978.

Bouchon, M., The rupture mechanism of the Coyote Lake earthquake of August 6, 1979 inferred from near field data, *Bull. Seismol. Soc. Am., 72,* 745-757, 1982.

Branner, J. C., J. F. Newson, and R. Arnold, Description of the Santa Cruz quadrangle, in *Geological Atlas,* Folio 163, 11 pp., U.S. Geological Survey, Reston, Va., 1909.

Brown, R. D., Jr., and J. G. Vedder, The Parkfield-Cholame California earthquakes of June-August 1966: Surface tectonic fractures along the San Andreas fault, *U.S. Geol. Surv. Prof. Pap., 579,* 2-22, 1967.

Brune, J. N., Seismic moment, seismicity, and rate of slip along major fault zones, *J. Geophys. Res., 73,* 777-784, 1968.

Brune, J. N., and C. R. Allen, A low stress-drop, low-magnitude earthquake with surface faulting: The Imperial, California, earthquake of March 4, 1966, *Bull. Seismol. Soc. Am., 57,* 501-514, 1967.

Bryant, W. A., Southern Hayward fault zone, Alameda and Santa Clara counties, California, Proceedings Conference on Earthquake Hazards in the Eastern San Francisco Bay Area, edited by E. W. Hart et. al., *Calif. Div. Mines Geol. Spec. Publ. 62,* 35-44, 1982.

Bucknam, R. C., G. Plafker, and R. V. Sharp, Fault movement (afterslip) following the Guatemala earthquake of February 4, 1976, *Geology, 6,* 170-173, 1978.

Bulletin of the Seismological Society of America, 14, Seismological notes, 169-170, 1924.

Burdick, L., and G. R. Mellman, Inversion of the body waves from the Borrego Mountain earthquake to source mechanism, *Bull. Seismol. Soc. Am., 66,* 1485-1499, 1976.

Burford, R. D., and P. W. Harsh, Slip on the San Andreas fault in central California from alignement array surveys, *Bull. Seismol. Soc. Am., 70,* 1233-1261, 1980.

Burford, R. D., and R. V. Sharp, Slip on the Hayward and Calaveras faults determined from offset powerlines, Proceedings Conference on Earthquake Hazards in the Eastern San Francisco Bay area, edited by E. W. Hart et al., 261-269, 1982.

Burke, D. B., and M. M. Clark, Late Quaternary activity along the Garlock fault at Koehn Lake, California, *Eos Trans. AGU, 59,* 1126, 1978.

Butler, R., G. S. Stewart, and H. Kanamori, The July 27, 1976 Tangshan, China earthquake-A complex sequence of intraplate events, *Bull. Seismol. Soc. Am., 69,* 207-220, 1979.

Buwalda, J. P., and P. St. Amand, Geological effects of the Arvin-Tehachapi earthquake, *Bull. Calif. Div. Mines Geol., 171,* 41-56, 1955

California Department of Water Resources, Sea-water intrusion, Bolsa-Sunset area, Orange County, *Bull. Calif. Dep. Water Resour., 63-2,* 167 pp., 1968.

Canitez, N., and M. N. Toksoz, Static and dynamic study of earthquake source mechanism: San Fernando earthquake, *J. Geophys. Res., 77,* 2583-2594, 1972.

Carpenter, D. W., and R. J. Clark, Geologic studies for seismic hazard assessment, Las Positas fault zone, Proceedings Conference on Earthquake Hazards in the Eastern San Francisco Bay Area, edited by E. W. Hart et al., *Spec. Rep. Calif. Div. Mines Geol., 62,* 147-154, 1982.

Carter, B. A., Quaternary displacement on the Garlock fault, California, in *Geology and Mineral Wealth of the California Desert, Dibblee Volume,* edited by D. L. Fife and A. R. Brown, pp. 457-466, South Coast Geological Society, Santa Ana, Calif., 1980.

Carter, B., Neogene displacement on the Garlock fault, California, *Eos Trans. AGU, 63,* 1124, 1982.

Carver, G. A., Quaternary tectonics of the Mendocino Triple Junction, the Mad River fault zone, in *American Geomorphological Field Trip Group Guidebook,* edited by H. M. Hulsey, T. E. Lisle, and M. E. Savina, pp. 155-167, American Geomorphological Field Group, University of California, Berkeley, 1985.

Carver, G. A., T. A. Stephens, and J. C. Young, Quaternary reverse and thrust faults, Mad River fault zone, in *Late Cenozoic History and Forest Geomorphology of Humboldt County, California: Friends of the Pleistocene, Pacific Cell, Field Trip Guidebook,* edited by D. R. Harden, D. C. Marron, and A. McDonald, pp. 93-97, 1982.

Castle, R. O., Geologic map of the Baldwin Hills area, California, scale 1:12,000, *U.S. Geol. Surv. Open File Rep.,* 1960.

Castle, R. O., and R. F. Yerkes, Recent surface movements in the

Baldwin Hills, Los Angeles County, California, *U.S. Geol. Surv. Prof. Pap., 882,* 125 pp., 1976.

Chen, W.P., and P. Molnar, Seismic moments of major earthquakes and the average rate of slip in Central Asia, *J. Geophys. Res., 82,* 2945-2969, 1977.

Christensen, M. N., Late Cenozoic crustal movements in the Sierra Nevada of California, *Geol. Soc. Am. Bull., 77,* 163-182, 1966.

Christodoulidis, D. C., D. E. Smith, R. Kolenkiewicz, S. M. Klosko, M. H. Torrence, and P. J. Dunn, Observing tectonic plate motions from satellite laser ranging, *J. Geophys. Res., 90,* 9249-9263, 1985.

Clark, M. M., Pleistocene glaciation of the drainage of the West Walker River, Sierra Nevada, California, Ph.D. thesis, 130 pp., Stanford Univ., Stanford, Calif., 1967.

Clark, M. M., Surface rupture along the Coyote Creek fault, The Borrego Mountain Earthquake of April 9, 1968, *U.S. Geol. Surv. Prof. Pap., 787,* 55-86, 1972.

Clark, M. M., Range-front faulting: Cause of the difference in height between Mono Basin and Tahoe moraines at Walker Creek, in *Field Guide to Relative Dating Methods Applied to Glacial Deposits in the Third and Fourth Recesses and Along the Eastern Sierra Nevada, California, With Supplementary Notes on Other California Localities: The Friends of the Pleistocene, Pacific Cell, Field Trip Guidebook,* edited by R. M. Burke and P. W. Birkeland, pp. 54-57, 1979.

Clark, M. M., Map showing recently active breaks along the Elsinore and associated faults, Clalifornia, between Lake Henshaw and Mexico, *U.S. Geol. Surv. Misc. Invest. Ser. Map, I-1329,* 1982.

Clark, M. M., and A. R. Gillespie, Record of the late Quaternary faulting along the Hilton Creek fault in the Sierra Nevada, California (abstract), *Earthquake Notes, 52,* 46, 1981.

Clark, M. M., and K. R. Lajoie, Holocene behavior of the Garlock fault (abstract), *Geol. Soc. Am. Abstr. Programs, 6,* 156-157, 1974.

Clark, M. M., and J. C. Yount, Surface faulting along the Hilton Creek fault associated with the Mammoth Lakes, California earthquakes of May 1980, *Earthquake Notes, 52,* 45-46, 1981.

Clark, M. M., A. Grantz, and M. Rubin, Holocene activity of the Coyote Creek fault as recorded in sediments of Lake Cahuilla, The Borrego Mountain Earthquake of April 9, 1968, *U.S. Geol. Surv. Prof. Pap., 787,* 55-86, 1972.

Clark, M., K. Harms, J. Lienkaemper, J. A. Perkins, M. J. Rymer, and R. V. Sharp, The search for surface faulting, The Coalinga Earthquake Sequence of May 2, 1983, *U.S. Geol. Surv. Open File Rep., 83-511,* 8-11, 1983.

Clark, M. M., K. K. Harms, J. J. Lienkaemper, D. S. Harwood, K. R. Lajoie, J. C. Matti, J. A. Perkins, M. J. Rymer, A. M. Sarna-Wojcicki, R. V. Sharp, J. D. Sims, J. C. Tinsley and J. I. Ziony, Preliminary slip-rate table for late Quaternary faults of California, *U.S. Geol. Surv. Open File Rep., 84-106,* 12, 1984.

Clark, M. M., A. C. Darrow, K. K. Harms, J. J. Lienkaemper, and R. H. Patterson, Uncertainties in slip rates, manuscript in preparation, 1986.

Cockerham, R. S., and J. P. Eaton, The April 24, 1984 Morgan Hill earthquake and its aftershocks: April 24 through September 30, 1984, *Calif. Div. Mines Geol. Spec. Publ. 68,* 215-236, 1984.

Coppersmith, K. J., Activity assessment of the Zayante-Vergeles fault, central San Andreas fault system, California, Ph.D. thesis, 210 pp., Univ. of Calif., Santa Cruz, 1979.

Crone, A. J., M. N. Machette, M. G. Bonilla, J. J. Lienkaemper, K. L. Pierce, W. E. Scott, and R. C. Bucknam, Characteristics of surface faulting accompanying the Borah Peak earthquake, central Idaho, *U. S. Geol. Sur. Open File Rep., 85-290,* 43-58, 1985.

Crook, R., Jr., C. R. Allen, B. Kamb, C. M. Payne, and R. J. Proctor, Quaternary geology and seismic hazard of the Sierra Madre and associated faults, western San Gabriel Mountains, California, Recent Reverse Faulting in the Transverse Ranges, California, *U. S. Geol. Surv. Prof. Pap.,* in press, 1986.

Crouch, J. K., S. B. Bachman, and J. T. Shay, Post-Miocene compressional tectonics along the central California margin, in *Tectonics and Sedimentation Along the California Margin,* edited by J. K. Crouch and S. B. Bachman, pp. 37-54, Pacific Coast Section, Society for Economic Paleontologists and Mineralogists, Bakersfield, Calif., 1984.

Crowell, J. C., Problems concerning the San Andreas fault system in southern California, Proceedings of the Conference on Tectonic Problems of the San Andreas Fault System, edited by R. L. Kovach and A. Nur, *Stanford Univ. Publ. Geol. Sci., 13,* 125-135, 1973.

Crowell, J. C., and A. G. Sylvester, Tectonics of the juncture between the San Andreas fault system and the Salton Trough, southeastern California, report, Dep. of Geol. Sci., Univ. of Calif., Santa Barbara, 1979.

Cummings, J. C., The Santa Clara Formation and possible post-Pliocene slip on the San Andreas fault in central California, Proceedings of the Conference on Geologic Problems of the San Andreas Fault System, edited by W. R. Dickinson and A. Grantz, *Stanford Univ. Publ. Geol. Sci., 11,* 191-207, 1968.

Cummings, J. C., The Woodside facies, Santa Clara Formation and late Quaternary slip on the San Andreas fault, San Mateo County, California, paper presented at 58th Annual Meeting, Pac. Coast Sect., Soc. of Econ. Paleontol. and Mineral., Sacramento, Calif., 1983.

Darrow, A. C., and P. J. Fisher, Activity and earthquake potential of the Palos Verdes fault, final technical report, contract 14-08-001-19786, 90 pp., U.S. Geol. Surv., Menlo Park, Calif., 1983.

Davies, G. F., and J. N. Brune, Regional and global fault rates from seismicity, *Nature Phys. Sci., 229,* 101-107, 1971.

Davis, T. L., Late cenozoic structure and tectonic history of the western "Big Bend" of the San Andreas fault and adjacent San Emigdio Mountains, Ph.D. thesis, 580 pp., Univ. of Calif., Santa Barbara, 1983.

Davison, F.C., Jr., and C. H. Scholz, Frequency moment distribution of earthquakes in the Aleutian Arc: A test of the characteristic earthquake model, *Bull. Seismol. Soc. Am., 75,* 1349-1362, 1985.

Dibblee, T. W., Jr., Geology of the central Santa Ynez mountains, Santa Barbara County, California, *Bull. Calif. Div. Mines Geol., 186,* 99 pp., 1966.

Dibblee, T. W., Jr., Existence of major lateral displacement on the Pinto Mountain Fault, southeastern California, *Spec. Pap. Geol. Soc. Am., 115,* 322, 1968*a*.

Dibblee, T. W., Jr., Geology of the Fremont Peak and Opal Mountain quadrangles, California, *Bull. Calif. Div. Mines Geol., 188,* 64 pp., 1968*b*.

Dibblee, T. W., Jr., Late Quaternary uplift of the San Bernardino Mountains on the San Andreas and related faults, *Spec. Rep. Calif. Div. Mines Geol., 118,* 127-146, 1975.

Dokka, R. K., Displacements on late Cenozoic strike-slip faults of the central Mojave Desert, California, *Geology, 11,* 305-308, 1983.

Doser, D. I., Source parameters and faulting processes of the 1959 Hebgen Lake, Montana, earthquake sequence, *J. Geophys. Res., 90,* 4537-4555, 1985.

Doser, D. I., and H. Kanamori, Long period surface waves of four western U.S. earthquakes recorded by the Pasadena strainmeter, *Bull. Seismol. Soc. Am.,* in press, 1986.

Doser, D. I., and R. B. Smith, Seismic moment rates in the Utah Region, *Bull. Seismol. Soc. Am., 72,* 525-552, 1982.

Doser, D. I., and R. B. Smith, Source parameters of the 28 October 1983 Borah Peak, Idaho, earthquake from body wave analysis, *Bull. Seismol. Soc. of Am., 75,* 1041-1051, 1985.

Duffield, W. A., and G. I. Smith, Pleistocene history of volcanism and the Owens River near Little Lake, California, *U.S. Geol. Surv. J. Res., 6,* 395-408, 1978.

Dupre, W. R., Quaternary history of the Watsonville lowlands, north-central Monterey Bay region, California, Ph.D. thesis, 145 pp. Stanford Univ., Stanford, Calif., 1975.

Durham, D. L., Evidence of large strike-slip displacement along a fault in the southern Salinas Valley, California, *U.S. Geol. Surv. Prof. Pap., 525-D,* D106-D111, 1965.

Ehlig, P. L., History, seismicity, and engineering geology of the San Gabriel fault, Geology, Seismicity and Environmental Impact, pp. 247-251, Association of Engineering Geologists, University Publishers, Los Angeles, Calif., 1973.

Ehlig, P. L., Geologic framework of the San Gabriel mountains, *Bull. Calif. Div. Mines Geol., 196,* 7-18, 1975.

Ekstrom, G., and A. M. Dziewonski, Centroid-moment tensor solutions for 35 earthquakes in western North America (1977-1983), *Bull. Seismol. Soc. Am., 75,* 23-40, 1985.

Ellsworth, W. L., Bear Valley, California earthquake sequence of

February-March 1972, *Bull. Seismol. Soc. Am., 65,* 483-506, 1975.

Ferrand, G. T., C. G. Bemis, and L. T. Jansen, Radiocarbon dates of alluvium, Rose Canyon fault zone, San Diego, California, *Geol. Soc. Am. Abstr. Programs, 13,* 55, 1981.

Field, M. E., S. H. Clarke, Jr., and M. E. While, Geology and Geologic Hazards of offshore Eel River Basin, northern California continental margin, *U.S. Geol. Surv. Open File Rep., 80-1080,* 80 pp., 1980.

Fitch, T. J., and C. H. Scholz, Mechanisms of underthrusting in southwest Japan: A model of convergent plate interactions, *J. Geophys. Res., 76,* 7260-7292, 1971.

Frizzell, U. A., Jr., and R. D. Brown, Jr., Map showing recently active breaks along the Green Valley fault, Napa and Solano counties, California, *U.S. Geol. Surv. Map, MF-743,* 1976.

Fuis, G. S., Displacement on the superstition Hills fault triggered by the earthquake, *U.S. Geol. Surv. Prof. Pap., 1254,* 145-154, 1982.

Fukao, Y., and M. Furumoto, Mechanisms of large earthquakes along the eastern margin of the Japan Sea, *Tectonophysics, 25,* 247-266, 1975.

Gardner, D. A., and I. Stahl, Geotechnical-seismic investigation of the proposed 330 zone water storage reservoir and water conditioning facilities site for the City of San Buenaventura, California, *Rep. V77151,* 19 pp., Geotech. Consult., Inc., Ventura, Calif., 1977.

Garfunkle, Z., Model for the late Cenozoic tectonic history of the Mojave Desert, California, and for its relation to adjacent region, *Geol. Soc. Am. Bull., 85,* 1931-1944, 1974.

Gilbert, G. K., A theory of earthquakes of the Great Basin with practical applications, *A. M. J. Sci., 27,* 49-53, 1884.

Gillespie, A. R., Quaternary glaciation and tectonics in the southeastern Sierra Nevada, Inyo County, California, Ph.D. thesis, 695 pp., Calif. Inst. of Tech., Pasadena, 1982.

Gordon, S. A., Relations between the Santa Ynez fault zone and the Pine Mountain thrust fault system, Piru Mountains, California, *Geol. Soc. Am. Abstr. Programs, 11,* 80, 1979.

Graham, S. A., and W. R. Dickinson, Apparent offsets of on-land geologic features across the San Gregorio-Hosgri fault trend, *Spec. Rep. Calif. Div. Mines Geol., 137,* 13-23, 1978.

Greene, H. G., W. H. K. Lee, D. S. McCulloch, and E. E. Brabb, Faults and earthquakes in the Monterey bay region, California, *U.S. Geol. Surv. Misc. Field Maps, MF-518,* 14, 1973.

Greene, H. G., K. A. Bailey, S. H. Clarke, J. I. Ziony, and M. P. Kennedy, Implications of fault patterns of the inner California continental borderland between San Pedro and San Diego, in *Earthquake and Other Perils in the San Diego Region,* edited by P. L. Abbot and W. J. Elliot, pp. 21-28, Geological Society of America, Boulder, Colo., 1979.

Gutenberg, B., and C. F. Richter, Frequency of earthquakes in California, *Bull. Seismol. Soc. Am., 34,* 185-188, 1944.

Hall, C. A., Jr., San Simeon-Hosgri fault system, coastal California: Economic and environmental implications, *Science, 190,* 1291-1294, 1975

Hall, N. T., Holocene history of the San Andreas fault between Crystal Springs Reservoir and San Andreas Dam, San Mateo County, California, *Bull. Seismol. Soc. Am., 74,* 281-300,1984*b*.

Hall, N. T., Late Quaternary history of the eastern Pleito thrust fault, northern transverse ranges, California, Ph.D. thesis, 89 pp., Stanford Univ., Stanford, Calif., 1984.

Hall, N. T., W. R. Cotton, and E. A. Hay, Recurrence frequency of large earthquakes on the San Andreas Fault near Dogtown and on the San Francisco Peninsula, paper presented at AGU Chapman Conference on Fault Behavior and the Earthquake Generation Process, AGU, Snowbird, Utah, 1983.

Hamilton, D. H., and C. R. Willingham, Hosgri fault zone; structure, amount of displacement, and relationship to structures of the western Transverse Ranges, *Geol. Soc. Am. Abstr. Programs, 9,* 429, 1977.

Hamilton, R. M., Aftershocks of the Borrego Mountain earthquake from April 12 to June 12, 1968, The Borrego Mountain Earthquake of April 9, 1968, *U.S. Geol. Surv. Prof. Pap., 787,* 31-54, 1972.

Hanks, T., β values and ω^γ seismic source models: Implications for tectonic stress variations along active crustal fault zones and the estimation of high-frequency strong ground motion, *J. Geophys. Res., 84,* 2235-2242, 1979.

Hanks, T., and H. Kanamori, A moment magnitude scale, *J. Geophys. Res., 84,* 2348-2350, 1979.

Hanks, T. C., and M. Wyss, The use of body-wave spectra in the determination of seismic-source parameters, *Bull. Seismol. Soc. Am., 62,* 561-589, 1972.

Harden, J. W., and D. E. Marchand, Quaternary stratigraphy and interpretation of soil data from Auburn, Oroville, and Sonora areas along the Foothill fault system, western Sierra Nevada, California, *U.S. Geol. Surv. Open File Rep., 80-305,* 39 pp., 1980.

Harsh, P. W., and R. O. Burford, Alignment-array measurements of fault slip in the eastern San Francisco Bay area, California, Proceedings Conference on Earthquake Hazards in the Eastern San Francisco Bay Area, edited by E. W. Hart et al., *Calif. Div. of Mines Geol. Spec. Publ., 62,* 251-260, 1982.

Harsh, P. W., and N. Pavoni, Slip on the Pacines Fault, *Bull. Seismol. Soc. Am., 68,* 1191-1193, 1978.

Harsh, P. W., E. H. Pampeyan, and J. M. Coakley, Slip on the Willits fault, California, *Earthquake Notes, 49,* 22, 1978.

Hart, E. W., Basic geology of the Santa Margarita area, San Luis Obispo County, California, *Bull. Calif. Div. Mines Geol., 199,* 45 pp., 1976.

Harwood, D. S., and E. J. Helley, Preliminary structure-contour map of the Sacramento Valley, California, showing major late Cenozoic structural features and depth to basement, scale 1:250,000, *U.S. Geol. Surv. Open File Rep., 82-737,* 1982.

Harwood, D. S., E. J. Helley, J. A. Barker, and E. A. Griffin, Preliminary geologic map of the Battle Creek fault zone, Shasta and Tenama counties, California, scale 1:24,000, *U.S. Geol. Surv. Open File Rep., 80-474,* 1980.

Harwood, D. S., E. J. Helley, and M. P. Doukas, Geologic map of the Chico monocline and northeastern part of the Sacramento Valley, California, scale 1:62,500, *U.S. Geol. Surv. Misc. Invest. Map, I-1238,* 1981.

Hay, E. A., W. R. Cotton, and N. T. Hall, Shear couple tectonics and the Sargent-Berrocal fault system in northern California, Studies of the San Andreas Fault Zone in Northern California, *Spec. Rep. Calif. Div. Mines Geol., 140,* 41-50, 1980.

Hearn, B. C., Jr., J. M. Donelly, and F. E. Goff, Preliminary geologic map of the Clear Lake volcanic field, Lake County, California, scale 1:24,000, *U.S. Geol. Surv. Open File Rep., 76-751,* 3 plates., 1976.

Heath, E. G., D. E. Jensen, and D. W. Lukesh, Style and age of deformation on the Chino fault, in *Neotectonics in Southern California,* compiled by J. D. Cooper, pp. 123-134, Geological Society of America, Cordilleran Section, Anaheim, Calif., 1982.

Heaton, T. H., and H. Kanamori, Seismic potential associated with subduction in the northwestern United States, *Bull. Seismol. Soc. Am., 74,* 933-941, 1984.

Hedel, C. W., Late Quaternary faulting in western Surprise Valley, Modoc County, Calif., M.S. thesis, 113 pp., San Jose State Univ., San Jose, Calif., 1980.

Helley, E. J., et al., Geologic map of the Battle Creek fault zone and adjacent parts of the northern Sacramento Valley, California, scale 1:62,500, *U.S. Geol. Surv. Misc. Field Stud. Map, MF-1298,* 12 pp., 1981.

Herd, D. G., Intracontinental plate boundary east of Cape Mendocino, *Calif. Geol., 6,* 721-725, 1978.

Herd, D. G., Neotectonic framework of central California and its implications to microzonation of the San Francisco Bay region, *U.S. Geol. Surv. Circ., 807,* 3-12, 1979.

Herd, D. G., and E. E. Brabb, Evidence for tectonic movement on the Las Positas fault, Alameda County, California, *U.S. Geol. Surv. Open File Rep., 79-1658,* 7 pp., 1979.

Herd, D. G., and E. E. Brabb, Faults at the General Electric test reactor site, Vallecitos Nuclear Center, Pleasanton, California, *U.S. Geol. Surv. Admin. Rep., 77,* 1980.

Herd, D. G., and E. J. Helley, Faults with Quaternary displacement northwestern San Francisco Bay region, California, *U.S. Geol. Surv. Misc. Field Stud. Map, MF-818,* 1977.

Herd, D. G., and C. R. McMaster, Surface faulting in the Sonora, Mexico, earthquake of 1886, *Geol. Soc. Am. Abstr. Programs, 14,* 4, 1982.

Hill, R. I., Geology of Garner Valley and Vicinity, in *Geology of the San Jacinto Mountains, Field Trip Guideb. 9,* edited by A. R. Brown and R. W. Ruff, pp. 90-99, South Coast Geological Society, Irvine, Calif., 1981.

Hooke, R. L., Geomorphic evidence for late Wisconsin and Holocene tectonics deformation, Death Valley, California, *Geol. Soc. Am. Bull., 83,* 2073-2098, 1972.

Hope, R. A., The Blue Cut fault, southeastern California, *U.S. Geol. Surv. Prof. Pap. 650-D,* D116-D121, 1969.

Imamura, A., Topographic changes accompanying earthquakes or volcanic eruptions, *Publ. 25,* pp. 1-143, Earthquake Invest. Comm. on Foreign Languages, Tokyo, 1930.

Ishimoto, M., and K. Iida, Observations sur les seisms enregistre par le microseismograph construite derniermente (I), *Bull. Earthquake Res. Inst., Univ. Tokyo, 17,* 443-478, 1939

Jennings, C. W., Fault map of California, California geologic data map series, Dep. of Conserv., San Francisco, Calif., 1975.

Joyner, W. B., and T. E. Fumal, Predictive mapping of earthquake ground motion, Evaluating Earthquake Hazards in the Los Angeles Region-An Earth-Science Perspective, edited by J. I. Ziony, *U.S. Geol. Surv. Prof. Pap., 1360,* 203-220, 1985.

Junger, A., and H. C. Wagner, Geology of the Santa Monica and San Pedro basins, California continental borderland, *U.S. Geol. Surv. Misc. Field Stud. Map, MF-820,* 1977.

Kahle, J. E., Megabreccias and sedimentary structures of the Plush Ranch Formation, northern Ventura County, California, M. A. thesis, 125 pp., Univ. of Calif., Los Angeles, 1966.

Kanamori, H., Mode of strain release associated with major earthquakes in Japan, *Annu. Rev. Earth Planet. Sci., 1,* 213-239, 1973.

Kanamori, H., Mechanism of the 1983 Coalinga earthquake determined from long-period surface waves, *Calif. Div. Mines Geol. Spec. Publ., 66,* 233-240, 1983.

Kanamori H., and C. R. Allen, Earthquake repeat time and average stress drop, in *Earthquake Source Mechanics, Geophys. Monogr. Ser., vol. 37,* edited by S. Das, J. Boatwright, and C. Scholz, pp. 227-235, AGU, Washington, D.C., 1986.

Kanamori, H., and J. Regan, Long-period surface waves, *U.S. Geol. Surv. Prof. Pap. 1254,* 55-58, 1982.

Kanamori, H., and G. S. Stewart, Mode of strain release along the Gibb's fracture zone, Mid-Atlantic Ridge, *Phys. Earth Planet. Inter., 11,* 312-332, 1976.

Kanamori, H., and G. S. Stewart, Seismological aspects of the Guatemala earthquake of February 4, 1976, *J. Geophys. Res., 83,* 3427-3434, 1978.

Kawasaki, I., The focal process of the Kita-Mino earthquake of August 19, 1961, and its relationship to a Quaternary fault, the Hatogayu-Koike fault, *J. Phys. Earth, 24,* 227-250, 1975.

Keaton, J. R., Geomorphic evidence for late Quaternary displacement along the Santa Ynez fault zone, Blue Canyon, eastern Santa Barbara County, California (abstract), *Geol. Soc. Am. Abstr. Programs, 10,* 111, 1978.

Kelleher, J. A., Space-time seismicity of the Alaska-Aleutian seismic zone, *J. Geophys. Res., 75,* 5745, 1970.

Kelleher, J. A., Rupture zones of large south American earthquakes and some predictions, *J. Geophys. Res., 77,* 2087-2103, 1972.

Keller, E. A., M. S. Bonkowski, R. J. Korsch, and R. J. Salemon, Tectonic geomorphology of the San Andreas fault zone in the southern Indio Hills, Coachella Valley, California, *Geol. Soc. Am. Bull., 93,* 46-56, 1982.

Kennedy, M. P., Geology of the San Diego metropolitan area, California, *Bull. Calif. Div. Mines Geol., 200,* 1-39, 1975.

Kern, J. P., Origin and history of upper Pleistocene marine terraces, San Diego, California, *Geol. Soc. Am. Bull., 88,* 1553-1566, 1977.

Kilbourne, R. T., C. W. Chesternman, and S. W. Wood, Recent volcanism in the Mono Balin-Long Valley region of Mono County, California, *Spec. Rep. Calif. Div. Mines Geol., 150,* 7-22, 1980.

King, G., and J. Nabelek, Role of fault bends in the initiation and termination of earthquake rupture, *Science, 228,* 984-987, 1985.

King, N. E., and J. C. Savage, Strain-rate profile across the Elsinore, San Jacinto, and San Andreas faults near Palm Springs, California, 1973-81, *Geophys. Res. Lett., 10,* 55-57, 1983.

Knuepfer, P. L., Geomorphic investigations of the Vaca and Antioch fault systems, Solano and Contra Costa counties, California, M.S. thesis, 53 pp., Stanford Univ., Stanford, Calif., 1977.

Koto, B., On the cause of the great earthquake in central Japan, *J. Coll. Sci. Imp. Univ. Tokyo, 5,* 295-353, 1893.

Lahr, J. C., and C. D. Stephens, Alaska seismic zone: Possible example of non-linear magnitude distribution for faults, *Earthquake Notes, 53,* 66, 1982.

Lajoie, K. R., and D. Keefer, Investigations of the 8 November 1980 earthquake in Humboldt County, California, *U.S. Geol. Surv. Open File Rep., 81-397,* 30 pp., 1981.

Lajoie, K. R., A. M. Sarna-Wojcicki, and R. F. Yerkes, Quaternary chronology and rates of crustal deformation in the Ventura area, California, in *Neotectonics in Southern California,* compiled by J. D. Cooper, pp. 43-51, Geological Society of America, Cordilleran Section, Anaheim, Calif., 1982.

Lamar, D. L., Structural evolution of the northern margin of the Los Angeles Basin, Ph.D. thesis, Univ. of Calif., Los Angeles, 142 pp., 1961.

Lamar, D. L., P. M. Merifield, and R. J. Proctor, Earthquake recurrence intervals on major faults in southern California, in *Geology, Seismicity and Environmental Impact,* edited by D. E. Moran, J. E. Slosson, R. O. Stone, and C. A. Yelverton, pp. 265-275, Association of Engineering Geologists, University Publishers, Los Angeles, Calif., 1973.

La Violette, J. W., G. E. Christenson, and J. C. Stepp, Quaternary displacement on the western Garlock fault, southern California, in *Geology and Mineral Wealth of the California Desert, Dibblee Volume,* edited by D. L. Fife, and A. R. Brown, pp. 449-456, South Coast Geological Society, Santa Ana, Calif., 1980.

Lawson, A. C., et al., The California earthquake of April 18, 1906, in *Report of the State Earthquake Investigation Commission,* vol. 1-2, 451 pp., Carnegie Institution of Washington, Washington, D. C., 1908.

Lee, W. H. K., R. F. Yerkes, and M. Samirenko, Recent earthquake activity and focal mechanisms in the western Transverse Ranges, California, *U.S. Geol. Surv. Circ., 799-A,* 37 pp., 1979.

Legg, M. R., and M. P. Kennedy, Faulting offshore San Diego and northern Baja California, in *Earthquake and other Perils in the San Diego Region,* edited by P. L. Abbot and W. J. Elliot, pp. 29-46, Geological Society of America, Boulder, Colo., 1979.

Lettis, W. R., Late Cenozoic stratigraphy and structure of the western margin of the central San Joaquin Valley, California, *U.S. Geol. Surv. Open File Rep., 82-526,* 203 pp., 1982.

Lisowski, M., and W. H. Prescott, Short-range distance measurements along the San Andreas fault system in central California, 1975 to 1979, *Bull. Seismol. Soc. Am., 71,* 1607-1624, 1981.

Lindh, A. G., Preliminary assessment of long-term probabilities for large earthquakes along selected fault segments of the San Andreas fault system in California, *U.S. Geol. Surv. Open File Rep., 83-63,* 1-15, 1983.

Lindh, A. G., and D. M. Boore, Control of rupture by fault geometry during the 1966 Parkfield earthquake, *Bull. Seismol. Soc. Am., 71,* 95-116, 1981.

Liu, H., and D. V. Helmberger, The near-source ground motion of the 6 August 1979, Coyote Lake, California, earthquake, *Bull. Seismol. Soc. Am., 73,* 201-218, 1983.

Louderback, G. D., Central California earthquakes of the 1830's, *Bull. Seismol. Soc. Am., 37,* 33-74, 1947.

Louie, J. N., C. R. Allen, D. C. Johnson, and P. C. Haase, Fault slip in southern California, *Bull. Seismol. Soc. Am., 75,* 811-834, 1985.

Lowman, P. D., Vertical displacement on the Elsinore fault of southern California: Evidence from orbital photographs, *J. Geol., 88,* 415-432, 1980.

Lubetkin, L. K. C., Late Quaternary activity along the Lone Pine fault, Owens Valley fault zone, California, M.S. thesis, 85 pp., Stanford Univ., Stanford Calif., 1980.

Lubetkin, L. K. C., and M. M. Clark, Late Quaternary activity along the Lone Pine fault, eastern California (abstract), *Eos, Trans. AGU, 61,* 1042, 1980.

Magistrale, H., C. Sanders, and H. Kanamori, The rupture patterns of large earthquakes in the San Jacinto fault zone, *Eos Trans. AGU, 65,* 992, 1984.

Matsuda, T., Surface faults associated with Kita-Izu earthquake of 1930 in Izu Peninsula, Japan (in Japanese), in *Izu Peninsula,* edited by M. Hoshino and H. Aoki, pp. 73-93, Tokai University Press, Tokyo, 1972.

Matsuda, T., Surface faults associated with Nobi (Mino-Owari) earthquake of 1891, Japan, *Spec. Bull. Earthquake Res. Inst., Univ. Tokyo, 13,* 85-126, 1974.

Matsuda, T., Estimation of future destructive earthquakes from active faults on land in Japan, *J. Phys. Earth, 25,* suppl., S251-S260, 1977.

Matsuda, T., H. Yamazaki, T. Nakata, and T. Imaizumi, The surface faults associated with the Rikuu earthquake of 1896, *Bull. Earthquake Res. Inst., Univ. Tokyo, 55,* 795-855, 1980.

Matti, J. C., and D. M. Morton, Geologic history of the Banning fault zone, southern California, *Geol. Soc. Am. Abstr. Programs, 14,* 184, 1982.

Matti, J. C., J. C. Tinsley, D. M. Morton, and L. D. McFadden, Holocene faulting history as recorded by alluvial stratigraphy within the Cucamonga fault zone: A preliminary view, in *Late Quaternary Pedogenesis and Alluvial Chronologies of the Los Angeles and San Gabriel Mountain Areas, Southern California, and Holocene Faulting and Alluvial Stratigraphy Within the Cucamonga Fault Zone,* edited by J. C. Tinsley, L. D. McFadden, J. C. Matti, pp. 21-44, Geological Society of America, Cordilleran Section, Anaheim, Calif., 1982.

Matti, J. C., D. M. Morton, and B. F. Cox, Distribution and geologic relations of fault systems in the vicinity of the Central Transverse Ranges, southern California, *U.S. Geol. Surv. Open File Rep., 85-365,* 27 pp., 1985.

McCulloch, D. S., H. G. Greene, and K. S. Heston, A summary of the geology and geologic hazards in proposed lease sale 53, central California outer continental shelf, *U.S. Geol. Surv. Open File Rep., 80-1095,* 76 pp., 1980.

McGill, J. T., Recent movement on the Potrero Canyon fault, Pacific Palisades area, Los Angeles, California, *U. S. Geol. Surv. Prof. Pap., 1175,* 258-259, 1981.

McGill, J. T., Preliminary geologic map of the Pacific Palisades area, City of Los Angeles, California, scale 1:4800, *U.S. Geol. Surv. Open File Rep., 82-194,* 15 pp., 1982.

Meisling, K. E., Neotectonics of the north frontal fault system of the San Bernardino Mountains, southern California: Cajon Pass to Lucerne Valley, Ph.D. thesis, 394 pp., Calif. Inst. of Tech., Pasadena, 1984.

Mezger, L., and R. J. Weldon, Tectonic implications of the Quaternary history of lower Lytle Creek, southeast San Gabriel Mountains, *Geol. Soc. Am. Abstr. Programs, 15,* 418, 1983.

Michael, E. D., Large lateral displacement on Garlock fault, California, as measured from offset fault system, *Geol. Soc. Am. Bull., 77,* 111-114, 1966.

Mikumo, T., Faulting mechanism of the Gifu earthquake of Sept. 9, 1969, and some related problems, *J. Phys. Earth, 21,* 191-212, 1973.

Mikumo, T., Some considerations on the faulting mechanism of the southeastern Akita earthquake of October 16, 1970, *J. Phys. Earth, 22,* 87-108, 1974.

Mikumo, T., and M. Ando, A search into the faulting mechanism of the 1891 great Nobi earthquake, *J. Phys. Earth, 24,* 63-87, 1976.

Miller, F. K., and D. M. Morton, Potassium-argon geochronology of the eastern Transverse Ranges and southern Mojave Desert, southern California, *U.S. Geol. Surv. Prof. Pap., 1151,* 30, 1980.

Miller, S. T., Geology and mammalian biostratigraphy of a part of the northern Cady Mountains, Mojave Desert, California, *U.S. Geol. Surv. Open File Rep., 80-878,* 122 pp., 1980.

Millman, D. E., and T. K. Rockwell, Lateral offset of mid and late Quaternary deposits along the northern Elsinore fault, southern California, *Geol. Soc. Am. Abstr. Programs, 17,* 370, 1985.

Minster, J. B., and T. H. Jordan, Present-day plate motions, *J. Geophys. Res., 83,* 5331-5354, 1978.

Minster, J. B., and T. H. Jordan, Vector constraints on Quaternary deformation of the western United States, in *Tectonics and Sedimentation Along the California Margin,* edited by J. K. Crouch, and S. B. Burcham, pp. 1-16, Pacific Coast Section, Society for Economic Paleontologists and Mineralogists, Bakersfield, Calif., 1984.

Molnar, P., Earthquake recurrence intervals and plate tectonics, *Bull. Seismol. Soc. Am., 69,* 115-134, 1979.

Moore, G. W., and M. P. Kennedy, Quaternary faults at San Diego Bay, California: *J. Res. U.S. Geol. Surv., 3,* 589-595, 1975.

Morton, D. M., Synopsis of the geology of the eastern San Gabriel Mountains, southern California, *Spec. Rep. Calif. Div. Mines Geol., 118,* 170-176, 1975.

Morton, D. M., F. K. Miller, and C. C. Smith, Photoreconnaissance maps showing young-looking fault features in the southern Mojave Desert, California, *U.S. Geol. Surv. Misc. Field Stud. Map, MF-1051,* 1980.

Morton, D. M., J. C. Matti, and J. C. Tinsley, Quaternary history of the Cucamonga fault zone, southern California, *Geol. Soc. Am. Abstr. Programs, 14,* 118, 1982.

Nakata, J. K., Distribution and petrology of the Anderson-Coyote Reservoir volcanic rocks, M.S. thesis, 105 pp., San Jose State Univ., San Jose, Calif., 1977.

Nur, A., Nonuniform friction as a physical basis for earthquake mechanics, *Pure Appl. Geophys., 116,* 1-26, 1978.

Okal, E. A., A surface wave investigation of the Gobi-Altai (December 4, 1957) earthquake, *Phys. Earth Planet. Inter., 12,* 319-328, 1976.

Page, B. M., Basin-Range faulting in Pleasant Valley, Nevada, *J. Geol., 43,* 690-707, 1935.

Page, B. M., Modes of Quaternary tectonic movement in the San Francisco Bay region, California, Proceedings Conference on Earthquake Hazards in the Eastern San Francisco Bay Area, edited by E. W. Hart, *Calif. Div. Mines Geol. Spec. Publ., 62,* 1-16, 1982.

Pampeyan, E. H., P. W. Harsh, and J. M. Coakley, Recent breaks along Maacana fault zone, Laytonville to Hopland, California, *U.S. Geol. Surv. Map, MF-1217,* 1981.

Patterson, R. H., Tectonic geomorphology and neotectonics of the Santa Cruz Island fault, Santa Barbara county, California, M. A. thesis, Univ. of Calif., Santa Barbara, 141 pp., 1979.

Pinault, C. T., and T. K. Rockwell, Rates and sense of Holocene faulting on the southern Elsinore fault: Further constraints on the distribution of dextral shear between the Pacific and North American plates, *Geol. Soc. of Am. Abstr. Programs, 16,* 624, 1984.

Plafker, G., T. Hudson, T. Bruns, and M. Rubin, Late Quaternary offsets along the Fairweather fault and crustal plate interactions in southern Alaska, *Can. J. Earth Sci., 15,* 805-816, 1978.

Poland, J. F., and A. M. Piper, Ground water geology of the coastal zone Long Beach-Santa Ana area, California, *U.S. Geol. Surv. Water Supply Pap., 1109,* 126 pp., 1956.

Prescott, W. H., and M. Lisowski, Deformation along the Hayward and Calaveras faults: Steady aseismic slip or strain accumulation, Proceedings Conference on Earthquake Hazards in the Eastern San Francisco Bay Area, edited by E. W. Hart, *Calif. Div. Mines Geol. Spec. Publ., 62,* 261-269, 1982.

Prescott, W. H., and S.-B. Yu, Geodetic measurement of horizontal deformation in the northern San Francisco Bay region, California, *J. Geophys. Res., 91,* 7475-7484, 1986.

Prescott, W. H., M. Lizowski, and J. C. Savage, Geodetic measurement of crustal deformation on the San Andreas, Hayward and Calaveras faults near San Francisco, California, *J. Geophys. Res., 86,* 10,853-10,869, 1981.

Proctor, R. J., R. Crook, Jr., M. H. McKeown, and R. L. Moresco, Relation of known faults to surface ruptures, 1977 San Fernando earthquake, southern California, *Geol. Soc. Am. Bull., 83,* 1601-1618, 1972.

Rasmussen, G. S., Geologic features and rate of movement along the south branch of the San Andreas fault, San Bernardino, California, in *Neotectonics in Southern California,* compiled by J. D. Cooper, pp. 109-114, Geological Society of America, Cordilleran Section, Anaheim, Calif., 1982.

Reasenberg, P., and W. L. Ellsworth, Aftershocks of the Coyote Lake, California, earthquake of August 6, 1979: A detailed study, *J. Geophys. Res., 87,* 10,637-10,655, 1982.

Reid, H. F., The California earthquake of April 18, 1906, the mechanics of the earthquake, in *The State Earthquake Investigation Committee Report,* vol. 2, 192 pp., Carnegie Institute of Washington, D. C., 1910.

Richins, W. D., R. B. Smith, C. J. Langer, J. E. Zollweg, J. J. King, and J. C. Pechman, The 1983 Borah Peak, Idaho, earthquake: Relationship of aftershocks to the main shock, surface faulting, and regional tectonics, *U.S. Geol. Surv. Open File Rep., 85-290,* 285-310, 1985.

Richter, C. F., *Elementary Seismology,* 768 pp., W. H. Freeman, New York, 1958.

Richter, C. F., C. R. Allen, and J. M. Nordquist, The Desert Hot Springs earthquakes and their tectonic environment, *Bull. Seismol. Soc. Am., 48,* 315-337, 1958.

Riddihough, R., Gorda plate motions from magnetic anomaly analysis, *Earth Planet. Sci. Lett., 51,* 163-170, 1980.

Roberts, C. T., and T. L. T. Gross, Late Cenozoic extensional

strain rates and directions in the Honey Lake-Eagle Lake region, northeast California, *Eos, Trans. AGU, 63,* 1107, 1982.

Rockwell, T. K., Soil chronology, geology, and neotectonics of the north-central Ventura basin, California, Ph.D. thesis, Univ. of Calif., Santa Barbara, 1983.

Rockwell, T. K., E. A. Keller, M. N. Clark and D. L. Johnson, Chronology and rates of faulting of Ventura River terraces, California, *Geol. Soc. Am. Bull., 95,* 1466-1474, 1984.

Rockwell, T. K., D. L. Lamar, R. S. McElwain, and D. E. Millman, Late Holocene recurrent faulting on the Glen Ivy north strand of the Elsinore fault, southern California, *Geol. Soc. Am. Abstr. Programs, 17,* 404, 1985.

Rogers, G. C., Juan de Fuca plate map: Seismicity analysis, *Open File Rep. 80-3,* Seismol. Serv., Can. Earth Phys. Branch, Sidney, B.C., Canada, 1980.

Roquemore, G. R., Active faults and associated tectonic stress in the Coso Range, California. *Rep. NWC JP 6270,* 101 pp., Nav. Weapons Cent., China Lake, Calif., 1981.

Rust, D. J., Radiocarbon dates for the most recent prehistoric earthquake and for late Holocene slip rates. San Andreas fault in part of the Transverse Ranges north of Los Angeles (abstract), *Geol. Soc. Am. Abstr. Programs, 14,* 229, 1982*a*.

Rust, D. J., Trenching studies of the San Andreas fault bordering western Antelope Valley, southern California, in Summaries of Technical Reports, vol. XIV, *U.S. Geol. Surv. Open File Rep., 82-840,* 89-91, 1982*b*.

Rust, D. J., Evidence for uniformity of large earthquakes in the "big bend" of the San Andreas fault, *Eos Trans. AGU, 63,* 1030, 1982*c*.

Sage, O. J., Paleocene geography of the Los Angeles region, Proceedings of the Conference on Tectonic Problems of the San Andreas Fault System, edited by R. L. Kovach, and A. Nur, *Stanford Univ. Publ. Geol. Sci., 13,* 348-357, 1973.

Saint-Amand, P., and G. R. Roquemore, Tertiary and Holocene development of the southern Sierra Nevada and Coso Range, California, *Tectonophysics, 52,* 409-410, 1979.

Salyards, S. L., Patterns of offset associated with the 1983 Borah Peak, Idaho, earthquake and previous events, Proceedings of Workshop XXVIII on the Borah Peak, Idaho, Earthquake, *U.S. Geol. Surv. Open File Rep., 85-290,* 59-75, 1985.

Sanders, C. O., and H. Kanamori, A seismotectonic analysis of the Anza seismic gap, San Jacinto fault zone, southern California, *J. Geophys. Res., 89,* 5873-5890, 1984.

Sarna-Wojcicki, A. M., and R. F. Yerkes, Comment on article by R. S. Yeats on "Low-shake faults of the Ventura basin, California," in *Neotectonics in Southern California,* compiled by J. D. Cooper, pp. 17-19, Geological Society of America, Cordilleran Section, Anaheim, Calif., 1982.

Sarna-Wojcicki, A. M., K. M. Williams, and R. F. Yerkes, Geology of the Ventura fault, Ventura County, California, scale 1:6,000, *U.S. Geol. Surv. Misc. Field Stud. Map, MF-781,* 1976.

Sarna-Wojcicki, A. M., K. R. Lajoie, S. W. Robinson, and R. F. Yerkes, Recurrent Holocene displacement on the Javon Canyon fault, rates of faulting and regional uplift, western Transverse Ranges, California, *Geol. Soc. Am. Abstr. Programs, 11,* 125, 1979.

Savage, J. C., and R. O. Burford, Geodetic determination of relative plate motion in central California, *J. Geophys. Res., 78,* 832-845, 1973.

Savage, J. C., and W. H. Prescott, Strain accumulation on the San Jacinto fault near Riverside, California, *Bull. Seismol. Soc. Am., 66,* 1749-1754, 1976.

Savage, J. C., W. H. Prescott, and W. T. Kinoshita, Geodimeter measurements along the San Andreas fault, Proceedings Conference on Tectonic Problems of the San Andreas Fault System, *Stanford Univ. Publ. Geol. Sci., 13,* 44-53, 1973.

Savage, J. C., W. H. Prescott, M. Lisowski, and N. King, Geodetic measurements of deformation near Hollister, California, 1971-1978, *J. Geophys. Res., 84,* 7599-7615, 1979.

Scholz, C. H., and T. Kato, The behavior of a convergent plate boundary: Crustal deformation in the South Kanto District, Japan, *J. Geophys. Res., 83,* 783-797, 1978.

Scholz, C. H., M. Wyss, and S. W. Smith, Seismic and aseismic slip on the San Andreas fault, *J. Geophys. Res., 74,* 2049-2069, 1969.

Scholz, C. H., C. A. Aviles, and S. G. Wesnousky, Scaling differences between large intraplate and interplate earthquakes, *Bull. Seismol. Soc. Am., 76,* 65-70, 1986.

Schwartz, D. P., and K. J. Coppersmith, Fault behavior and characteristic earthquakes: Examples from the Wasatch and San Andreas fault zones, *J. Geophys. Res., 89,* 5681-5698, 1984.

Schwartz, D. P., and A. J. Crone, The 1983 Borah Peak earthquake: A calibration event for quantifying earthquake recurrence and fault behavior on Great Basin normal faults, Proceedings of Workshop XXVIII on the Borah Peak, Idaho, Earthquake, *U.S. Geol. Surv. Open File Rep., 85-290,* 153-160, 1985.

Segall, P., and D. D. Pollard, Mechanics of discontinuous faults, *J. Geophys. Res., 85,* 4337-4350, 1980.

Sharp, R. V., San Jacinto fault zone in the peninsular ranges of southern California, *Geol. Soc. Am. Bull., 78,* 705-730, 1967.

Sharp, R. V., Map showing recent tectonic movement on the Concord fault, Contra Costa and Solano counties, California, *U.S. Geol. Surv. Misc. Field Stud. Map, MF-505,* 1973.

Sharp, R. V., En echelon fault patterns of the San Jacinto fault zone, *Spec. Rep. Calif. Div. Mines Geol., 118,* 147-151, 1975*a*.

Sharp, R. V., Displacement on tectonic ruptures, *Bull. Calif. Div. Mines Geol., 196,* 187-194, 1975*b*.

Sharp, R. V., 1940 and prehistoric earthquake displacements on the Imperial fault, Imperial and Mexicali Valleys, in *Proceedings Symposium on Human Settlements on the San Andreas Fault,* pp. 68-81, California Seismic Safety Commission, Sacramento, 1980.

Sharp, R. V., Variable rates of late Quaternary strike slip on the San Jacinto fault zone, southern California, *J. Geophys. Res., 86,* 1754-1762, 1981.

Sharp, R. V., Comparison of the 1979 surface faulting to earlier displacements in central Imperial Valley, The Imperial Valley, California, Earthquake, October 15, 1979, *U.S. Geol. Surv. Prof. Pap., 1254,* 213-221, 1982.

Sharp, R. V., and J. J. Lienkaemper, Preearthquake and postearthquake nearfield leveling across the Imperial fault and Brawley fault zone, The Imperial Valley, California, Earthquake of October 15, 1979, *U.S. Geol. Surv. Prof. Pap., 1254,* 169-182, 1982.

Sharp, R. V., J. L. Lienkaemper, M. G. Bonilla, D. B. Burke, B. F. Fox, D. G. Herd, D. M. Miller, D. M. Morton, D. J. Pont, M. J. Rymer, J. C. Tinsly, J. C. Yound, J. E. Kahle, E. W. Hart and K. E. Sieh, Surface faulting in the central Imperial Valley, The Imperial Valley, California, Earthquake of October 15, 1979, *U. S. Geol. Surv. Prof. Pap., 1254,* 119-144, 1982.

Shedlock, K. M., R. K. McGuire, and D. G. Herd, Earthquake recurrence in the San Francisco Bay region, California, from fault slip and seismic moment, *U.S. Geol. Surv. Open File Rep., 80-999,* 20 pp., 1980.

Shimazaki, K., Nemuro-Oki earthquake of June 17, 1973: A lithospheric rebound at the upper half of the interface, *Phys. Earth Planet. Inter., 9,* 314-327, 1974.

Shimazaki, K., and P. Somerville, Static and dynamic parameters of the Izu-Oshima, Japan, earthquake of Jan. 14, 1978, *Bull. Seismol. Soc. Am., 69,* 1343-1378, 1979.

Sibson, R. H., Fault zone models, heat flow, and the depth distribution of earthquakes in the continental crust of the United States, *Bull. Seismol. Soc. Am., 72,* 151-163, 1982.

Sibson, R. H., Rupture interactions with fault jogs, in *Earthquake Source Mechanics, Geophys. Monogr.,* vol. 37, edited by S. Das, J. Boatwright, and C. H. Scholz, pp. 157-167, Washington, D. C., 1986.

Sieh, K. E., Prehistoric large earthquakes produced by slip on the San Andreas fault at Pallett Creek, California, *J. Geophys. Res., 83,* 3907-3939, 1978*a*.

Sieh, K. E., Slip along the San Andreas fault associated with the great 1857 earthquake, *Bull. Seismol. Soc. Am., 68,* 1421-1448, 1978*b*.

Sieh, K. E., Central California foreshocks of the great 1857 earthquake, *Bull. Seismol. Soc. of Am., 68,* 1731-1749, 1978*c*.

Sieh, K. E., Lateral offsets and revised dates of large prehistoric earthquakes at Pallett Creek, southern California, *J. Geophys. Res., 89,* 7641-7670, 1984.

Sieh, K. E., and R. H. Jahns, Holocene activity of the San Andreas at Wallace Creek, California, *Geol. Soc. Am. Bull., 95,* 883-896, 1984.

Silver, E. A., Tectonics of the Mendocino triple junction, *Geol. Soc. Am. Bull., 82,* 2965-2978, 1971.

Silver, E. A., Structural interpretation from free-air gravity on the

California continental margin, 35° to 40° N, *Geol. Soc. Am. Abstr. Programs, 9,* 524, 1974.

Silver, E. A., The San Gregorio-Hosgri fault zone: An overview, *Spec. Rep. Calif. Div. Mines Geol., 137,* 1-2, 1978

Singh, S. K., L. Astiz, and J. Havskov, Seismic gaps and recurrence periods of large earthquakes along the Mexican subduction zone: A reexamination, *Bull. Seismol. Soc. Am., 71,* 827-843, 1981.

Singh, S. K., M. Rodriguez, and L. Esteva, Statistics of small earthquakes and frequency of occurrence of large earthquakes along the Mexican subduction zone, *Bull. Seismol. Soc. Am., 73,* 1779-1798, 1983.

Slemmons, D. B., Geological effects of the Dixie Valley-Fairview Peak, Nevada, earthquakes of December 16, 1954, *Bull. Seismol. Soc. Am., 47,* 353-373, 1957.

Slemmons, D. B., State of the art for assessing earthquake hazards in the United States: Determination of the design earthquake magnitude from fault length and maximum displacement data, 109 pp., U.S. Army Eng. Waterways Exp. St., Vicksburg, Miss., 1977.

Smith, G. I., Large lateral displacement on Garlock fault, California, as measured from offset dike swarms, *Am. Assoc. Pet. Geol. Bull., 46,* 85-104, 1962.

Smith, G. I., Holocene movement on the Garlock fault, Geological Survey Research, *U.S. Geol. Surv. Prof. Pap., 975,* 202, 1975.

Smith, G. I., Holocene offset and seismicity along the Panamint Valley fault zone, western Basin and Range Province, California, *Tectonophysics, 52,* 411-415, 1979.

Smith, G. I., B. W. Troxel, C. H. Gray, Jr., and R. Von Huene, Geologic reconnaissance of the Slate Range, San Bernardino and Inyo counties, California, *Spec. Rep. Calif. Div. Mines Geol., 96,* 33 pp., 1968.

Stein, R. S., and W. Thatcher, Seismic and aseismic deformation associated with the 1952 Kern County, California, earthquake and relationship to Quaternary history of the White Wolf fault, *J. Geophys. Res., 86,* 4913-4928, 1981.

Sykes, L. R., Aftershock zones of great earthquakes, seismicity gaps, and earthquake prediction for Alaska and the Aleutians, *J. Geophys. Res., 76,* 8021-8041, 1971.

Sykes, L. R., and S. P. Nishenko, Probabilities of occurrence of large plate rupturing earthquakes for the San Andreas, San Jacinto, and Imperial faults, California, *J. Geophys. Res., 89,* 5905-5927, 1984.

Sykes, L. R., and R. C. Quittmeyer, Repeat times of great earthquakes along simple plate boundaries, in *Earthquake Prediction: An International Review, Maurice Ewing Ser.,* vol. 4, edited by D. W. Simpson and P. G. Richards, pp. 297-332, AGU, Washington, D. C., 1981.

Sylvester, A. G., and A. C. Darrow, Structure and neotectonics of the western Santa Ynez fault system in southern California, *Tectonophysics, 52,* 389-405, 1979.

Takeo, M., K. Abe, and H. Tsuji, Mechanism of the Shizuoka earthquake of July 11, 1935 (in Japanese with English abstract), *J. Seismol. Soc. Jpn., 32,* 423-434, 1979.

Tanimoto, T., and H. Kanamori, Linear programming approach to moment tensor inversion of earthquake sources and some tests on the three-dimensional structure of the upper mantle, *Geophys. J. R. Astron. Soc., 84,* 413-430, 1986.

Taylor, G. C., and W. A. Bryant, Surface rupture associated with the Mammoth Lakes earthquakes of 25 and 27 May, 1980, *Spec. Rep. Calif. Div. Mines Geol., 150,* 49-68, 1980.

Thatcher, W., Strain accumulation and release mechanism of the 1906 San Francisco earthquake, *J. Geophys. Res., 80,* 4862-4872, 1975.

Thatcher, W., J. A. Hileman, and T. C. Hanks, Seismic slip distribution along the San Jacinto fault zone, southern California, and its implications, *Geol. Soc. Am. Bull., 86,* 1140-1146, 1975.

Thatcher, W., T. Matsuda, T. Kato, and J. B. Rundle, Lithospheric loading by the 1896 Rikuu earthquake in northern Japan: Implications for plate flexure and asthenospheric rheology, *J. Geophys. Res., 85,* 6429-6435, 1980.

Tocher, D., Movement on the Rainbow Mountain fault, *Bull. Seismol. Soc. Am., 46,* 10-14, 1956.

Toppozada, T. R., History of earthquake damage in Santa Clara County and comparison of the 1911 and 1984 earthquakes in the in the Morgan Hill, California earthquake, *Calif. Div. Mines Geol. Spec. Publ., 68,* 237-248, 1984.

Toppozada, T. R., and D. L. Parke, Areas damaged by California earthquakes, 1900-1949, *Calif. Div. Mines Geol. Open File Rep., 82-17 SAC,* 65 pp., Sacramento, Calif., 1982.

Toppozada, T. R., C. R. Real, and D. L. Parke, Preparation of isoseismal maps and summaries of reported effects for pre-1900 California earthquakes, *Calif. Div. Mines Geol. Open File Rep., 81-11 SAC,* 182 pp., Sacramento, Calif., 1981.

Toppozada, T. R., C. R. Real, and D. L. Parke, Earthquake history of California, *Calif. Geol., 39,* 27-33, 1986.

Trifunac, M. D., Tectonic stress and the source mechanism of the Imperial Valley, California, earthquake of 1940, *Bull. Seismol. Soc. Am., 62,* 1283-1302, 1972.

Troxel, B. W., and P. R. Butler, Tertiary and Quaternary fault history of the intersection of the Garlock and Death Valley fault zones, southern Death Valley, California, Summaries of Technical Reports, National Earthquake Hazards Reduction Program, *U.S. Geol. Surv. Open File Rep., 80-6,* 45-47, 1980.

Tsai, Y. B., and K. Aki, Simultaneous determination of the seismic moment and attenuation of seismic surface waves, *Bull. Seismol. Soc. Am., 59,* 275-287, 1969.

Urhamner, R. A., Observations of the Coyote Lake, California earthquake sequence of August 6, 1979, *Bull. Seismol. Soc. Am., 70,* 559-570, 1980.

Urhamner, R. A., R. D. Darragh, and B. Bolt, The 1983 Coalinga earthquake sequence: May 2 through Aug. 1, *Spec. Rep. Calif. Div. Mines Geol., 66,* 221-232, 1983. br

Utsu, T., Aftershocks and earthquake statistics (III), *J. Fac. Sci., Hokkaido Univ. Ser. 7, 3,* 379-441, 1971.

von Seggern, D., A random stress model for seismicity statistics and earthquake prediction, *Geophys. Res. Lett., 7,* 637-664, 1980.

Wallace, R. E., Earthquake recurrence intervals on the San Andreas fault, *Geol. Soc. Am. Bull., 81,* 2875-2890, 1970.

Wallace, R. E., Patterns of faulting and seismic gaps in the Great Basin province, Proceedings of Conference VI, Methodology for Identifying Seismic Gaps, *U.S. Geol. Surv. Open File Rep., 78-943,* 857-868, 1978.

Wallace, R. E., and R. A. Whitney, Late Quaternary history of the Stillwater seismic gap, Nevada, *Bull. Seismol. Soc. Am., 74,* 301-314, 1984.

Weber, F. H., Jr., Total right lateral offset along the Elsinore fault zone, southern California, paper presented at 73rd Annual Meeting, Cordilleran Sect., Geol. Soc. of Am., Sacramento, Calif., 1977.

Weber, F. H., Jr., Geological features related to character and recency of movement along faults, north-central Los Angeles County, California, Earthquake Hazards Associated With the Verdugo-Eagle Rock and Benedict Canyon Fault Zones, Los Angeles County, California, edited by F. H. Weber, Jr., J. H. Bennett, R. H. Chapman, G. W. Chase, and R. B. Saul, *Calif. Div. Mines Geol. Open File Rep., 80-10 LA,* B1-B116, 1980.

Weber, G. E., Geologic investigation of the marine terraces of the San Simeon region and Pleistocene activity on the San Simeon fault zone, San Luis Obispo County, California, final technical report contract, 14-08-0001-18230, 66 pp., U.S. Geol. Surv., Menlo Park, Calif., 1981.

Weber, G. E., and W. R. Cotton, Geologic investigation of recurrence intervals and recency of faulting along the San Gregorio fault zone, San Mateo County, California, *U.S. Geol. Surv. Open File Rep., 81-263,* 133 pp., 1981.

Weber, G. E., and K. R. Lajoie, Map of Quaternary faulting along the San Gregorio fault zone, San Mateo and Santa Cruz counties, California, scale 1:24,000, *U.S. Geol. Surv. Open File Rep., 80-907,* 1980.

Weldon, R. J., Climatic control for the formation of terraces in Cajon Creek, southern California (abstract), *Geol. Soc. Am. Abstr. Programs, 15,* 429, 1983.

Weldon, R., and E. Humphreys, A kinematic model of California, *Tectonics, 5,* 33-48, 1986.

Weldon, R. J., and K. E. Sieh, Holocene rate of slip along the San Andreas fault and related tilting near Cajon Pass, southern California, *Geol. Soc. Am. Abstr. Programs, 12,* 159, 1980.

Weldon, R. J., and K. E. Sieh, Holocene rate of slip and tentative recurrence interval for large earthquakes on the San Andreas fault, Cajon Pass, southern California, *Geol. Soc. Am. Bull., 96,* 793-812, 1985.

Wesnousky, S. G., C. H. Scholz, and K. Shimazaki, Deformation

of an island arc: Rates of moment release and crustal shortening in intraplace Japan determined from seismicity and Quaternary fault data, *J. Geophys. Res., 87,* 6829-6852, 1982.

Wesnousky, S. G., C. H. Scholz, K. Shimazaki, and T. Matsuda, Earthquake frequency distribution and the mechanics of faulting, *J. Geophys. Res., 88,* 9331-9340, 1983.

Wesnousky, S. G., C. H. Scholz, K. Shimazaki, and T. Matsuda, Integration of geological and seismological data for the analysis of seismic hazard: A case study of Japan, *Bull. Seismol. Soc. Am., 74,* 687-708, 1984.

Whitney, J. D., The Owens Valley earthquake, *Overland Mon., 9,* (2 and 3), 130-140, 226-278, 1872.

Willis, B., A fault map of California, *Bull. Seismol. Soc. Am., 13,* 1-12, 1923.

Wilson, J. T., Foreshocks and aftershocks of the Nevada earthquake of December 20, 1932, and the Parkfield earthquake of June 7, 1934, *Bull. Seismol. Soc. Am., 26,* 189-194, 1936.

Witkind, I. J., Reactivated faults north of Hebgen Lake, *U.S. Geol. Surv. Prof. Pap., 435,* 37-50, 1964.

Wong, I. G., Reevaluation of the 1892 Winters, California, earthquakes based upon comparison with the 1983 Coalinga earthquake, *Eos Trans. AGU, 65,* 996, 1984.

Woodward-Clyde Consultants, Earthquake evaluation studies of the Auburn Dam area, report prepared for U.S. Bureau of Reclamation, 8 vol., San Francisco, Calif., 1977.

Woodward-Clyde Consultants, Evaluation of the potential for resolving the geologic and seismic issues at the Humboldt Bay Power Plant Unit No. 3, report prepared for Pacific Gas and Electric Co., 74 pp., San Francisco, Calif., 1980.

Wright, L. A., and B. W. Troxel, Limitations on right-lateral, strike-slip displacement, Death Valley and Furnace Creek fault zones, California, *Geol. Soc. Am. Bull., 78,* 933-950, 1967.

Wright, R. H., D. H. Hamilton, T. D. Hunt, M. L. Traubenik, and R. J. Shlemon, Character and activity of the Greenville structural trend, Proceedings Conference on Earthquake Hazards in the Eastern San Francisco Bay Area, edited by E. W. Hart, *Calif. Div. Mines Geol. Spec. Publ., 62,* 187-196, 1982.

Wright, T. L., E. S. Parker, and R. C. Erickson, Stratigraphic evidence for timing and nature of late Cenozoic deformation in Los Angeles region, California (abstract), *Am. Assoc. Pet. Geol. Bull., 57,* 813, 1973.

Wyss, M., Preliminary source parameter determination of the San Fernando earthquake, *U.S. Geol. Surv. Prof. Pap., 733,* 38-40, 1971.

Yeats, R. S., Newport-Inglewood fault zone, Los Angeles Basin, California, *Am. Assoc. Pet. Geol. Bull., 57,* 117-135, 1973.

Yeats, R. S., Stratigraphy and paleogeography of the Santa Susana fault zone, Transverse ranges, California, in *Cenozoic Paleogeography of the Western United States, Pacific Coast Paleogeography Symposium,* edited by J. M. Armentrout, M. R. Cole, H. Ferbest, Jr., pp. 191-204, Los Angeles, Calif., 1979.

Yeats, R. S., Low-shake faults of the Ventura basin, California, in *Neotectonics of Southern California,* compiled by J. D. Cooper, pp. 3-23, Geological Society of America, Cordilleran Section, Anaheim, Calif., 1982.

Yeats, R. S., Large-scale Quaternary detachments in Ventura Basin, southern California, *J. Geophys. Res., 88,* 569-583, 1983*a*.

Yeats, R. S., Simi: A structural essay, in *Cenozoic Geology of the Simi Valley Area, Southern California,* edited by S. R. Squires and M. V. Filewicz, pp. 233-240, Pacific Coast Section, Society for Economic Paleontologists and Mineralogists, Bakersfield, Calif., 1983*b*.

Yeats, R. S. and and, D. J. Olson, Alternate fault model for the Santa Barbara, California, earthquake of 13 August 1978, *Bull., Seismol. Soc. Am., 74,* 1545-1553, 1984.

Yeats, R. S., M. N. Clark, E. A. Keller, and T. K. Rockwell, Active fault hazard in southern California: Ground rupture versus seismic shaking, *Geol. Soc. Am. Bull., 92,* 189-196, 1981.

Yerkes, R. F., and C. M. Wentworth, Structure, Quaternary history, and general geology of the Corral Canyon area, Los Angeles County, California, *U.S. Geol. Surv., Open File Rep., 864,* 215, 1965.

Yerkes, R. F., T. H. McCulloch, J. E. Schoellhamer, and J. G. Vedder, Geology of the Los Angeles Basin, California--An introduction, *U.S. Geol. Surv. Prof. Pap., 420-A,* 57, 1965.

Yerkes, R. F., and W. H. K. Lee, Faults, fault activity, epicenters, focal depths, and focal mechanisms, 1970-1975 earthquakes, western Transverse Ranges, California, scale 1:250,000, *U.S. Geol. Surv. Misc. Field Stud. Map, MF-1032,* 1979.

Yerkes, R. F., H. G. Greene, J. C. Tinsley, and K. R. Lajoie, Seismotectonic setting of the Santa Barbara Channel area, southern California, *U.S. Geol. Surv. Misc. Field Map, 1169,* 1981.

S. G. Wesnousky, Tennessee Earthquake Information Center, Memphis State University, Memphis, TN 38152

(Received August 13, 1985;
revised April 21, 1986;
accepted May 29, 1986.)